

A thesis submitted for the degree of
Master of Science

**A STUDY OF STRUCTURAL PARAMETERS
AFFECTING FLUTTER STABILITY
OF SUSPENSION BRIDGES**

by

GEORGE FRANGOPOULOS

Department of Civil Engineering
University of Glasgow



Copyright G. Frangopoulos

June 1992

ProQuest Number: 13815387

All rights reserved

INFORMATION TO ALL USERS

The quality of this reproduction is dependent upon the quality of the copy submitted.

In the unlikely event that the author did not send a complete manuscript and there are missing pages, these will be noted. Also, if material had to be removed, a note will indicate the deletion.



ProQuest 13815387

Published by ProQuest LLC (2018). Copyright of the Dissertation is held by the Author.

All rights reserved.

This work is protected against unauthorized copying under Title 17, United States Code
Microform Edition © ProQuest LLC.

ProQuest LLC.
789 East Eisenhower Parkway
P.O. Box 1346
Ann Arbor, MI 48106 – 1346

Thesis
9414
copy 1

GLASGOW
UNIVERSITY
LIBRARY

Acknowledgements

The work described herein was carried out in the Department of Civil Engineering at the University of Glasgow with the supervision of Doctor Alan Agar.

I wish to express my thanks to my supervisor for the provision of the program ANSUSP and for his close guidance and great patience throughout the progress of the present work.

Thanks are due to Mrs Janet Sutherland for her guidance in my introduction to the various software facilities of the department and also to Ian Dickson and Ken Ryan for their valuable help.

I wish to express my gratitude to my friends and colleagues Emanuel Awoleye, Zhang Binsheng and for their help to my adaptation to the working environment of the University. I also want to thank Manuel Lorena, Saleh Gaderbouh, Giovanni Scilipoti, Libor Jendele, Suhol Bu and Waseem Khalifa for their friendly support during my work in the University. Thanks are also due to Olubyo Famiyensin, Mohamed Abdel-Kader and Bensalem Abdelmadjid for their interesting spiritual discussions.

I wish also to express my thanks to John Fisher for helping me with the English at the final stages of this thesis.

Finally I wish to express my special thanks to my family for their continual support and encouragement throughout the years.

Abstract

The cable suspended bridges have been used worldwide to connect two remote points, separated usually by water. These bridges may be largely affected by wind because of the sites where they are erected, being usually near estuaries, their large proportions and their particularly flexible design because of the cables involvement in the overall stiffness of the bridge.

In the present work a parametric analysis is carried out of the basic structural properties of the cable suspended bridge and the effects of these properties on the flutter stability of the bridge are investigated. In the present work two numerical approaches were used being available with the computer program 'ANSUSP'.

The natural modes were firstly computed for a cable suspended bridge with the Severn bridge nominal structural properties and for each modified bridge configuration and an effort was made to explain the effects of the alteration of the structural properties on the aero-elastic behaviour of the bridge.

Modal analysis method was used for a wide variety of bridge structural properties and critical windspeeds were predicted.

Secondly the time history method was used only for some selected bridge structural properties, being the more time consuming method of the two and flutter speeds were predicted. The results of the two methods are

presented in graphs and are compared between each other and also with the results of Selberg's semi-empirical equation.

Table of Contents

	<u>Page No</u>
Chapter 1	
1. Introduction.....	1
1.1 Suspension bridge history.....	1
1.2 Suspension bridge failures due to wind.....	4
1.3 Suspension bridge aero-elastic problems.....	6
1.4 Static analysis of suspension bridges.....	8
1.5 Dynamic analysis of suspension bridges.....	9
1.6 Scope of present work.....	13
Chapter 2	
2.1 Review of aerodynamic instabilities.....	17
2.2 Classical flutter theory.....	21
2.3 Significance of natural frequencies.....	22
2.4 Wind tunnel tests.....	23
2.5 Empirical approach.....	26
2.6 Equations of aerodynamic forces.....	27
2.7 General equations of motion at flutter.....	30
2.7.1 Equations of motion in a 2 degree of freedom system.....	30
2.7.2 Multi degree of freedom system.....	32
2.8 Flutter instability of suspension bridges.....	34

Chapter 3

3.1	The computer program 'ANSUSP'.....	41
3.2	3-D modelling.....	42
3.3	Structural model.....	45

Chapter 4

4.1	Modal flutter analysis.....	49
4.2	Time step analysis.....	52

Chapter 5

	<u>Parametric study using ANSUSP</u>	58
5.1	Modal flutter analysis by ANSUSP.....	60
5.1.1	The effect of cable sag.....	60
5.1.2	The effect of cable sag with deck torsional stiffness reduced to 7% the nominal value.....	62
5.1.3	The effect of horizontal separation of the cables.....	64
5.1.4	The effect of horizontal separation of the cables with deck torsional stiffness reduced to 4% of its nominal value.....	66
5.1.5	The effect of horizontal separation of the cables with tower stiffness increased to 10 times the nominal value.....	69
5.1.6	The effect of horizontal separation of the cables with tower torsional and flexural stiffness increased to 10,000 times the nominal value.....	70
5.1.7	The effect of cables' mass per unit length...	73

5.1.8	The effect of rotational deck inertia.....	74
5.1.9	The effect of deck mass.....	75
5.1.10	The effect of the deck torsional stiffness..	76
5.1.11	The effect of deck vertical stiffness.....	78
5.1.12	The effect of cables Young's modulus.....	79
5.1.13	Effects of air density.....	81
5.1.14	The effect of full aerodynamic width.....	82
5.2	3-D Time history method.....	82
5.2.1	The effect of horizontal separation of the cables.....	83
5.2.2	The effect of deck mass factor.....	84
5.2.3	The effect of deck torsional stiffness.....	84
5.2.4	The effect of full aerodynamic width.....	85
Chapter 6		
	<u>Discussion of results</u>	87
Chapter 7		
	<u>Conclusions</u>	91
Chapter 8		
	<u>Further work proposals</u>	97
Chapter 9		
	<u>Reference</u>	99

Declaration

I hereby declare that the following thesis has been composed by me, that it is a record of work carried out by myself and that it has not been presented in any previous application for a higher degree.

Chapter 1

Introduction

1.1 Suspension bridge history

Among the earliest examples of structures of this kind (Fig.1), is the rope suspended bridge over the Indus river near Swat [2] and the Iron chain bridge over the Pan-Po river in China, believed by tradition to have been erected in A.D.65, [2]. These structures have evolved from the simple idea of bridging two points with ropes. The lower ones could support the dead weight and live loading, which was applied on girders, positioned transversely. The upper cables were connected to the lower through vertical ropes (hangers) and were carrying part of the loads. Another utility of the upper ropes was the role of a handle for the people who used the passage since the structure was too flexible and oscillated wildly under dynamic loading of steps. Later stiffening girders positioned longitudinally helped redistribute the forces to more hangers and the bridges grew more stable and more practical.

The substitution of natural ropes by metal chains brought a big advance in suspension bridge design and construction and enabled the construction of larger span bridges. These innovations started in China (eg. Hwa Kiang river bridge of 200ft span, 1632). In the western world suspension bridges gained popularity in the early years of the eighteenth century (eg. Tees river bridge

near Middleton of 70ft span, 1741, Lahn Bridge in Germany of 98ft span, 1785, Uniontown bridge in Pennsylvania, USA, of 70ft span, 1796). By the end of 19th century, wire cables were used instead of chains and the whole layout had been modified, (Fig.2).

The suspension bridge profits considerably from the advances of theoretical engineering, during the beginning of the 19th century. By then the main three simple cable shapes, simple catenary, catenary of uniform strength and parabola were fully studied mathematically. In 1823 Navier [1] presented his work on elastic theory. Later Clericetti [26] and Melan, J. [3] on deflection theory and even later Timoshenko [25], on energy methods and Castigliano's strain energy work and its application on arches were developed, the cable suspended bridge being practically an 'inverted' arch with tension instead of compression, without the disadvantage of local buckling of the arches and so providing a more effective use of the material.

In the early third of 20th century, the expansion of the cable suspended bridges was immense especially in the U.S.A where a series of such bridges were built. The length of the main span reached 4200ft in the Golden Gate bridge at San Francisco, 1937. Simultaneously the demand for more aesthetically acceptable structures as well as more economical and lighter ones highlighted the requirement for more slender bridges. One example is the Tacoma Narrows bridge in Washington of 2800ft span, 1940. The deck section was constructed from two plate girders

of 8ft deep each, (Fig.3) giving to it a slender side profile. The structure was in service only for a few months when it started oscillating vertically in a wind of approximately 40mph. The oscillations developed in a combination of flexural and torsional galloping motion and after a slight increase of the windspeed the bridge collapsed.

The bridges which followed since are tested in wind tunnels extensively in order to ascertain that they are aerodynamically stable.

After the Tacoma Narrows collapse, engineers turned to open lattice stiffening girders (second Tacoma Narrows bridge, Forth Road bridge in Scotland of 3240ft span, 1964, Verrazano Narrows bridge of 4200ft, 1965, Tagus river bridge in Portugal of 3300ft span, 1966).

The Severn bridge of 3400ft span linking England and Wales was completed in 1966. It's deck is 10ft deep with the cross section shaped as a closed box (Fig.4), with a streamlined shape not unlike an aircraft wing. The closed box section provided a high torsional deck stiffness. This innovative design was studied in wind tunnels for aerodynamic stability and behaved very satisfactorily, providing low drag and reduced flow separation. Other features included the employment of inclined hangers, instead of vertical, in order to increase structural damping. This was the first design of this kind and was adopted in later structures. Many of the long span bridges which have been built since have similar features. Some examples are the Bosphorus bridges

in Turkey [24], the Lillebaelt bridge in Denmark, Burrard Inlet, Humber, etc.

1.2 Suspension bridge failures due to wind.

The first failures of suspension bridges are reported back in 19th century. The Tweed river bridge in Berwick, Scotland, 1817, [28], the Tweed river Union bridge at Nordham Ford, 1820, which collapsed after six months only in operation.

Damage was reported in 1836 on the Brighton Chain Pier bridge with four spans of 255ft, suspended by four chains. Built in 1823, it collapsed in a storm in 1833, when one span was destroyed. After three years the same span collapsed again. The motion mechanism that was involved in the collapse of the structure has been compared to that of the Tacoma Narrows bridge and was very similar.

The Telford bridge over the Menai Straits was built in 1826, with a main span of 580ft. It was damaged three times; twice in 1836, the central span collapsed and later on in 1839 the same span collapsed again. Finally alterations to its deck structure improved its behaviour in wind.

Other examples of collapses include Nassau bridge over the Lahn River in Germany, built in 1830 with a main span of 245ft, and Wheeling bridge in West Virginia in USA with a main span of 1010ft, built in 1848. By then the stiffening trusses were becoming increasingly deep

with each new structure, affecting as a result the weight of the deck. The extreme was reached in 1903 with the Williamsburgh bridge in U.S.A with stiffening trusses reaching 40ft deep. After this structure the trusses started to give way to plate girders. This trend led to shallower, more slender structures, reaching an extreme in 1940 with the construction of Tacoma Narrows bridge. This was a perfectly safe structure for the static weight and static wind loads and live loading it was designed to carry, however as no precautions had been taken against potential dynamic wind loads or aeroelastic instability, the strong tendency it | for flexural and torsional oscillations resulted in its collapse.

The development of vertical oscillations during its erection caused some extra measures to be taken. This included installation of hydraulic buffers at the towers, diagonal cable ties at the centre of the main span and tie-down cables installed at the side spans anchored firmly to the ground, restricting their movements. These efforts though were unable to prevent the vibration of the main span. In November on 1940, in a wind of 38mph the bridge started oscillating in a vertical flexural mode with small amplitude. After a few hours the wind speed reached 42mph and the mode of oscillation changed to a combination of vertical and torsional modes with large amplitudes, leading to the collapse of the bridge approximately 75 minutes later.

Eventhough the wind sensitivity of cable suspended bridges was known from previous occasions, it was always

related to the static wind forces [4]. Only after the destruction of the first Tacoma Narrows bridge did the engineering community realise the importance of the dynamic wind loading on those structures.

1.3 Suspension bridge aeroelastic problems.

Cable suspended bridges are subjected to aerodynamic instabilities. Some of the most important ones are described in the following:

Divergence is a phenomenon of static instability. The air flow induces a static force on the side of the deck, essentially reducing the torsional stiffness of the deck. When this force overlaps the critical one, the deck inclines. The angle of attack then produces higher lift forces which lead to increased moments applied to the deck which inclines more and finally flips over. The critical force is applied to the structure at the critical windspeed. If this is not reached the deck maintains its position. This phenomenon, once critical windspeed is reached, cannot be reversed at any higher than the critical windspeed. Therefore it has only a lower bound windspeed.

Classical flutter, torsional divergence, vortex shedding, buffeting and galloping are the most important aerodynamic instabilities, [4]. They are all dynamic instabilities. The former is the most dangerous of all

for the modern streamlined deck cross sections and will be discussed in detail in a later chapter.

Vortex shedding is a phenomenon affecting bluff bodies as wide H-type deck sections. The boundary layer alternately detaches from and re-attaches to the body. Depending on the value of the Reynold's number and the type of cross section, this may become periodical, creating turbulence across the leeward side of the deck leading to alternating forces. These forces are directed across-wind and vertically to the bridge deck and generate a dynamic excitation. If a natural frequency of the bridge is similar to one half of the vortex shedding frequency, resonance may occur where the oscillations tend to increase to large values.

Buffeting is due to the sudden variation of intensity of the air-flow caused by the turbulent texture of atmospheric wind. Usually its frequency is too low to exert some kind of resonance, but the variation of wind force intensity applied to different parts of the span in some organised pattern could initiate oscillations.

Galloping, finally, is a phenomenon affecting cross sections with non circular shapes. As the wind direction fluctuates around a mean direction, forces are applied on the section, asymmetrically, causing a periodical oscillation. It usually affects electric conductors when subjected to ice accretion.

1.4 Static analysis of suspension bridges.

The examination of cable suspended bridges is still continuing even though many long-span suspension bridges have been designed and constructed successfully, many of which in the first half of the century. The simplicity of the design and the redundancy it provides, made it a very versatile and adaptable structure. A structure, with the shape of an inverted arch, relying on tensile instead of compressive forces carrying the deck beam and all its loads. The shape is either second order or catenary or even catenary of uniform strength, formed by the cable freely under the loading, and has the freedom to transform under live loads. Usually it has the shape of the second order curve as the moment diagram of a beam loaded with continuously distributed loads. The hangers support the deck and transfer dead and live loads to the main support element which is the cable. Finally the cables are suspended from the towers, transferring to them all their vertical loads.

Studies on suspension bridge static forces go back as far as 1888 with deflection theory by Melan,[4]. In the first half of 20th century through advances in deflection theory raised hopes for the solution of the cable equilibrium. A big advance was the introduction of the theories on energy and potential energy which were initiated by Timoshenko [25] and later by F. Bleich [29] using trigonometric series for the approximate representation of deflections. On the same principles was

based the work of Bowen and Charlton [46] , and later Van der Woude [30].

The analytical solution for the cable and cable mesh was solved by Panagiotopoulos [18]. Even though cable finite elements have appeared, they are still in experimental level and have not been introduced yet for the study of cable suspended bridges.

A method which was developed in 1976 [13] was the employment of a step-by-step numerical integration of the equations of motion of a heavily damped dynamic model of the bridge. Given an initial condition of displacements and velocities of the structure in each degree of freedom, the structure oscillates freely with a very high damping ratio. After a few oscillation cycles the structure comes to rest at its equilibrium position.

1.5 Dynamic analysis of suspension bridges.

The first large steps in aerodynamic instabilities were achieved by Frazer and Duncan [37] in 1928. They developed the model of the flutter mechanism of a wing. The equations of motion were solved by the test functions of Frazer. Theodorsen's [45] paper on the incompressible flow flutter was published in 1935.

Later on, in 1948 Bleich [28] published a paper applying the flutter theory as used in aircraft designing to suspension bridge decks. He developed the equations of motion for a suspension bridge deck represented as a flat

plate, with vertical flexural and torsional d.o.f.s using Theodorsen's aerodynamic forces.

Farquharson [38] worked experimentally on the original Tacoma Narrows Bridge and on various proposed designs for the second Tacoma Narrows bridge.

Steinman [39] introduced into the designs, additional damping devices in order to increase the resistance of bridges to flutter. Most of these have been adopted in later designs.

Selberg [40], after working on wind tunnel tests experimentally, produced a very simple formula for the prediction of flutter windspeeds.

Smith [41] investigated in 1964 the Severn bridge proposed designs. His aim was to detect aerodynamic instabilities in the erection stages. When deck sections of a bridge are raised into place and before they are fully connected, the deck has minimal torsional stiffness and so is very susceptible to flutter. This conclusion opposed the previously accepted conception that the fully connected sections would provide a longer plate to the wind-stream than the unconnected sections and hence would be more susceptible to flutter than the unconnected deck sections.

Sabzevari et al [42], [43] worked with a combination of analytical and experimental approaches. They used experimentally derived results to evaluate the air forces which are then used in the analytical formulations. In this way the shape of the cross section of the deck can be taken into account during the

investigations of the stability of the bridge in flutter.

Recently, Chaudhury [33] analysed the vertical bending vibrations by using his own numerical integration method, to integrate the Newtonian equations of motion and obtain the dynamic response of the bridge with time.

Allman [34] developed a relaxation method. According to this method the restraint forces are gradually relaxed when the correct solution for the acceleration is reached.

Bell and Brotton [36] developed a numerical integration method for the determination of the flutter windspeed of a structural system. Calculating damping for different windspeeds, he finally finds the flutter windspeed of the bridge, when the damping of the motion is zero.

Iwegbue [13], followed on these principles, and presented his work on time-step analysis, for representation of the bridge reaction to Theodorsen's wind forces.

Today the dynamic analysis of structures is founded on the implementation of discretized mass and stiffness properties. According to this, the mass of the system is often assumed to be concentrated at discrete points, so that their displacements can be described by a finite number of coordinates. The equilibrium conditions may be expressed by a number of ordinary differential equations rather than partial ones which would be more adequate for the description of the original system of continuous mass distribution. The simultaneous differential equations can

be formulated as matrix equations. From this point on, two different approaches can be followed for the solution; the modal analysis methods and the time history integration methods.

The modal analysis method leads to the solution of the eigenvalue problem, extracting the natural frequencies of the bridge, when it oscillates freely, and the characteristic shapes of the system (natural modes). The forced motion problem leads also to the eigenvalue-eigenvector problem with the real part of the eigenvalues being the logarithmic damping of the system.

The advantage of this method lies in the fact that the response of most systems which concern engineers is dominated by a few modes of vibration. The oscillation of the structure is assumed to be a combination of a very few natural modes of the structure. It also gives an estimate of the behaviour of the structure with low computational cost.

On the other hand this method is based on the assumption that the structure behaves linearly which may be untrue in situations where cable bridges undergo large deflections and there may be significant geometrical non-linear effects.

The time-history analysis is capable of reproducing the non-linear behaviour of the structure and record its time history of oscillations, enabling the study of the amplitudes of displacements of the structure, and also the forces which have been developed in each element. A

more detailed description of both methods will follow in a later chapter.

1.6 Scope of present work.

The present work is based on the use of the computer program ANSUSP, enabling the study of a cable suspended bridge, for static and dynamic loading, focusing on flutter instability and the structural factors that affect its onset.

The aim is to achieve a better understanding of the role of different factors which affect the aeroelastic stability of conventional 2-cable 3-span suspended bridge configuration.

For dynamic wind loads, the two most important methods are implemented. The modal analysis method, [31] and the time history method, [13].

A series of variables are examined in order to predict the limits of aeroelastic stability, and the influence of these variables, structural, geometrical or aerodynamical on flutter windspeeds.

The structural model used in the present project is a three dimensional finite element idealization of a bridge subjected to aerodynamic forces.

In the time history method, the model oscillates under the influence of wind forces, resulting in a detailed representation of the behaviour of the original structure. The results can include the stress history of

the structure, during oscillations, revealing momentary stresses in excess of the strength of construction materials, or even need for alterations of the design. However the main goal here is the flutter windspeed prediction of each particular configuration, when some properties of the bridge are altered.

The modal analysis has been shown [15] to give good estimates of the behaviour of the structure likely to occur in flutter windspeeds using much smaller amount of CPU, than the time step analysis so the later method was used to focus on the more interesting parameters. In conclusion the use of a combination of both methods proves more efficient and more reliable than the use of each one of the two, alone. Finally comparative diagrams follow with the results of the two methods and Selberg's [40] semi-empirical one, in order to provide a visual comparison.

The contents of the present thesis are organized under the following headings:

Major categories of aerodynamic instabilities where the main aeroelastic phenomena are described and flutter is described in more detail being the main theme of this thesis. Also methods which have been developed for the study of aeroelastic phenomena and application of special devices on bridges which have been constructed during the last forty years will be mentioned, followed by the mathematical models of the aerodynamic forces, used in this project and the equations of motion of the

structure. All these will be included in the second chapter.

The third chapter will contain a review of previous work on the problem of flutter instability and the progress which has been achieved during the last twenty years, including the experimentally established methods and prepositions for aerodynamic devices, in the attempt to improve the performance of these wind sensitive structures. Finally a short quotation on the ANSUSP work, introducing the 3-D modelling of the bridge, and the evolution of full bridge modelling will be included.

The ANSUSP program described in chapter 4, contains both modal analysis and time history method, enabling the comparison and combination of the two methods. A full description of both and their implementation in the program follows.

The parametric study which constitutes the backbone of the present project is described in chapter 5. The parameters which were investigated are geometrical, elastic, inertial and aerodynamic. The first category includes cables' sag and horizontal cable separation. In the second category are included vertical and torsional deck stiffness, stiffness of cable and tower and also cable and deck mass and torsional deck inertia. Finally in the third category aerodynamic width and air-density are included. The results, including the display of the critical curves and the comparison of the two methods are outlined in this chapter.

Results and conclusions are discussed with a view to the possibility of future study. The demand for accurate solutions, the availability of powerful computational devices, the need for quickly and economically raised structures and the introduction of new materials in the construction industry, place new challenges which must be met and investigated in future research work.

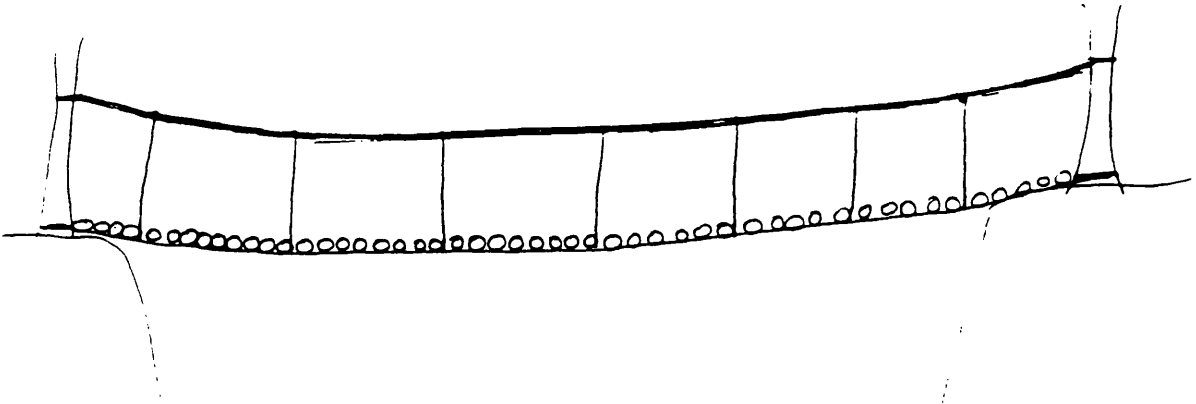


(Fig. 1) Primitive rope suspended bridge.

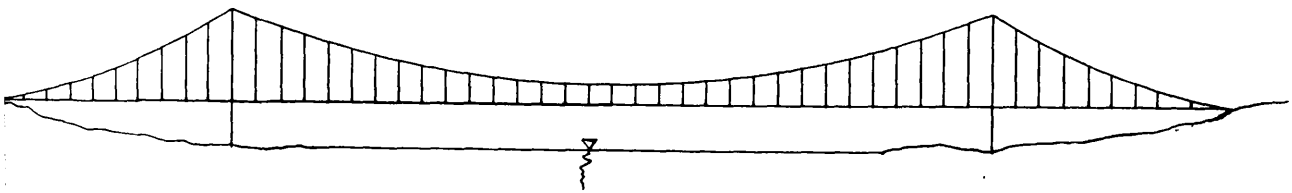


(Fig. 2) Typical layout of cable suspended bridge.

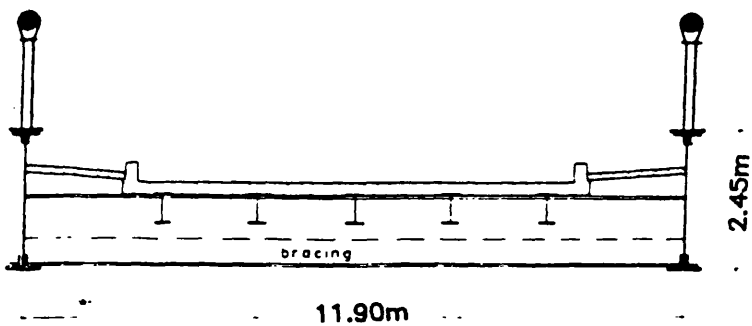


(Fig. 3) Cross section of First Tacoma Narrows bridge.

Chapter 2

2.1 Review of aerodynamic instabilities

As the range of materials used in human structures widened, stronger and lighter construction materials became available, which enabled engineers to create the large scale structures needed by the continuously growing demands of the increasing urban populations. In these massive structures wind forces became of paramount importance along with the effects of gravity loads. Collapses have occurred involving silos, huge storage bunkers, telescope reflectors, cable net roofs for stadiums and airports, factory chimneys, power station cooling towers, skyscrapers, antenna towers and long bridges, due to wind effects.

In these structures, the combination of wind forces, elastic and inertial forces, acted together creating destabilizing effects. These effects can be divided in two major categories: static and dynamic instabilities.

Static instabilities include those where wind forces are acting effectively as static external forces.

The static instability of divergence appears when the wind force acts on a long flat plate. The initial angle of the plate with the direction of the wind produces moments. The plate rotates as a result and the angle of attack increases. The moments increase accordingly and so on. As a result, the torsional stiffness of the structure essentially decreases. When

the wind speed is sufficiently high, the result is a zero torsional stiffness, and the structure suddenly deflects torsionally. This phenomenon is similar to that of structural buckling. The necessary study must be based on wind tunnel tests; however divergence is a phenomenon very unlikely to affect cable suspended bridges in practice.

Dynamic instabilities are more important for the cable suspended structures. Here are included vortex shedding, galloping, buffeting, separate flow torsional (or stall) flutter and classical flutter.

a) Vortex shedding occurs whenever a bluff or rounded body is positioned in a wind flow. Vortices are shed alternately with time from the opposite sides of the body (Fig.5) thus producing alternating transverse forces on it.

The stronger forces act transversely to the air-flow with frequency $= S =$ Strouhal number, while some in line with the flow are of secondary importance with frequency $= 2S$. When the frequency of vortex shedding approaches a structural natural frequency, the body starts to oscillate and resonant oscillations can occur. The vortex shedding frequency depends on the windspeed, so at the point where the oscillations start to develop, the critical windspeed for vortex shedding has been reached. In this case the wake vortices are influenced more strongly from the body motion frequency than from the natural Strouhal number.

The resonant condition is usually restricted to a narrow range of windspeeds, normal to the body. Out of this range, the structure returns to aerodynamic stability. The phenomenon is also self-limiting in amplitude. The entrance windspeed into lock-on conditions when windspeed is increasing is quite different from the escape windspeed from it, when windspeed is decreasing from the critical windspeed. It is by nature a non-linear phenomenon.

At Tacoma Narrows, vortex shedding was involved in the initiation of the vertical motion and sustained it but was not the reason for the final catastrophic motion, [4].

b) Separated flow torsional (or stall) flutter is a non-linear wind excited phenomenon, leading to periodical detachment and reattachment of the flow, around a body moving with predominantly one degree of freedom in torsion (Fig. 6). It can affect either 'aerofoils' in a large angle of attack or bluff bodies, such as rectangular prisms or flat H-sections, like the Tacoma Narrows deck section, truss stiffened deck structures or even electric power-transmission cables, subjected to ice-accretion.

The body subjected to an air-flow, develops an increasing angle of attack, caused by the wind forces, which become stronger as its inclination increases, until it reaches a point where the boundary layer detaches from the body, stall follows, the lift at the leading edge decreases and so does the angle of attack. Subsequently

the body moves to its equilibrium position, the wind-flow reattaches to the body and the motion repeats itself in the opposite transverse direction. The frequency of the motion depends on the velocity of the air-flow. As the windspeed increases, the motion frequency may approach a structural natural frequency and then the phenomenon will develop to a strongly destabilizing situation. If the windspeed continues to increase, the intensity of the motion will also increase and could lead to catastrophic effects since this condition has no upper windspeed limit. In the past this has been the main cause of bridge failures due to wind. Torsional flutter usually drives also the participation of vertical modes in a coupled motion, called classical flutter.

c) Classical flutter is a phenomenon affecting particularly streamlined 'faired' sections (Fig. 7). The airflow around the body remains attached. The phenomenon involves the coupling of vertical and torsional oscillation occurring together in common frequency with a phase difference, in a motion that extracts energy from the wind stream and feeds it into the structure increasing its amplitude of motion.

d) Galloping is the result of asymmetric aerodynamic forces associated with the cross flow (Fig. 8). It is a large amplitude oscillation, affecting mainly iced electric conductor cables or 'bundled conductor' configurations.

The fluid forces change fast around 'mean' values. The latter however vary much more slowly. Under these

conditions the slowly changing drag and lift forces induce to the body a low frequency oscillation with large amplitudes.

e) Buffeting is the result of the action of turbulence, created from the wake of a body upstream, or because of natural turbulence in the flow, [4], (Fig. 9). The oscillations are largest if the frequency of buffeting is close to a natural frequency of the structure.

2.2 Classical flutter theory.

Classical flutter is a self excited oscillation. The cycle of oscillation can be described as follows (Fig.10).

When the vertical displacement is near the equilibrium position, the torsional one takes its maximum value. As a result, the lift force takes its highest value and so the body moves vertically. When the vertical oscillation takes maximum value, the torsional one has decreased, so the combination of structural and gravity forces force the deck back to its equilibrium position. After it reaches that point, the phenomenon is repeated in the opposite direction and so one cycle is completed. The damping which is provided by the structure and wind-flow restrict the motion until flutter windspeed is reached. As the windspeed increases, the damping reduces, eventually becomes zero and the structure oscillates

violently with constant amplitude. Further increase of the wind will lead to the aerodynamic forces introducing negative damping where the oscillations will increase their amplitudes even more.

This phenomenon has been extensively studied in relation to cable suspended bridges, since it was found to endanger the stability of these structures.

According to some authors (Scanlan [4], [21], Hjorth-Hansen), exact correlation of faired deck sections with thin airfoil theory must be implemented cautiously because it is proved from experimental analysis that the aerodynamic forces expressed as functions of experimentally measured factors are quite different according to the section types used for the deck. However the deck sections used in the last twenty years and some proposed future structures are similar to the flat plate shape, thus substantiating the use of thin airfoil expressions for the aerodynamic forces, expressed by Theodorsen in 1935 [45].

2.3 Significance of natural frequencies.

As has been mentioned earlier, the natural frequencies of the structure play a very important role in all aerodynamic phenomena. The excitation of the structure by the wind initiates a motion which quickly develops to an oscillation, combining some of the first natural modes. If the windspeed is adequately high, the

vortex discharge frequency coincides with one of the first natural modes. The result is a feedback situation and increased shedding of vortices. Since the natural frequencies depend on inertial and elastic characteristics of the deck's cross section, it is essential that it is be designed in such a way that it will not facilitate resonance between aerodynamic forces and natural frequencies.

2.4 Wind tunnel tests

Wind tunnel test are commonly used in cable suspended bridge studies for measuring the lift, drag and moment coefficients of different deck cross sections and constitute the mean or time average of fluctuating values. This is because some fluid-structure interaction phenomena cannot be modelled analytically with enough accuracy so mean values are used to measure motion-dependent or time-dependent aerodynamic coefficients. These measurements are carried out in wind tunnels which have been used extensively for either scaled full-span models [4],[5],[9], of the whole structure or sectional models, when a section of the structure is tested and some particular properties are studied. Both model types are used in the experimental study of cable suspended bridges.

The full-span models are exact geometric copies of the original structures. They reproduce the exact mass,

stiffness and damping distribution, density ratio values, stiffness and structural damping under the scale they were assembled. In some studies, the characteristics of atmospheric wind were also reproduced in wind tunnels with the greatest possible accuracy, modelling densely built areas and hills which influence the wind flow vorticity and could affect its texture. Reynold's number, intensity of turbulence and wind speed variation with height are also characteristics which should be modelled appropriately. These models could reproduce the natural modes, frequencies amplitudes and critical flutter windspeeds. The frequency scale should be described by special scale parameters. The same will be necessary for the wind speeds and oscillation amplitudes of the original structure. However, there are difficulties in achieving the correct Reynold's number and structure of natural winds with turbulence texture. Other difficulties emerge from the restrictions on the size of the models, because of the restricted width of wind-tunnels and of the nature of such tests being very costly and time consuming to prepare and execute, especially if variations of the initial configuration need to be tested.

Linear-mode models are widely used to test specific sections of the structure under wind forces. The most usual section of cable bridges, which is extensively tested is the deck. Linear-mode models are geometric copies of the complete prototype, but rigid, mounted on gimbals to allow linear bending displacements (Fig.11).

They reproduce the elastic as well as aerodynamic properties of a section of the deck. However they are less complicated to construct, than full span models. They can also reproduce the first few natural frequencies of the structure and are used in the testing of several configurations of cross sections [5] and experimentation with aerodynamic stabilizers which can improve the behaviour of the bridge in wind [Long Creek bridge].

Another type of wind tunnel test is carried out on sectional models (Fig.12). They are geometric copies of a typical length of the original substructure, usually deck section, and reproduce its elastic properties by supporting the models on springs that represent the stiffness properties. They are commonly used for initial research models and are expected to supply some general information for the aerodynamic characteristics of the specific section and in particular here the cross section of the deck.

However these tests are 2D assuming the whole deck oscillates in phase along the span, which may not be true, since in real 3D conditions, displacements may vary from position to position along the span. These give rise to different wind forces and effectively lead to more complicated motion patterns than the 2D modelling can reproduce.

2.5 Empirical approach

Different approaches have been used in the past, concentrating on different aspects of the structure. The majority of studies were focused on the deck cross section, the aerodynamic aspects and vertical and torsional stiffness properties. The use of flat H plate girder section (Fig.13) was abandoned after the disaster of Tacoma Narrows bridge. Testing of different 'faired' cross sections was carried out in order to form a qualitative opinion on which section shapes were appropriate to be used in future designs [6]. Aerodynamic devices were tested, aiming to reduce the vertical vibrations of decks [8],[10] in order to establish some reference for following designers. A mono-cable bridge was designed, showing increased torsional stability in high wind speeds, postponing the onset of flutter [16]. Damping ratios of existing bridges were measured [19]. Closed box sections were introduced, providing low drag and lift forces and also high torsional stiffness. Side fairings helping in keeping the air-flow attached to the deck [10], and openings on the upper and lower surfaces, have shown to be necessary for bridges located in very high windspeed sites [12].

2.6 Equations of aerodynamic forces.

The main research on aerodynamic forces was introduced by Theodorsen and much work has been based on his analytical equations [13]. Later on, experimental results were published by Smith, Selberg and others [40], [41].

Theodorsen equations are based on the assumption that in a wind stream, a very thin flat plate is suspended, having only two degrees of freedom: one vertical and one torsional as shown in (Fig.14). This is true for the deck of a cable suspended bridge. The other assumption is that the air-flow is 2D and that the bridge oscillates in both vertical and torsional dof in a common frequency. The latter implies the deck is long enough in order to be free of any influence of end conditions and also that it moves as a rigid body. The length of the bridge is adequate to support the former assumption, but the deck does not necessarily oscillate as a rigid body. Concluding, these equations cannot be applied directly to the whole of the bridge, without considerable error. It should also be mentioned that air force expressions were derived for small amplitude harmonic oscillations, so they apply solely to a narrow band of transition from stable to unstable conditions. The rest of the resulting forces, out of these narrow bands of application have only qualitative value, and should be handled with extreme precaution. However this fact is not considered

restrictive, since our aim is to locate this narrow band and work in that space.

The explicit form of Theodorsen aerodynamic expressions calculate the wind forces, lift forces and moments which apply on an oscillating flat plate section.

$$L_h = -S\pi\rho b^2 (V\dot{\theta} + \ddot{y}) - 2S\pi\rho b VC(k) \left[V\theta + \dot{y} + \frac{b}{2} \dot{\theta} \right] \quad (1)$$

$$M_\alpha = -S\pi\rho b^2 \left[\frac{Vb}{2} \dot{\theta} + \frac{b^2}{8} \ddot{\theta} \right] + S\pi\rho b^2 VC(k) \left[V\theta + \dot{y} + \frac{b}{2} \dot{\theta} \right]$$

where k = reduced frequency $k = \frac{\omega b}{V}$

b being the half width of the deck,

S = span of section,

$C(k)$ = Theodorsen circulation function = $F(k) + iG(k)$

$F(k)$ and $G(k)$ being expressed in terms of Bessel functions of the first and second kind:

$$F(k) = \frac{J_1(J_1 + Y_0) + Y_1(Y_1 - J_0)}{(J_1 + Y_0)^2 + (Y_1 - J_0)^2} \quad (2)$$

$$G(k) = - \frac{Y_1 Y_0 + J_1 J_0}{(J_1 + Y_0)^2 + (Y_1 - J_0)^2}$$

Bessel functions J_0 , J_1 , Y_0 , Y_1 , are functions of k of the first and second order.

$F(k)$ and $G(k)$ can be plotted against k in (Fig.15).

The motion of the system at flutter speed is assumed to be simple harmonic and undamped, the displacements being expressed:

$$y_0 e^{-i\omega t} = y_0 [\cos(\omega t) + i \sin(\omega t)] \quad (3)$$

$$y = y_0 e^{i\omega t} = y_0 [\cos(\omega t) - i \sin(\omega t)]$$

So finally by substitution :

$$L_h = S\omega \left[\pi \rho b^3 \left[\frac{1}{b} - i \frac{2C(k)}{bk} \right] y - \pi \rho b^3 \left[\frac{i}{k} + \left[\frac{i}{k} + \frac{2}{k^2} \right] C(k) \right] \theta \right] \quad (4)$$

$$M_\alpha = S\omega^2 \left[\pi \rho b^4 \left[\frac{iC(k)}{bk} \right] y - \pi \rho b^4 \left[\frac{i}{2k} + \frac{i}{k^2} \right] C(k) + \left[\frac{1}{b} + \frac{i}{2k} \right] \theta \right]$$

2.7 General equations of motion at flutter.

2.7.1 Equations of motion in a 2 dof system.

In a system with two degrees of freedom and in particular a flat plate with vertical and torsional degrees of motion uncoupled, the equations which describe the motion are as follows:

$$\left. \begin{aligned} m\dot{h} + c_h \dot{h} + k_h h &= A_h + B_h \dot{h} \\ \theta \ddot{\alpha} + c_\alpha \dot{\alpha} + J\alpha &= A_\alpha + B_\alpha \dot{\alpha} \end{aligned} \right|$$

These have been derived from (4) where ^{the} lift force has been transformed to $A_h + B_h \dot{h}$ and aerodynamic moment has been transformed to $A_\alpha + B_\alpha \dot{\alpha}$.

c_h = damping in the vertical motion

c_α = damping in the torsional motion

m = vertical inertia of the system

θ = torsional inertia of the system

k_h = vertical stiffness

J = torsional stiffness

Bringing the right parts to the left side and braking up the aerodynamic forces as factors of displacements velocities and acceleration :

$$\left. \begin{aligned} m\dot{h} + (c_h - B_h)\dot{h} + (k_h - A_h)h &= 0 \\ \theta \ddot{\alpha} + (c_\alpha - B_\alpha)\dot{\alpha} + (J_\alpha - A_\alpha)\alpha &= 0 \end{aligned} \right| \quad (5)$$

For sinusoidal, motion the following solutions can be used:

$$\begin{array}{l} h=h_0 e^{\lambda t}, \dot{h}=\lambda h_0 e^{\lambda t}, \ddot{h}=\lambda^2 h_0 e^{\lambda t} \\ \alpha=\alpha_0 e^{\kappa t}, \dot{\alpha}=\kappa \alpha_0 e^{\kappa t}, \ddot{\alpha}=\kappa^2 \alpha_0 e^{\kappa t} \end{array} \quad \left| \right.$$

Substituting the latter in equation (5) :

$$\begin{array}{l} m\lambda^2 h_0 + (c_h - B_h)\lambda h_0 + (k - A_h)h_0 = 0 \\ \theta\kappa^2 \alpha_0 + (c_\alpha - B_\alpha)\kappa \alpha_0 + (J - A_\alpha)\alpha_0 = 0 \end{array} \quad \left| \right.$$

$$\begin{array}{l} \lambda^2 h_0 + \left[\frac{c_h - B_h}{m} \right] \lambda h_0 + \left[\frac{k - A_h}{m} \right] h_0 = 0 \\ \kappa^2 \alpha_0 + \left[\frac{c_\alpha - B_\alpha}{\theta} \right] \kappa \alpha_0 + \left[\frac{J - A_\alpha}{\theta} \right] \alpha_0 = 0 \end{array} \quad \left| \right.$$

$$\begin{array}{l} \left[\frac{c_h - B_h}{m} \right] \lambda h_0 + \left[\frac{k - A_h}{m} \right] h_0 = -\lambda^2 h_0 \\ \left[\frac{c_\alpha - B_\alpha}{\theta} \right] \kappa \alpha_0 + \left[\frac{J - A_\alpha}{\theta} \right] \alpha_0 = -\kappa^2 \alpha_0 \end{array} \quad \left| \right.$$

In matrix form :

$$\begin{bmatrix} \frac{c_h - B_h}{m} & \frac{k - A_h}{m} & \emptyset & \emptyset \\ 1 & \emptyset & \emptyset & \emptyset \\ \emptyset & \emptyset & \frac{c_\alpha - B_\alpha}{\theta} & \frac{J - A_\alpha}{\theta} \\ \emptyset & \emptyset & \emptyset & \emptyset \end{bmatrix} \begin{bmatrix} \lambda h_0 \\ h_0 \\ \kappa \alpha_0 \\ \alpha_0 \end{bmatrix} =$$

$$= \begin{bmatrix} \lambda & & & \\ & \lambda & & \\ & & \kappa & \\ & & & \kappa \end{bmatrix} \begin{bmatrix} \lambda h_0 \\ h_0 \\ \kappa \alpha_0 \\ \alpha_0 \end{bmatrix}$$

2.7.2 Multi degree of freedom system.

The cable suspended bridge will be modelled with finite elements. Assuming that the inertia properties of each element are concentrated at its nodes, the model of the structure can be reduced from a system of infinite number of masses to one of finite number. Structural damping is assumed to be zero.

Implementing the previous expressions for the wind forces we obtain:

$$M\ddot{X} + KX = A_1(k)\dot{X} + A_2(k)X \quad (6)$$

where :

$M = n \times n$ mass matrix

$K = n \times n$ structural stiffness matrix

$A_1, A_2,$ are $n \times n$ aerodynamic damping and stiffness matrices respectively, derived from the aeroelastic force expressions.

$X = n \times 1$ vector of displacements

When all the prerequisite factors are present and flutter occurs, the oscillation is pure harmonic motion:

$$X = X_0 e^{i\omega t} = X_0 (\cos\omega t + i\sin\omega t) \quad (7)$$

By substitution of (7) in (6) we conclude:

$$-\omega^2 MX + KX = \omega^2 WX \quad (8)$$

here W is a $n \times n$ matrix of the aerodynamic coefficients in (4). Further on we transform (8) in the eigenvalue form:

$$\left[MK^{-1} + WK^{-1} \right] X = \frac{1}{\omega^2} X \quad (9)$$

with solutions $\omega = \mu + i\lambda$. If we substitute these in (7) we obtain damped sinusoidal motion with circular frequency μ and logarithmic damping $-\lambda$.

Therefore we conclude that for a given frequency μ we can find the corresponding critical wind speed which causes flutter:

$$k = \frac{b\mu}{V}, \text{ testing } \mu \text{ and } V \text{ we obtain } k \text{ and } \lambda.$$

When λ equals zero, instability occurs. The lowest value of V for which λ takes negative values is the critical windspeed.

2.8 Flutter instability of Suspension bridges.

The beginning of theoretical work on flutter reaches back to Frazer and Duncan [37] when they published their fundamental paper in 1928. Their topic was the flutter phenomenon of aircraft wings under sharp angles of attack. They formulated the equations of motion using the test functions by Frazer. In 1935, the first major step was taken by Theodorsen [45] and his paper on incompressible flow flutter.

After the 1940 first Tacoma Narrows bridge collapse, the engineering world involved in bridge designs became interested in aerodynamic effects and aeroelastic interaction, [17]. Bleich [28] in 1948 published his work, applying the flutter theory for airfoils in the designing of the second Tacoma Narrows bridge.

Experimental work continued and in 1966 Sir Gilbert Roberts [47] first introduced the "closed box" deck

section with fairings in the Severn bridge (Fig.16), which was the first bridge built with a deck shaped so similar to an airfoil. The new shape being adopted by most engineers in their later structures, confirms the appropriateness of the thin plate flutter theory.

During the next twenty years, all cable suspended bridges with long spans were tested in wind tunnels in order to prevent aerodynamic instabilities.

In 1961, Selberg established a simple formula, which takes into account all the significant factors of the inertial and elastic properties of the bridge and produces a critical flutter windspeed, which can estimate fairly well the critical windspeed region for a given bridge configuration, [40]:

$$V_f = 0.88\omega_t \sqrt{\frac{\sqrt{\nu}}{\mu} \left[1 - \left(\frac{\omega_v}{\omega_t} \right)^2 \right]} \quad (10)$$

where $\nu = \frac{2r^2}{b^2}$, $\mu = \frac{2\pi\rho b^2}{m}$

ω_v = 1st vertical natural frequency

ω_t = 1st torsional ,, ,,

r = mass radius of gyration

ρ = density of air

m = 1/2 mass of bridge cross section / unit length

Later, Chaudhury and Brotton working on numerical methods, presented in 1966 their work, based on Theodorsen's aerodynamic force equations and on the same lines as Bleich, tackling also the partly built construction stages in a complete investigation of all the situations which can appear in the building process.

Wardlaw also worked in the same direction, [5], concluding the advantages of faired shaped sections in aerodynamic stability.

Another aspect of the shape investigation was covered by Ishiro Konishi et al [8] and Masara Matsumoto [48]. They experimented with the shapes of the kerbs and also attachments to them (Fig.17) in order to avoid the separation of the boundary layer and the generation of vortices from the leading edge. Their experiments with various fairing configurations revealed the influence of such stabilizers in the behaviour of the deck in high windspeeds and in air-flow inclined to the horizontal level. Some configurations showed a considerable reduction of vertical amplitudes of the deck.

A very daring step was taken by Leonhardt, [16]. His work on mono-cable suspended bridges, (Fig.18), is still unique. The deck is suspended by a single cable and forms a triangle with the hangers and the very thin and streamlined deck. Experiments with this type of bridge showed very good aerodynamic behaviour in high wind speeds. However the experimental study showed a tendency of some hangers to go slack, under heavy partial loading.

Because of that and in combination with the novelty of the design such a design has never been constructed.

In 1976 another major step in numerical approach was taken by Iwegbue in [13], who introduced the time step method in order to solve the static equilibrium position and forces, the dynamic response and to enable the evaluation of the flutter windspeed of a given bridge. He also included erection stages of the structure. However it must be commented that in his work he used the half span and the one cable only, exploiting the symmetry of the structure and reducing the high computational cost.

Finally mention should be made of the findings of the project undertaken by Simpson et al., for Tsing-Ma bridge in Hong-Kong [12], [23]. The region is often subjected to typhoon windspeeds. Experimental study in wind tunnels clearly indicated the limitations of the closed-box faired sections. They showed a tendency for coupled oscillations vertical and in torsion leading to classical flutter, in high windspeeds, which can be postponed if some gaps are left on the upper and lower surfaces of the deck, (Fig.19). These give rise to some oscillations, caused by vortex shedding, of somewhat minor importance, while guarantee stability, at a windspeed region where closed box sections would have been oscillating with flutter instability. The final design included a double carriageway on the upper deck, with a narrow gap in the middle, between the two directions and a lower deck with a single carriageway with a railway line each side of it (Fig.20). Between the

rails and the road lanes a narrow gap was introduced at each side. This configuration provides protection to the inner traffic even at high windspeeds which exploits to a larger extent the carrying surfaces of the deck. This design was based in the previous experience of gains in stability for truss stiffened decks with perforations at their upper surface.

In 1981, Agar [49] published his work on the implementation in a program called ANSUSP of all the previously expressed ideas by Iwegbue [21],[31] et al. In this package alternative methods can be used for analysing flutter behaviour of suspension bridges.

The assumption that the deck is a thin flat plate, enables the use of Theodorsen circulation functions, for the wind forces. Alternatively, experimental coefficients can be used in order to find the aerodynamic forces, applied on the structure.

Using the modal analysis we calculate the natural frequencies of the structure. The wind forces are assumed to be linear functions of displacements and their derivatives, allowing the formulation of an eigenvalue eigenvector problem. The results are the contribution of each mode in the final oscillations and the amount of damping of each mode. Here we neglect the non-linearities involved in the wind forces expressions and in the restoring forces.

When a satisfactory configuration is found, the time step method can be used to provide more accurate

information on what is happening to the structure, its flutter behaviour and even the stress history of the elements.

The advantage of this program is that it can provide an estimate of the influence of all the elements that don't usually take part in the sectional experimental tests which are the most commonly used ones, for example investigations of the influence of the distance between the cables, the sag of the cables, the different configurations of the connections between the deck and the towers, etc.

At a final stage, analysis of the behaviour for the incomplete structure in various erection stages, can be carried out to detect any unsafe conditions which need to be addressed.

Some comments on the characteristics of the different computational techniques will follow.

When the deck is represented by one element of its deck, the method is two dimensional (Fig.21). This model assumes that the whole length of the deck oscillates in the same manner as one rigid section with two degrees of freedom and with the same amplitude in vertical displacement and torsional displacement. However when the whole structure is subjected to wind, there is no reason to assume that the vertical displacements and torsional displacements will be constant along the span. In fact the boundary conditions at the ends of the span preclude this. Models that really fulfil all these requirements are 3D models. They represent more accurately the real

behaviour of the bridge, taking into account the adjacent bridge elements and the different wind force values, across the span, due to different displacements. The interaction of motion between the main span and the side spans is also included.

Of course the computational cost of the time history analysis of a 3-D model is much larger, but the rewards may well be significant. The 3D modelling is preferable and highly recommended for the specific type of study and since it can be handled by the computational efficiency of modern computers, it should be used.

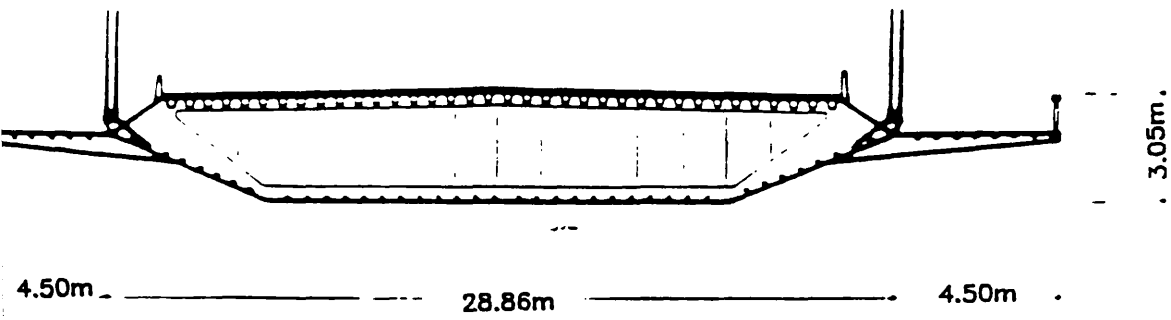


(Fig. 4) Cross section of Severn bridge.

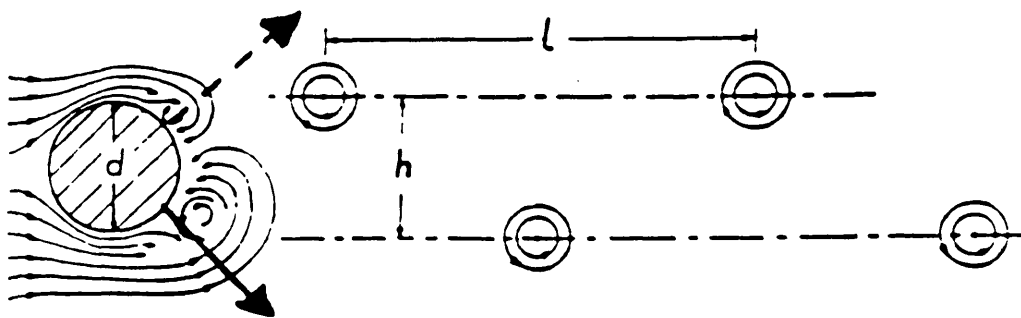


(Fig. 5) Vortex formation in a wind flow behind a circular obstacle.

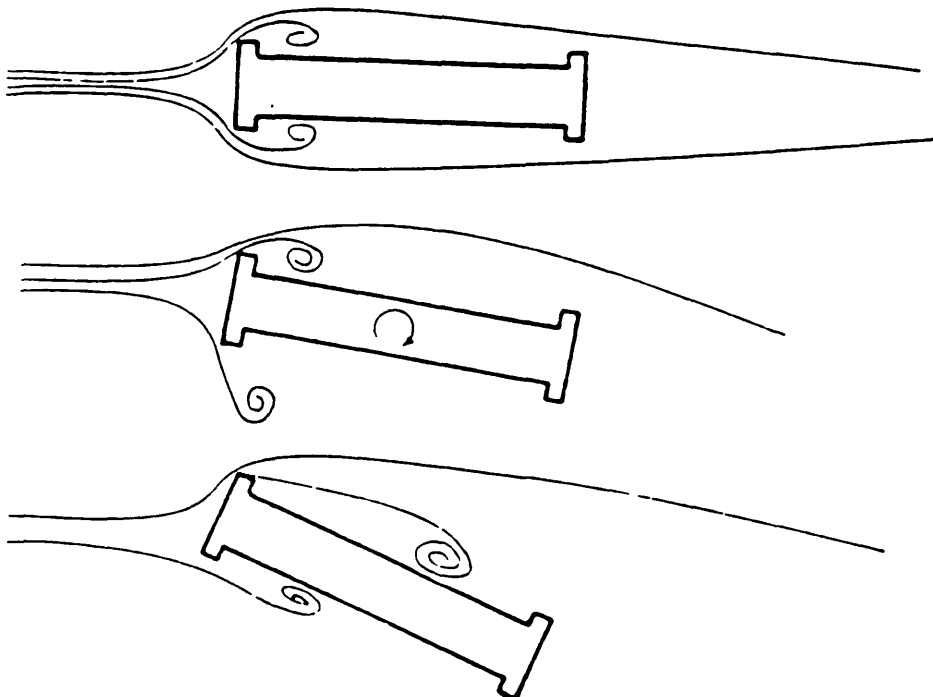


(Fig. 6) Flow pattern around a section similar to the First Tacoma Narrows cross section.

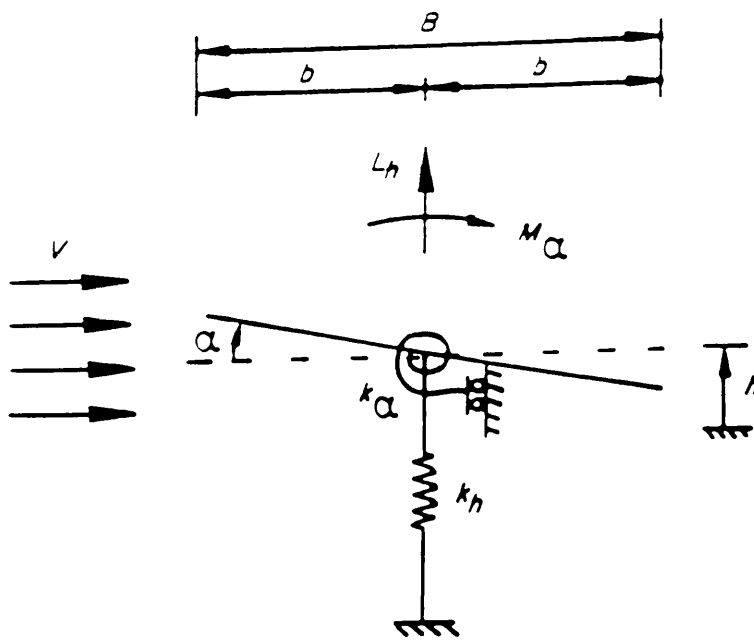


(Fig. 7) Thin flat plate aerofoil subjected to wind flow.

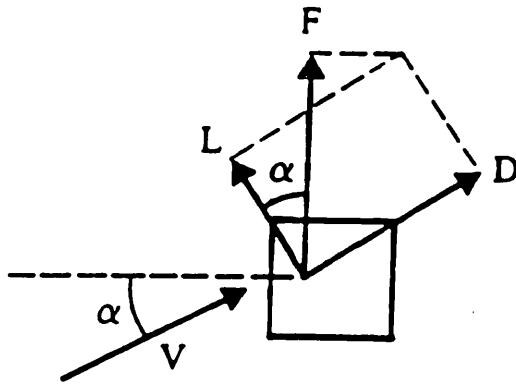


(Fig. 8) Model of a rectangular cross section subjected to wind flow producing galloping.

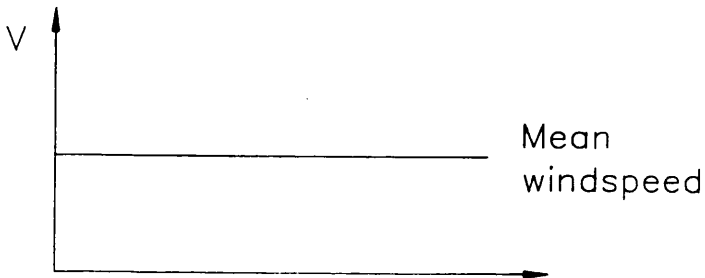
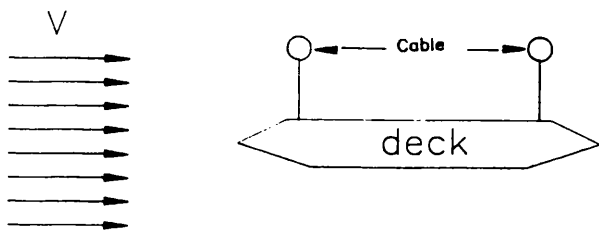
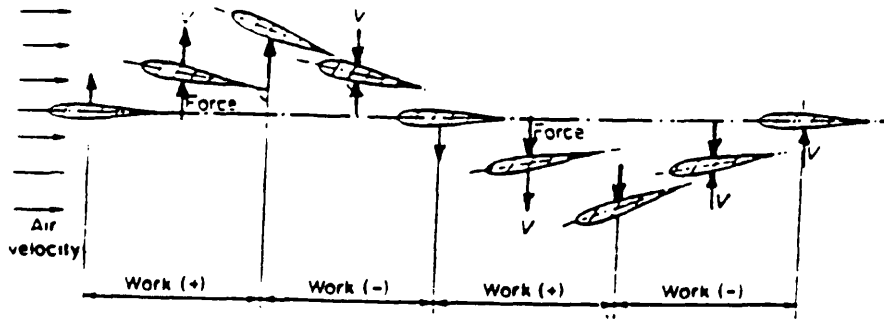
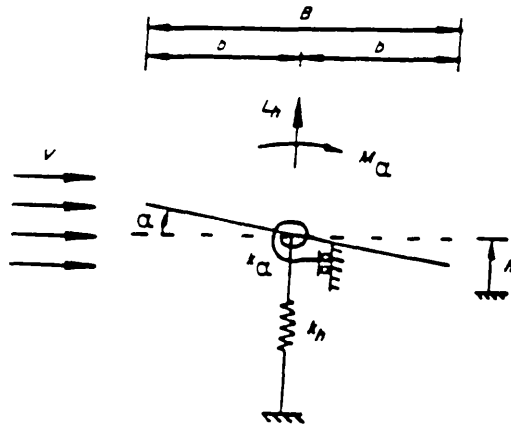
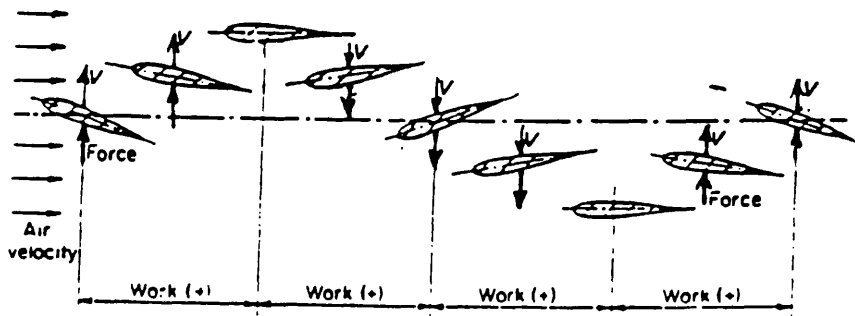


(Fig. 9) Variation of wind speed due to natural turbulence in atmospheric wind.



Vibrations in Phase : net work input : 0



Phase Difference 90° : net work input : +ve

(Fig. 10) Idealization of classical flutter effects on a thin aerofoil with 2 degrees of freedom subjected to wind-flow.

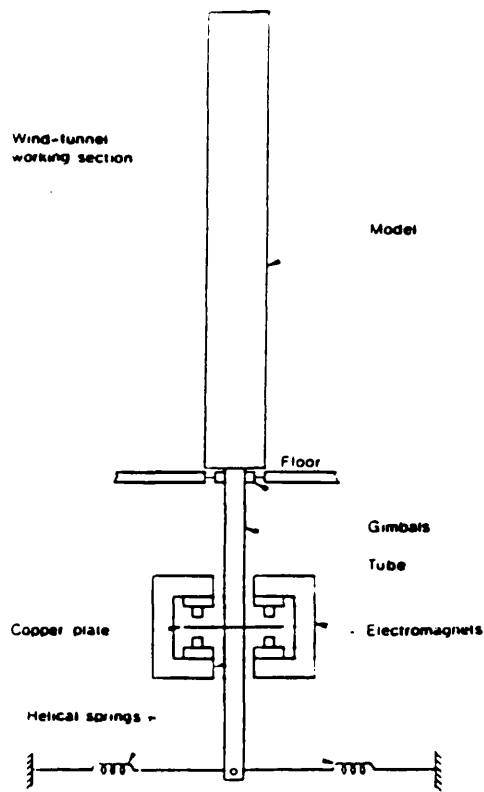


(Fig. 11) Linear mode models used in wind tunnel tests.[6]

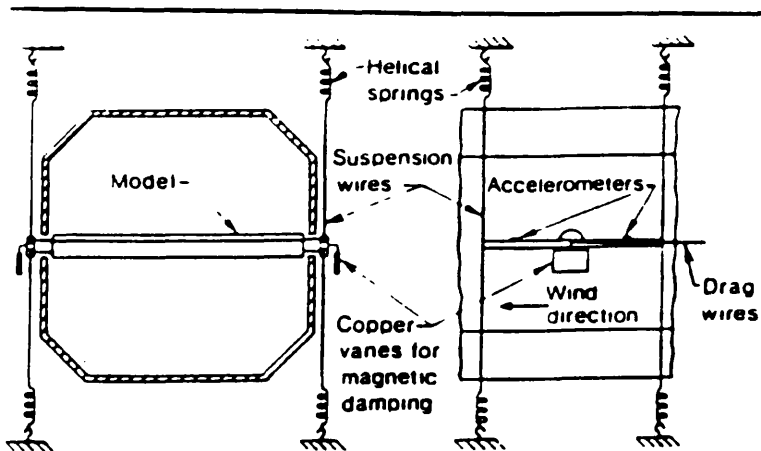


(Fig. 12) Sectional models used in wind tunnels tests.[6]

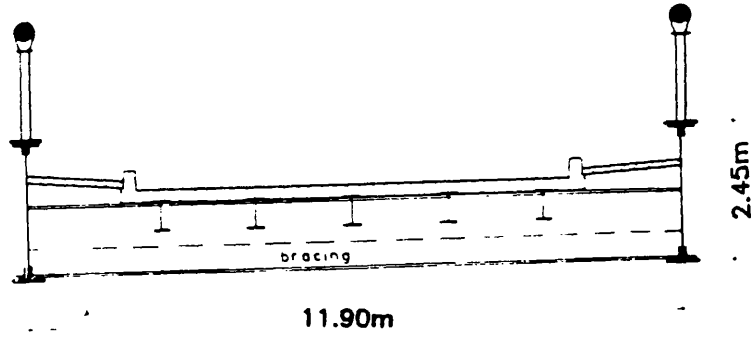


(Fig.13) Cross section of First Tacoma Narrows bridge.

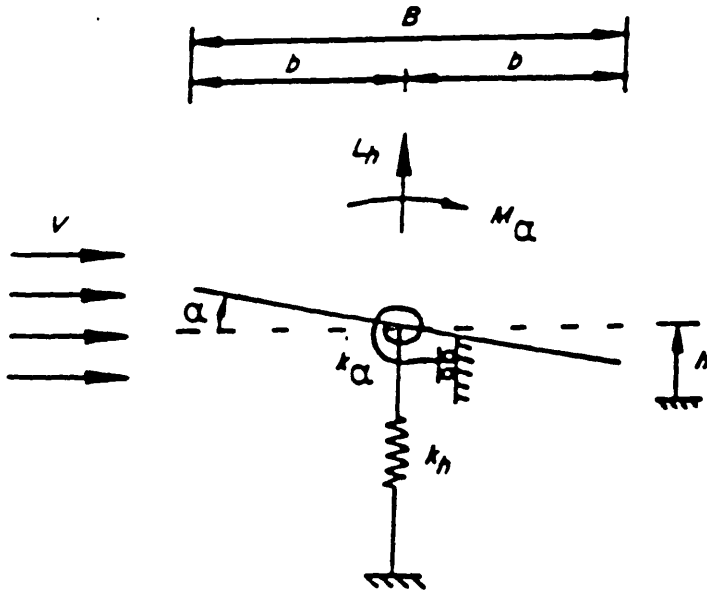


(Fig. 14) Simplified 2 degree of freedom model of a thin plate subjected to air-flow.

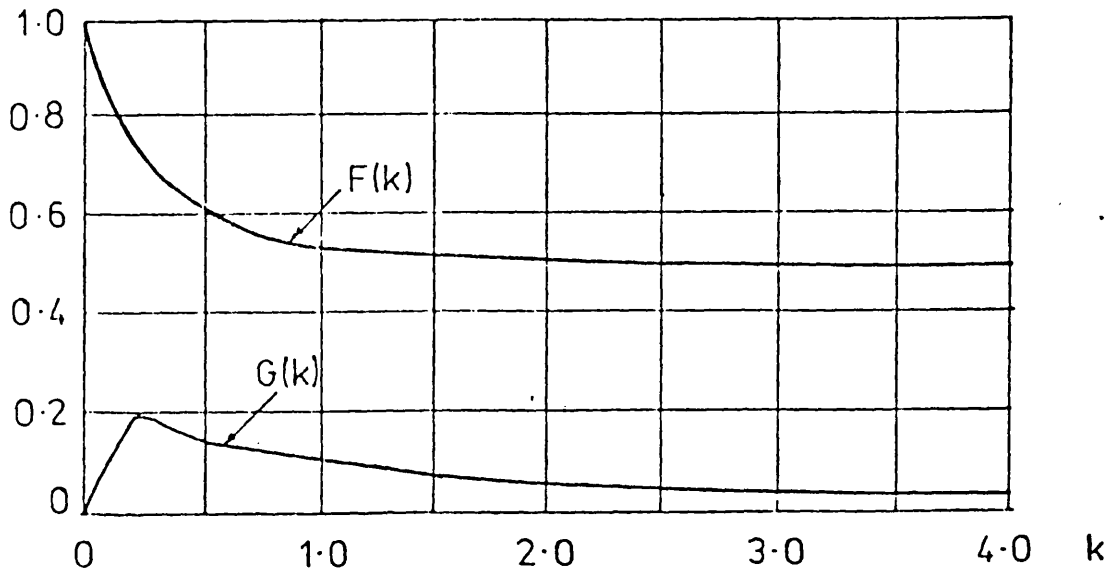


(Fig. 15) Curve of $F(k)$ and $G(k)$ versus k where k is reduced frequency.

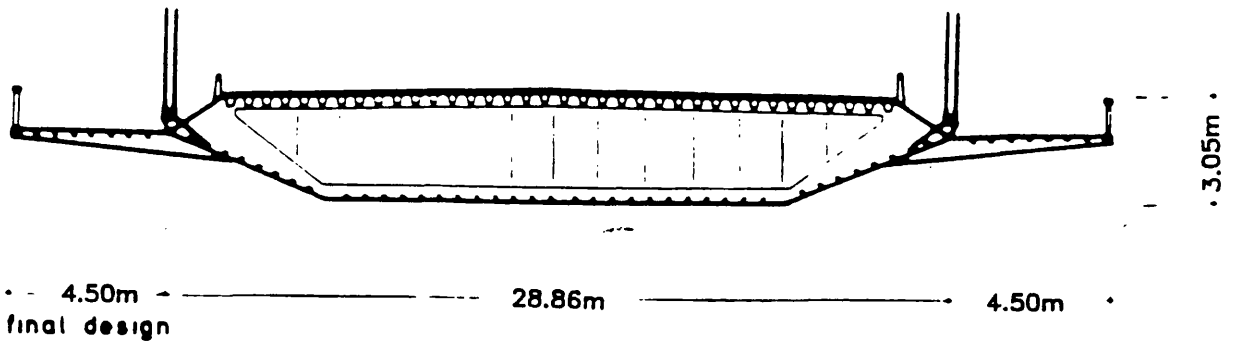


(Fig. 16) Cross section of Severn bridge.

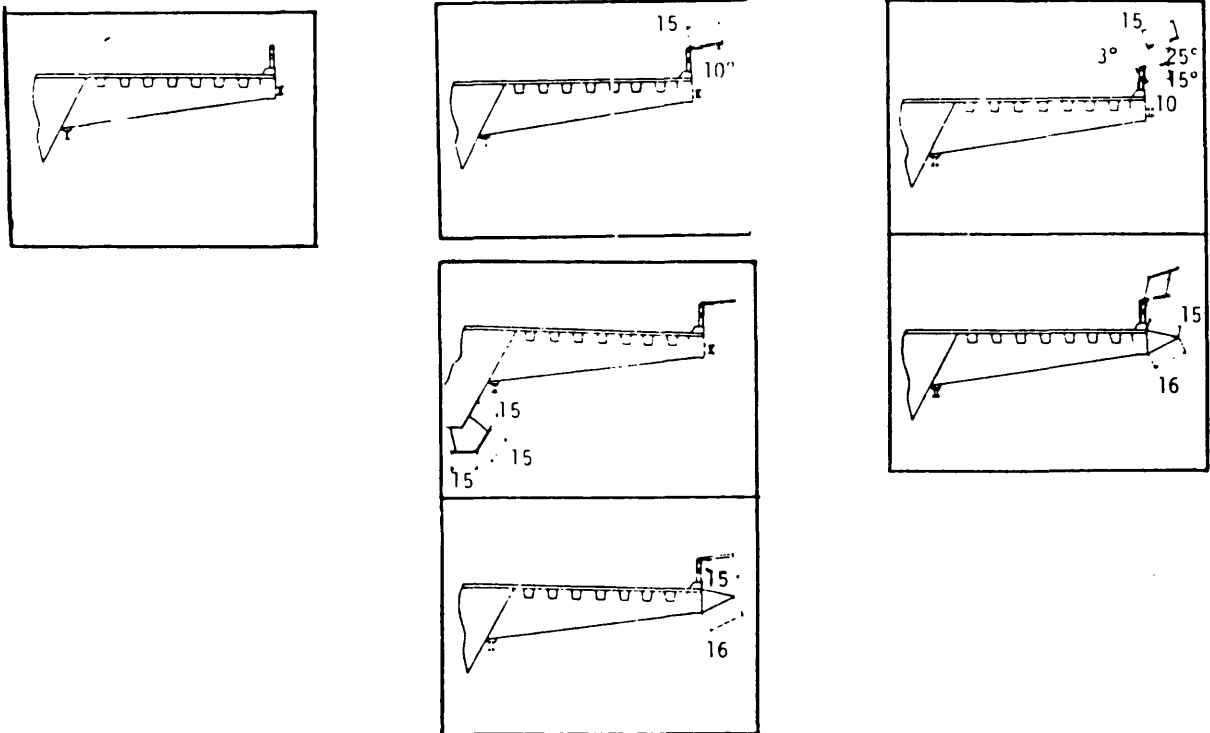


(Fig. 17) Stabilizers at the outer edges of a bridge cross section. [8]

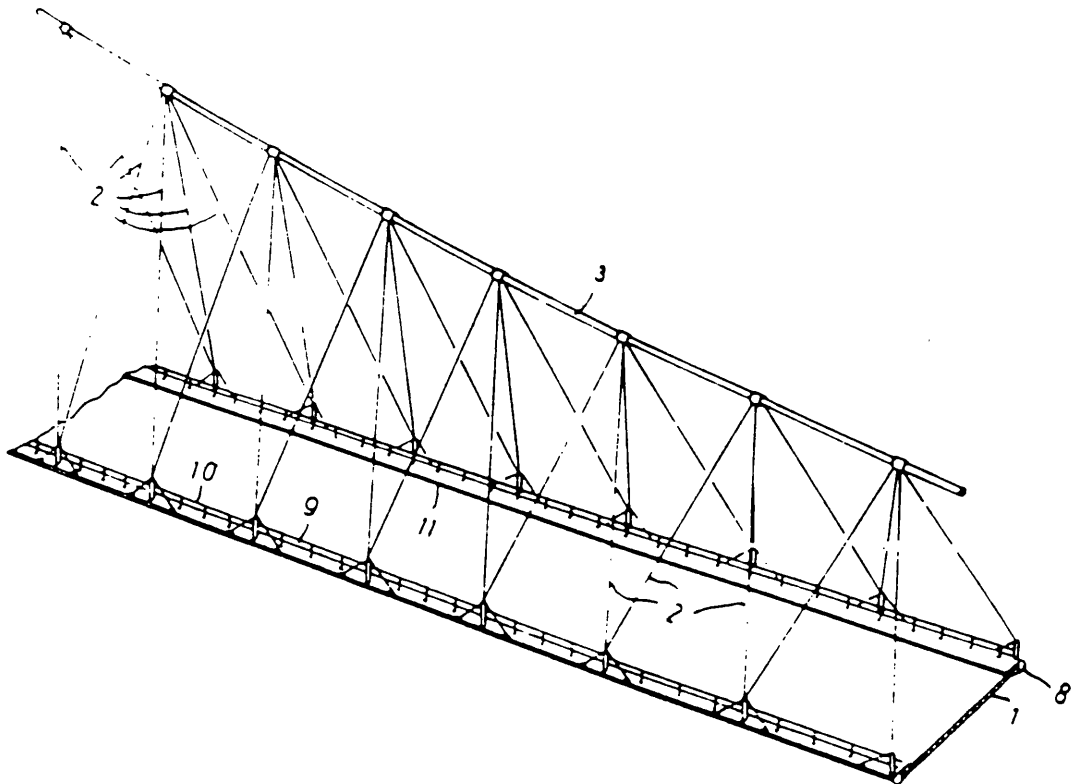
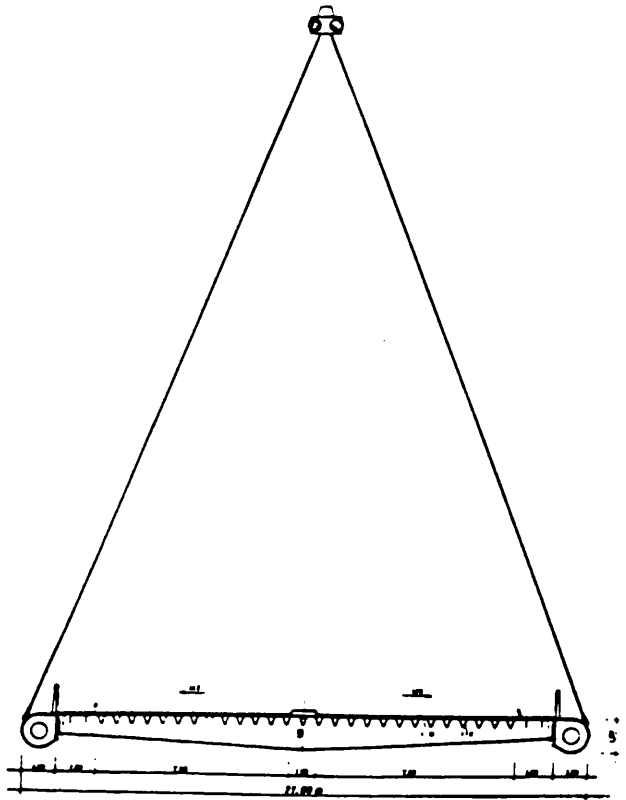
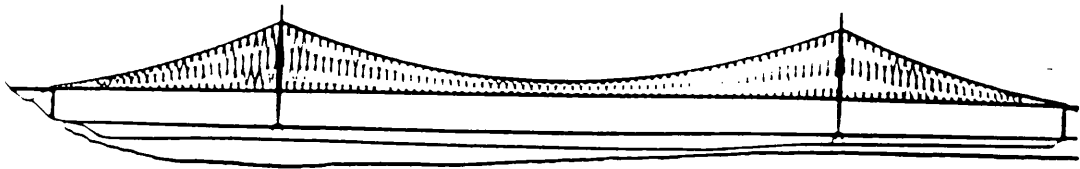


(Fig. 18) Monocable suspension bridge design proposals by Leonhardt. [16]

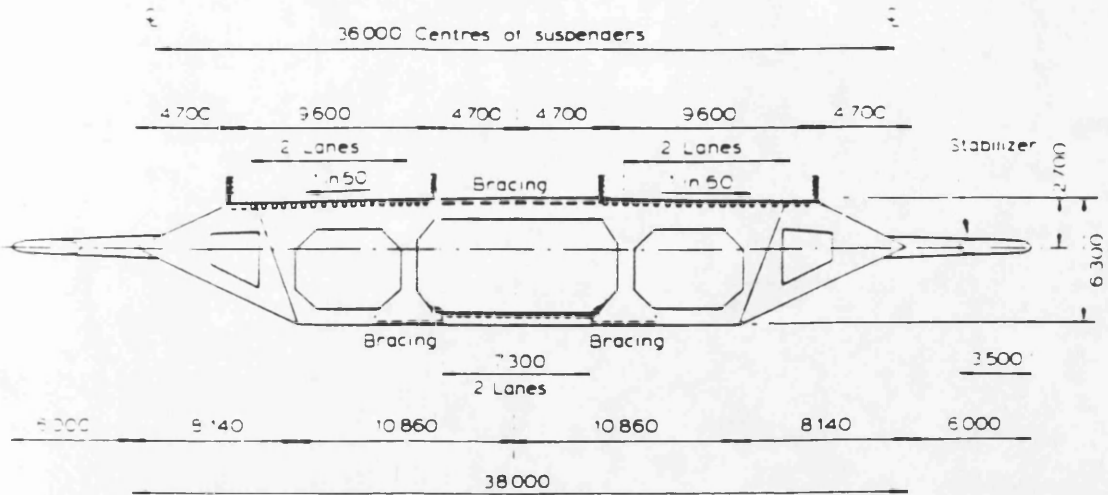


(Fig. 19) Preliminary design of Tsing-Ma cross section. [23]

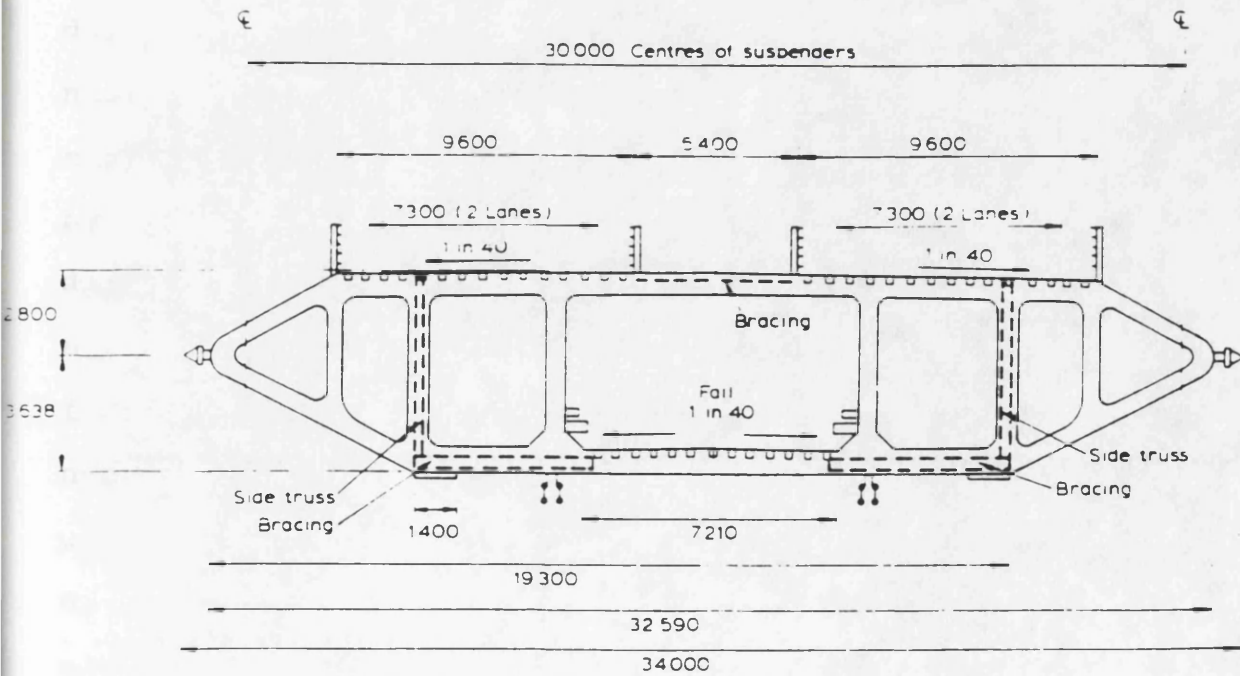


(Fig. 20) Final configuration of design of Tsing-Ma cross section. [23]

Chapter 3

3.1 The Computer Program 'A N S U S P'

The present project is based on the use of a program able to perform both the modal analysis and the time history method.

The numerical dynamic analysis solves the differential equations of motion for the modelled structure (Fig.22), where the inertial properties of the members are assumed to be concentrated at discrete points on the geometry of the structure. These lumped masses are assumed to be connected by members without mass, which have elastic properties reflecting the stiffness of the original structural elements. This discretization helps to reduce the infinitely large number of degrees of freedom of the prototype to a finite number and enables the handling of the dynamic analysis by the solution of a system of simultaneous ordinary differential equations. The number of these simultaneous equations is equal to the number of degrees of freedom of the model, the lumped masses being on the nodes of the FEM model. Alternatively, more nodes can be used as for example higher order elements or finer discretization, in order to increase accuracy if higher modes of oscillation are considered, in which case the mass distribution may have a substantial influence.

After the discretization of the structure, we proceed to the formation of the equations of motion:

$$M\ddot{U} + C\dot{U} + KU = P \quad (11)$$

M = diagonal matrix containing the mass attributed to each D.O.F.

C = diagonal damping matrix of structural damping

K = structural stiffness matrix

P = vector of forces at the nodes

U = square symmetric matrix of nodal displacements.

3.2 3-D modelling

When the whole structure is subjected to wind and all influences between the members of the structure are considered, a three-dimensional model is used. The aerodynamic equations which are used in the present analysis are derived for a thin flat plate and can be applied only approximately to faired closed box sections with a good degree of accuracy. These formulae (1) hold only at the region of windspeeds where the coupling between the vertical and torsional oscillation occurs producing an oscillation at a common frequency.

A bridge with a flat-plate deck is subjected to a smooth horizontal air-flow. The deck can oscillate in vertical and torsional motion. The first vertical and torsional mode shapes are plotted in (Fig.23). When the

two oscillations are coupled, their mode shapes and their frequencies are common; under these conditions the forces acting on the deck are lift L_h and moment M_α , while the common frequency of oscillation is ω . The expressions of the aerodynamic forces per unit length are given by the following expressions:

$$L_h = S\omega^2 \left[\pi\rho b^3 \left[\frac{1}{b} - i\frac{2C(k)}{bk} \right] y - \pi\rho b^3 \left[\frac{i}{k} + \left[\frac{i}{k} + \frac{2}{k^2} \right] C(k) \right] \right] \quad (12)$$

$$M_\alpha = S\omega^2 \left[\pi\rho b^4 \left[\frac{iC(k)}{bk} \right] y + \pi\rho b^4 \left[\left[\frac{i}{2k} + \frac{i}{k^2} \right] C(k) + \left[\frac{1}{b} - \frac{i}{2k} \right] \right] \right]$$

where $k =$ reduced frequency $\frac{\omega b}{V}$

b = the half width of the deck (Fig.24),
the bar over a symbol denotes a complex quantity,

S = span of section,

$C(k)$ = Theodorsen circulation function = $F(k) + iG(k)$

$F(k)$ and $G(k)$ being expressed in terms of

Bessel functions of the first and

second kind:

$$F(k) = \frac{J_1(J_1 + Y_0) + Y_1(Y_1 - J_0)}{(J_1 + Y_0)^2 + (Y_1 - J_0)^2} \quad (13)$$

$$G(k) = - \frac{Y_1 Y_0 + J_1 J_0}{(J_1 + Y_0)^2 + (Y_1 - J_0)^2}$$

In the previous formulae J_0 , J_1 and Y_0 , Y_1 are Bessel circulation functions of the first and second kind respectively.

An alternative way could also be used if the deck section differs considerably from the flat plate section, [51], [52], [53].

The following expressions are based on experimentally extracted parameters which describe the aerodynamic behaviour of the particular deck sections:

$$L_h = \frac{1}{2} \rho V^2 (2B) \left[KH_1^* \frac{\dot{h}}{V} + KH_2^* \frac{b\dot{\alpha}}{V} + K^2 H_3^* \alpha \right] \quad (14)$$

$$M_\alpha = \frac{1}{2} \rho V^2 (2B^2) \left[KA_1^* \frac{\dot{h}}{V} + KA_2^* \frac{b\dot{\alpha}}{V} + K^2 A_3^* \alpha \right]$$

where H_i^* , A_i^* are functions of $K = \frac{\omega B}{V}$

B = full aerodynamic width of the deck.

These expressions for lift and moment depend linearly on the displacements and velocities in each degree of freedom and according to Scanlan and Tomko, [18], they were proved to hold for small displacements.

3.3 Structural model

In the ANSUSP program, a suspension bridge is idealized as a three dimensional structure (Fig.22), based on the two dimensional modelling by Iwegbue et al [21].

The two cables are represented by parabolic curves, spanning between the tops of the towers, capable of carrying only tensile forces and modelled by bar elements.

The hangers are suspended vertically from the cable nodes, capable of carrying only tensile forces and are represented by bar elements. Their lower ends are connected to horizontal rigid arms, extending transversely from the centreline of the deck.

The deck is modelled by simple beam elements, with bending stiffness in both vertical and lateral directions and also torsional stiffness. They are positioned in the centreline of the original deck and carry their own dead load. They are connected to the hangers with horizontal rigid arms ($EI=\infty$), at the joints.

Each tower is idealized by one beam element, vertically positioned and fixed at their foundations;

their tops are connected to the two cables with horizontal rigid arms. The towers provide bending stiffness in both longitudinal and lateral directions to the bridge and also torsional stiffness. Second order phenomena are not included.

In the original structure, the degrees of freedom of the nodes are generally as follows (Fig.24):

The cable nodes, have the ability to move longitudinally, vertically and laterally.

The deck nodes can move vertically, laterally and torsionally.

The tower top nodes can move longitudinally, laterally and torsionally.

However, since the flutter phenomenon involves predominantly vertical and torsional deck motions, the lateral displacements of the bridge nodes are not considered to be significant and will be ignored in any further discussion.

The elements' inertia is always represented by lumped masses at the nodes, enabling the solution of equation (11) for \ddot{U} since M is diagonal.

In ANSUSP the basic geometry characteristics are given as the cable sag, the tower height, the deck shape (straight or circular curve) and the span lengths. Also the cross section areas of different elements, their moment of inertia and their Young modulus and material densities.

The operation of ANSUSP initiates with the mesh generator forming the dead load geometry of the structure and its mass matrix.

For the dead load geometry, the cable deforms under the self weight. When the cable and hanger forces are calculated, they are applied to the undeformed structure as internal forces. Equilibrium has to be restored before the cable and the deck resume their final dead load geometry.

The next step is to find the natural modes of the structure.

$$M\ddot{U} + C\dot{U} + KU = 0 \quad (15)$$

$C = 0$ because of the uncertainties in the damping factor:

$$\begin{aligned} \text{Substituting for : } U &= e^{sx}, \quad \dot{U} = se^{sx}, \quad \ddot{U} = s^2 e^{sx} \\ \underline{M}s^2 e^{sx} + \underline{K}e^{sx} &= 0 \Rightarrow (\underline{M}s^2) e^{sx} = (-\underline{K})e^{sx} \Rightarrow \quad (16) \\ s^2 &= -\underline{M}^{-1} \underline{K} \end{aligned}$$

where \underline{M} and \underline{K} are matrices and U vector

This is the usual eigenvalue problem.

The eigenvalues are complex quantities representing the natural frequencies (imaginary part) and the logarithmic damping (real part) of the system, while the eigenvectors enable us to describe the mode shapes as symmetric or antisymmetric, torsional or vertical.

The great importance of the natural frequencies cannot be over-emphasized since they give basic information on the behaviour of the structure revealing the tendency of the configuration to inflict instability in symmetric or antisymmetric motion, in lower or higher windspeeds.

Since flutter instability involves coupling of vertical and torsional modes of oscillation, it is essential to know how close are natural frequencies of similar mode shapes (torsional and vertical, both symmetric or antisymmetric).

From this point on, we will follow explicitly the procedure of solving the dynamic equations of motion with the modal analysis and the Newmark- β time-history methods.

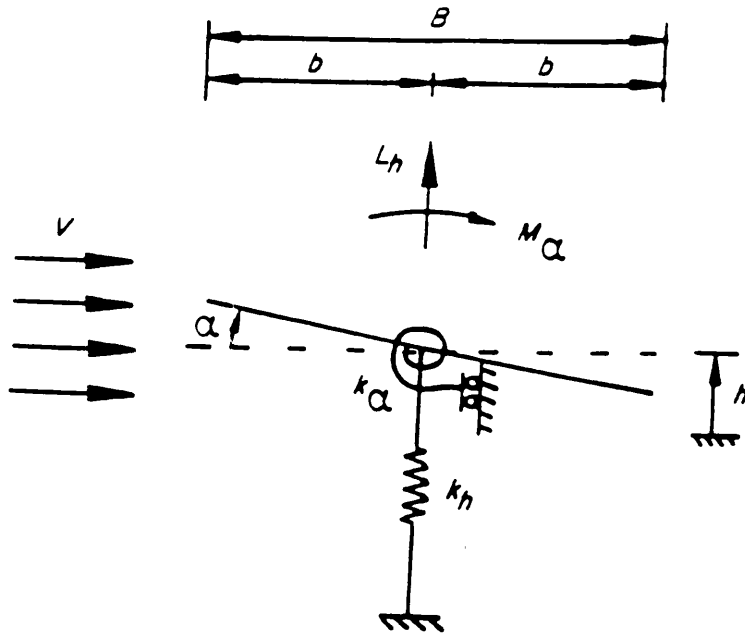


(Fig. 21) Simplified 2 degree of freedom model of a thin plate subjected to air-flow.

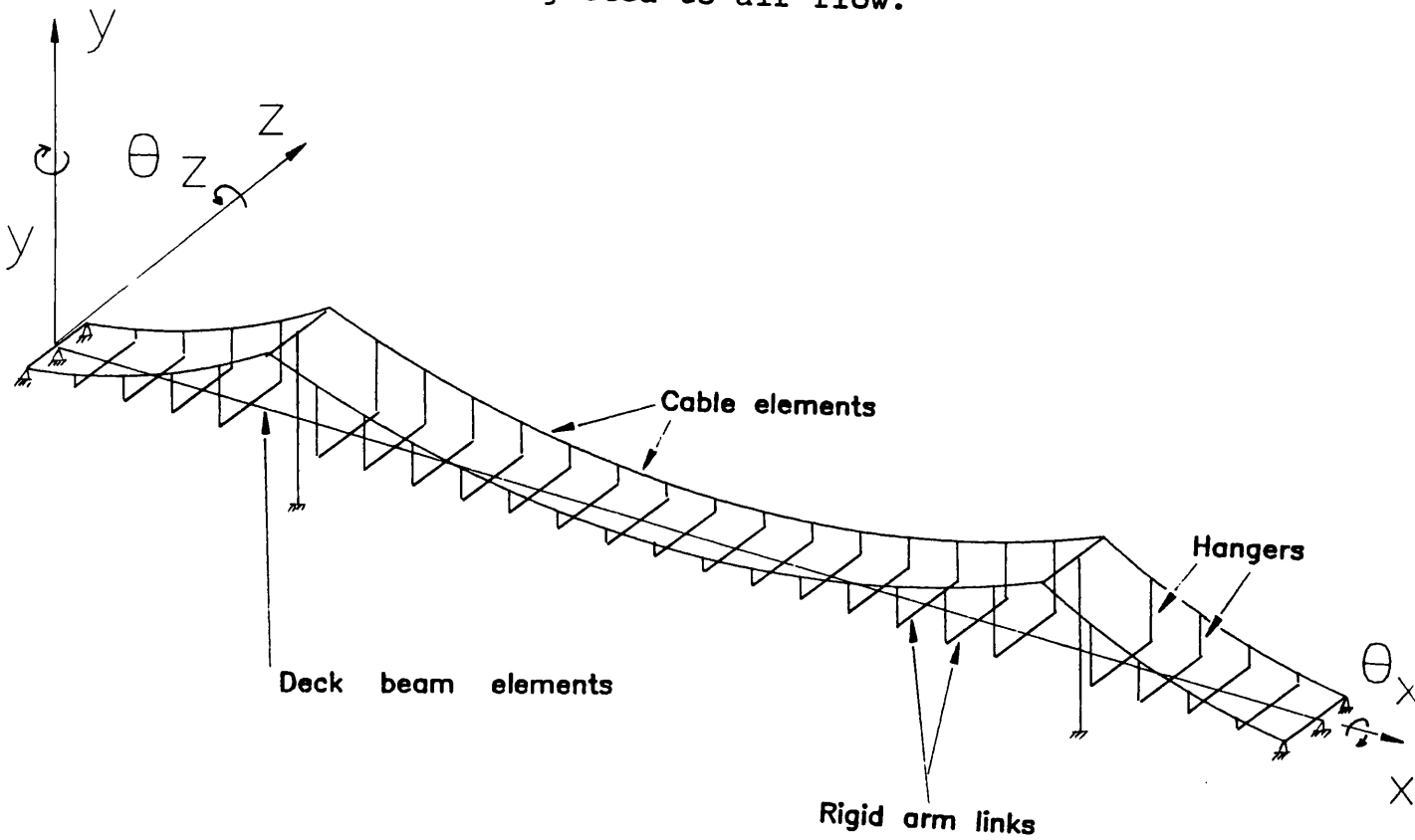


(Fig. 22) Suspension bridge idealization by ANSUSP.

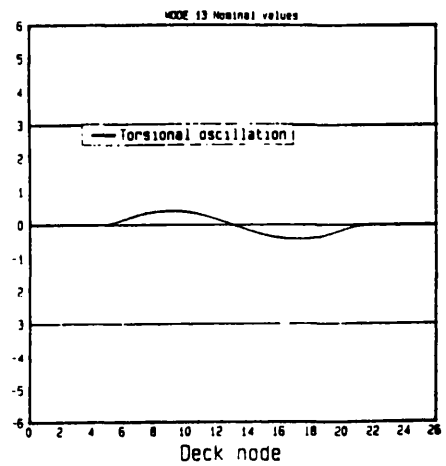
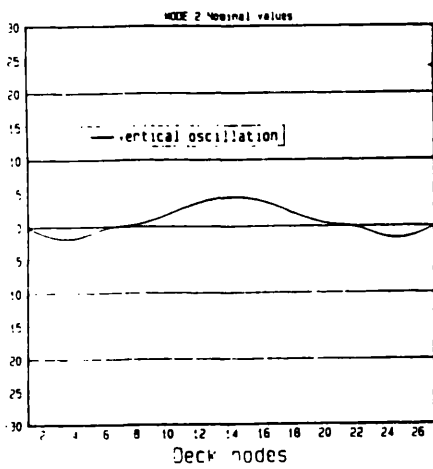
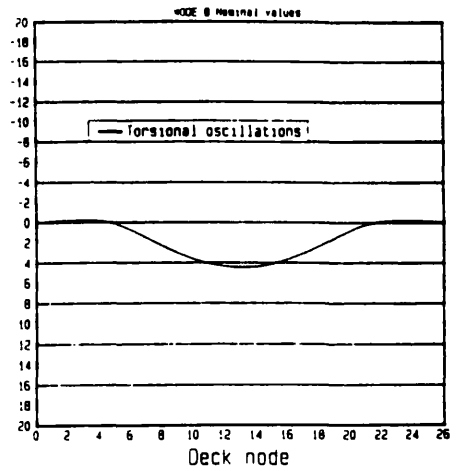
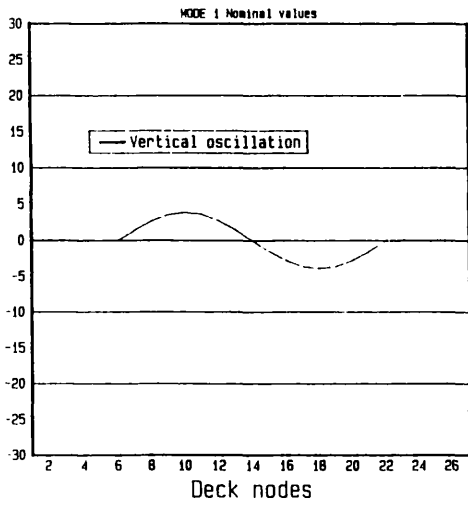


(Fig. 23) First two vertical and first two torsional mode shapes by ANSUSP for Severn nominal values.

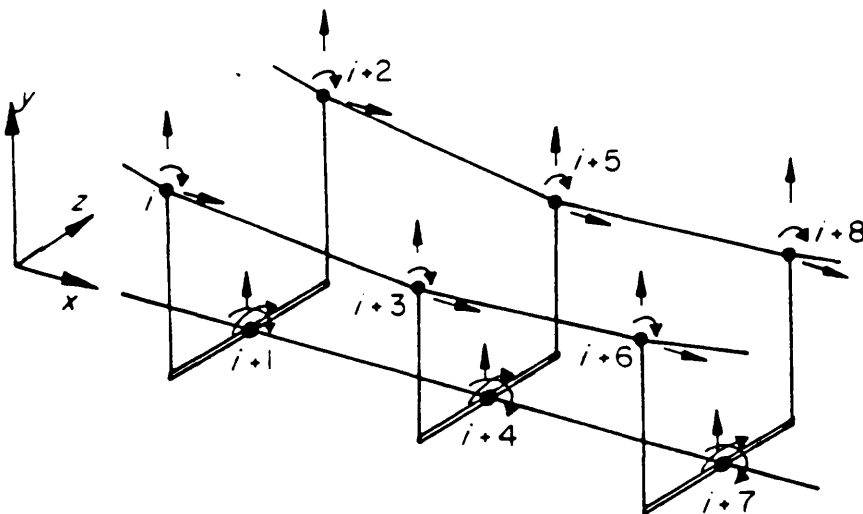


(Fig. 24) Degrees of freedom of the joints of a cable suspended bridge.

Chapter 4

4.1 Modal flutter analysis

This method is based on the following assumptions:

a) The wind forces acting at the deck near flutter windspeeds can be expressed as factors directly related by coefficients to deck displacements and velocities as in equation (1). These coefficients also depend however on the frequency of vibration through the coefficient

$$K = \frac{\omega b}{V}$$

b) The structure has a linear force-displacement behaviour which is true only for small displacements. The effect of large deflections causing geometrically non-linear effects is ignored.

c) The oscillation of the structure in the region of flutter occurring is assumed to be a composition of a number of the lower natural mode shapes including vertical modes and torsional modes in a resulting sinusoidal motion.

In the following the formulations of forced motion are presented:

$$P_{aero} = AU + B\dot{U} \quad (17)$$

where A and B are common multipliers of displacements and velocities, arising from the expressions for the wind forces, P_{aero} .

We now transform the initial equations:

$$M\ddot{U} + C\dot{U} + KU = P_{aero} = AU + B\dot{U} \Rightarrow \quad (18)$$

Substituting for: $U = e^{\lambda x}$, $\dot{U} = \lambda e^{\lambda x}$, $\ddot{U} = \lambda^2 e^{\lambda x}$

$$M\lambda^2 e^{\lambda x} + (C-B)\lambda e^{\lambda x} + (K-A)e^{\lambda x} = 0 \Rightarrow \quad (19)$$

$$\Rightarrow \lambda^2 e^{\lambda x} + M^{-1}(C-B)\lambda e^{\lambda x} + M^{-1}(K-A)e^{\lambda x} = 0 \Rightarrow$$

$$\Rightarrow e^{\lambda x} (\lambda^2 + C^*\lambda + K^*) = 0 \Rightarrow$$

$$\begin{bmatrix} -C^* & -K^* \\ I & 0 \end{bmatrix} = \lambda \begin{bmatrix} \lambda X \\ X \end{bmatrix}$$

which is an eigenvalue-eigenvector problem.

The λ are the eigenvalues which in general take complex values and can be written as:

$$\lambda = \mu + i\omega \quad , \quad \lambda = \mu - i\omega$$

The X are the eigenvectors, which also take complex values of the kind:

$$X = p + iq \quad , \quad X = p - iq$$

The response of the system can be written:

$$U = e^{\mu t} [(p+q)\sin\omega t + (q-p)\cos\omega t] \quad (20)$$

The characteristics of the resulting motion at a particular windspeed are obtained by the solution of the previous eigenvalue problem. These characteristics are monitored for increasing windspeeds, until overall damping is assessed as zero or negative.

The condition for dynamic stability is to ensure that the real parts μ of all eigenvalues are negative, since this means that the amplitude of any motion gradually decreases, eventually being damped out.

The flutter windspeed is the lowest windspeed which gives zero or positive value to μ .

However we must note here that since the wind-forces are dependent on the frequency of motion (1), an interactive loop must renew continuously the frequency ω which is used in Theodorsen expressions, until it agrees with one of the imaginary parts of the eigenvalues.

It is not clear though from the beginning which of the response frequency values is going to create instability and which one to use as a value for ω . However it was discovered that following the response frequency with the lowest damping $\mu \rightarrow 0$ is always leading to the flutter windspeed with convergence between ω_{trial} and ω_{result} . A simplified form of ANSUSP named ANSUSP2DE was used at the initial stage of familiarizing with the modal analysis. ANSUSP2DE calculates the response of a flat plate suspended in wind flow with 2 degrees of freedom (Fig.21). Using ANSUSP2DE the frequency of torsional oscillation could be plotted against corresponding damping for increasing windspeeds as shown in (Fig.25.a). When the damping crosses the axis of zero

damping the system oscillates under flutter conditions. The same operation has been followed for the full structure model in (Fig.25.b).

4.2 Time step analysis

This is more time consuming than the previous procedure, [49], having the advantage of being more reliable, because it enhances the versatility to include the geometric non-linearity.

In this method a pattern of initial nodal velocities is applied on the structure at zero time, to set the system in motion. The response is determined for a period of time and the logarithmic damping ratio is calculated. The results including corresponding frequencies are calculated and displacements in vertical and torsional motion can be plotted against time. A simplified version of ANSUSP, the ANSUSP2D was used to calculate the displacements and decay of a 2degree of freedom system. The displacements are plotted in (Fig.26.a,b,c,d). In this figure the smaller amplitude oscillation represents the torsional motion of the system. The diagrams presented in (Fig.26) correspond to windspeeds of 28, 33, 35, and 65m/sec and show the different pattern of oscillations, which is not always sinusoidal when the system oscillates in windspeeds significantly lower from the critical speed (Fig.26.a,b,c). Once the vertical and torsional motion oscillate coupled in a common frequency

(Fig.26d), the oscillation is apparently sinusoidal complying with one of Theodorsen assumptions.

At 65m/sec the 2dof model is almost at flutter motion. The amplitudes are very large and the slight decreasing trend is barely noticeable. Phase difference has not yet reached 90, but is near 130. The period of motion is clearly constant and the oscillation sinusoidal.

The previous procedure can be repeated for increasing windspeeds until the logarithmic damping becomes zero or takes positive values. In this way, the corresponding frequencies and damping can be plotted against windspeed (Fig.27) and critical windspeed can be found.

The nodal displacements and velocities after time Δt has elapsed are calculated with Newmark- β equations:

$$\dot{U}_{t+\Delta t} = \dot{U}_t + (1-\gamma)\Delta t \ddot{U}_t + \gamma \Delta t \ddot{U}_{t+\Delta t} , \quad (21)$$

$$U_{t+\Delta t} = U_t + \Delta t \dot{U}_t + \left[\frac{1}{2} - \beta \right] (\Delta t)^2 \ddot{U}_t + \beta (\Delta t)^2 \ddot{U}_{t+\Delta t}$$

β and γ are free dimensionless parameters of the quadrature.

The accelerations are determined from the equations of motion (18). The values of $\beta=1/6$ and $\gamma=1/2$ are used

here because the accelerations are assumed to vary linearly for every new time interval Δt .

The time step method is described in details in the following (Fig.28) :

i) In order to start the operation of the Newmark- β method we use initial values for displacements and velocities, usually in a pattern similar to the mode shapes. Estimated values for the oscillation frequency of the coupled motion are also necessary.

ii) The initial displacements and velocities are inserted in the aerodynamic equations (18) and nodal accelerations are calculated.

iii) The acceleration is used in special formulae which do not use $\ddot{U}_{t+\Delta t}$ given below:

$$\begin{aligned} \ddot{U}_{t+\Delta t} &= \ddot{U}_t + \Delta t \ddot{U}_t \\ U_{t+\Delta t} &= U_t + \Delta t \frac{(\dot{U}_t + \dot{U}_{t+\Delta t})}{2} \end{aligned} \quad (22)$$

and values for displacements $U_{t+\Delta t}$ and velocities $\dot{U}_{t+\Delta t}$ are calculated, after time Δt has elapsed.

iv) The resulting displacements and velocities are inserted again in the dynamic equations (18), and new values for acceleration $\ddot{U}_{t+\Delta t}$ are calculated. These values of $\ddot{U}_{t+\Delta t}$ are characterised as assumed since they are based on displacements and velocities extracted from approximation formulas.

v) The assumed values of $\dot{U}_{t+\Delta t}$ and the values of \dot{U}_t are inserted in Newmark- β formulas (21) and values for $\dot{U}_{t+\Delta t}$ and $U_{t+\Delta t}$ are calculated.

vi) The new values of displacements and acceleration are used in aerodynamic equations (18) and the accelerations which are calculated are characterised as calculated.

vii) The older values of the acceleration $\dot{U}_{t+\Delta t}$ and the new ones $\dot{U}_{t+\Delta t}$ are compared and if they do not satisfy the convergence criterion which has been set the calculations continue from step v) and onwards, using the last values for displacements, velocities and acceleration.

If convergence criterion is satisfied, displacements and velocities are substituted with their last values $\dot{U}_{t+\Delta t}$, $U_{t+\Delta t}$ and the procedure continues from step ii) and onwards for the next time step.

In this approach to the problem, the formation of the stiffness matrix has been avoided, since it would have to be transformed each time the displacements change, because it is displacement dependent. This is a big advantage of this technique, because large deformations of the structure are expected and particularly of the cables which are going to alter the geometric stiffness of the structure considerably.

The previous procedure is being followed for each wind speed for time-steps summing up to 30secs which is adequate, [47], [54] in order to include more than 10 periods' time of the fundamental mode. This is because

some time is needed for the bridge to build up any oscillation to a sinusoidal pattern. This period is also used in statistical studies, leading to the windspeed which must be designed for in practice.

The main disadvantage of this method is the computational cost; so it is advisable to have previously estimated the windspeed range where instability is expected by other methods, so that less analysis time is spent in this very costly procedure.

The advantages of this method include the possibility to plot the movements of some dofs of specific nodes and inspect closely the oscillations when reaching resonance conditions between vertical and torsional motions, the phase difference between them and also the maximum forces reached in all the elements during oscillations at the onset of flutter instability.

For a given windspeed, an initial pattern of nodal velocities is used to set the system in motion. An estimate of the value for the circular frequency of the structure is also used as the frequency of vibration is also needed in the equations of the aerodynamic forces. The results include the corresponding vertical frequency of oscillation ω_v , torsional frequency ω_t and logarithmic damping ratio for the vertical and torsional oscillation. If we follow this process for different windspeeds, we can plot the results as shown in (Fig.27).

For a given windspeed we can find the vertical and torsional displacements of the centrespan. If we plot

them against time, we get a plot similar to |
(Fig.26).

For the present analysis we will | use the
geometrical data of the Severn bridge, as given in
(Fig.29).

Predictions by ANSUSP2DE for torsional frequency against damping for a 2 degree of freedom system calculated by modal analysis with increasing windspeed by a step of 1m/sec.

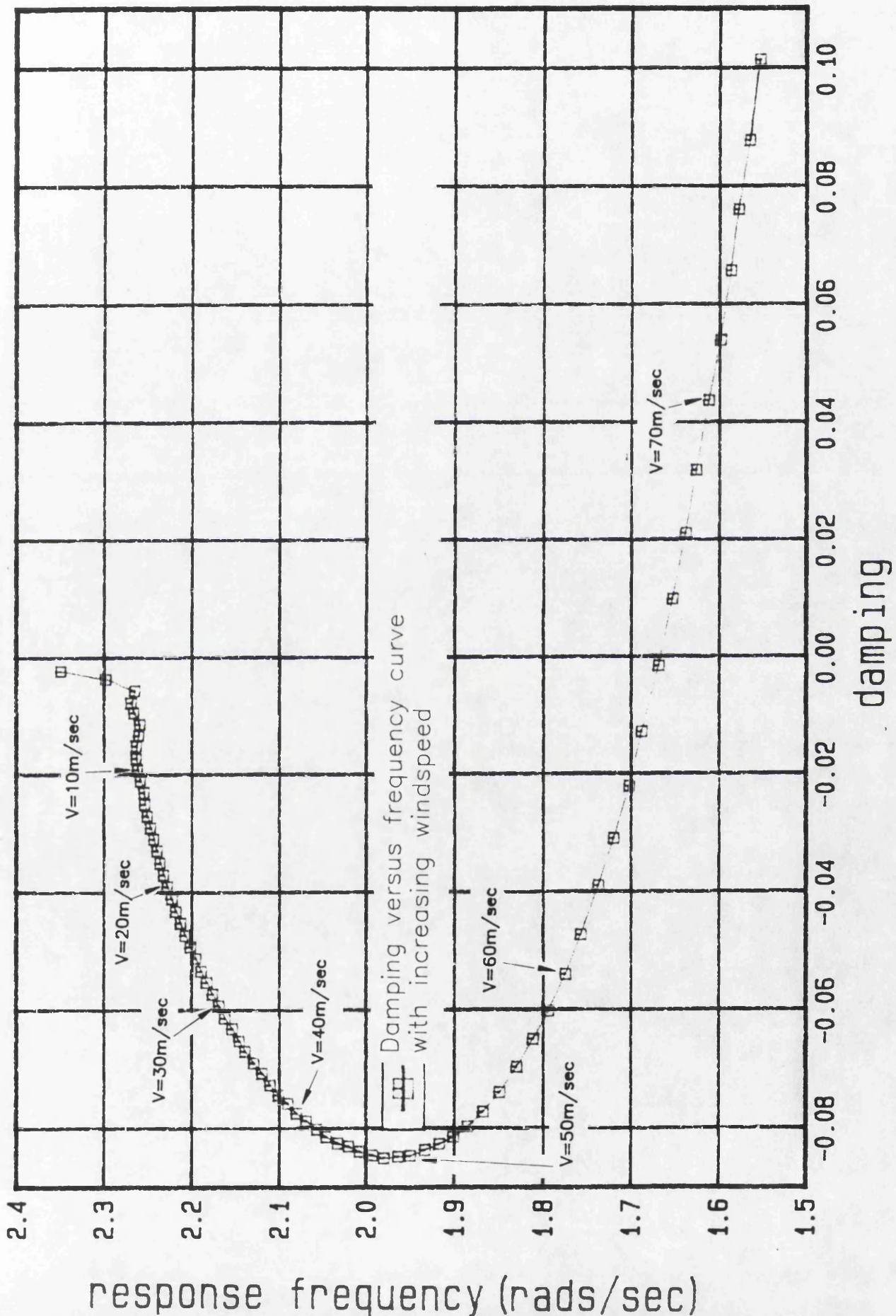


(Fig. 25.a) Argrand diagram of frequency vs damping of the torsional degree of freedom of a flat plate with 2 degrees of freedom plotted for different windspeeds calculated by ANSUSP2DE.

Predictions by ANSUSP of torsional frequency vs damping of a multi degree of freedom system when considering only a vertical and a torsional degree of freedom with modal analysis with increasing windspeed by a step of 4m/sec.

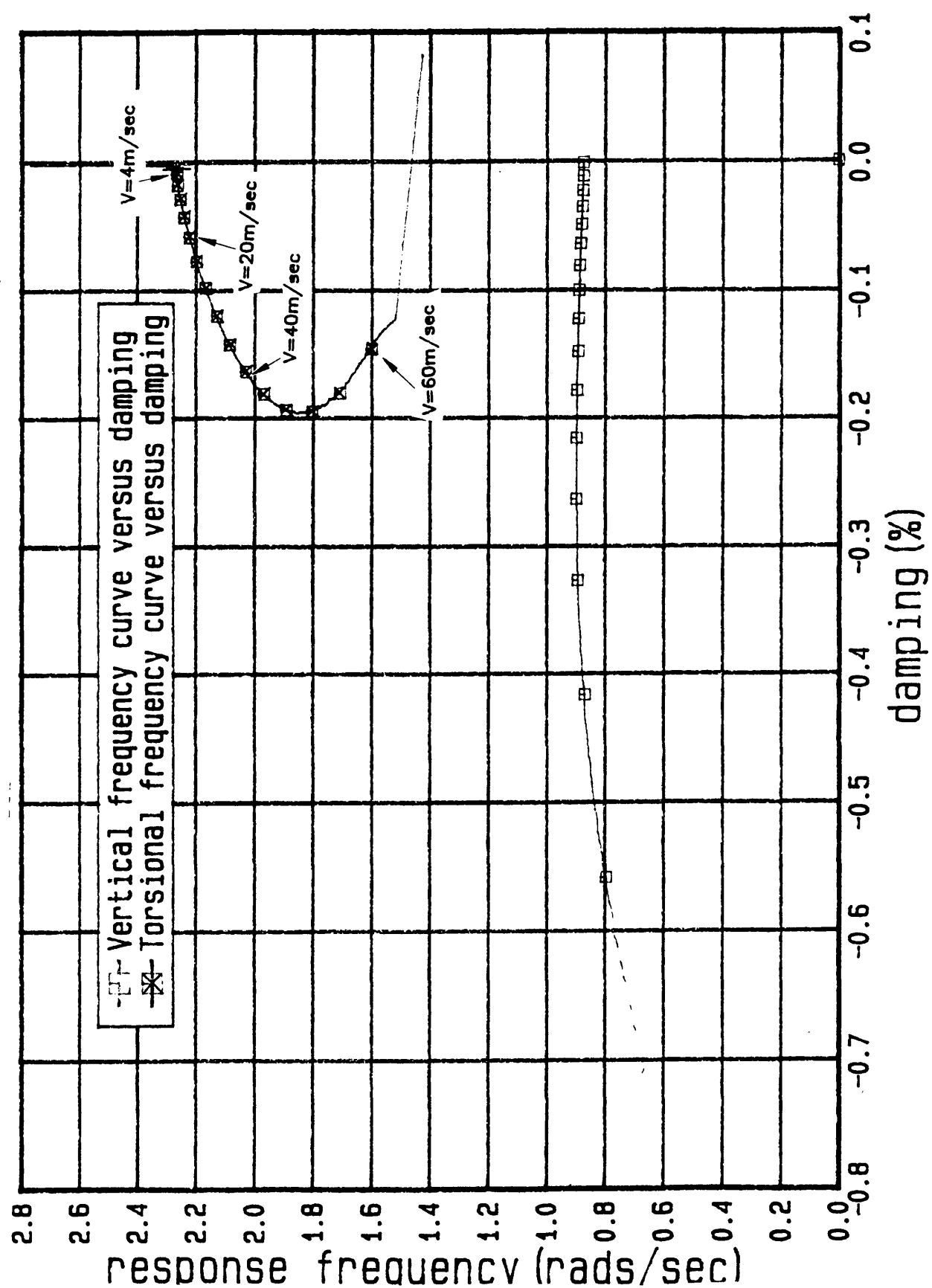


(Fig. 25.b) Argrand diagram of damping vs frequency plotted for different windspeeds considering only the first vertical symmetric and the first torsional symmetric degrees of freedom of a full bridge model calculated by ANSUSP.

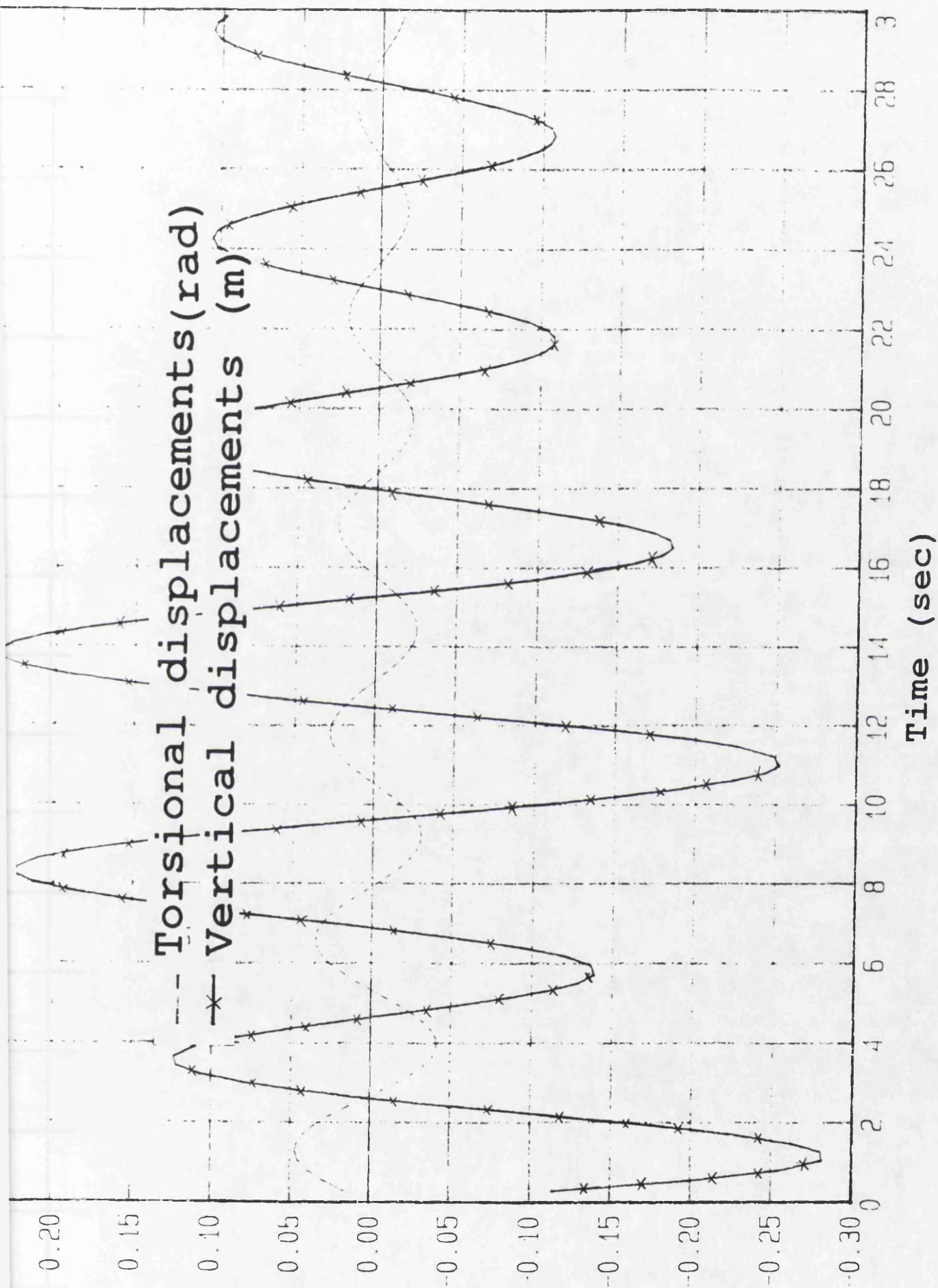


(Fig. 26.a) Oscillations of the centre of a thin flat plate in vertical and torsional motion against time in a windspeed of 28m/sec predicted by ANSUSP2D with the time history method.

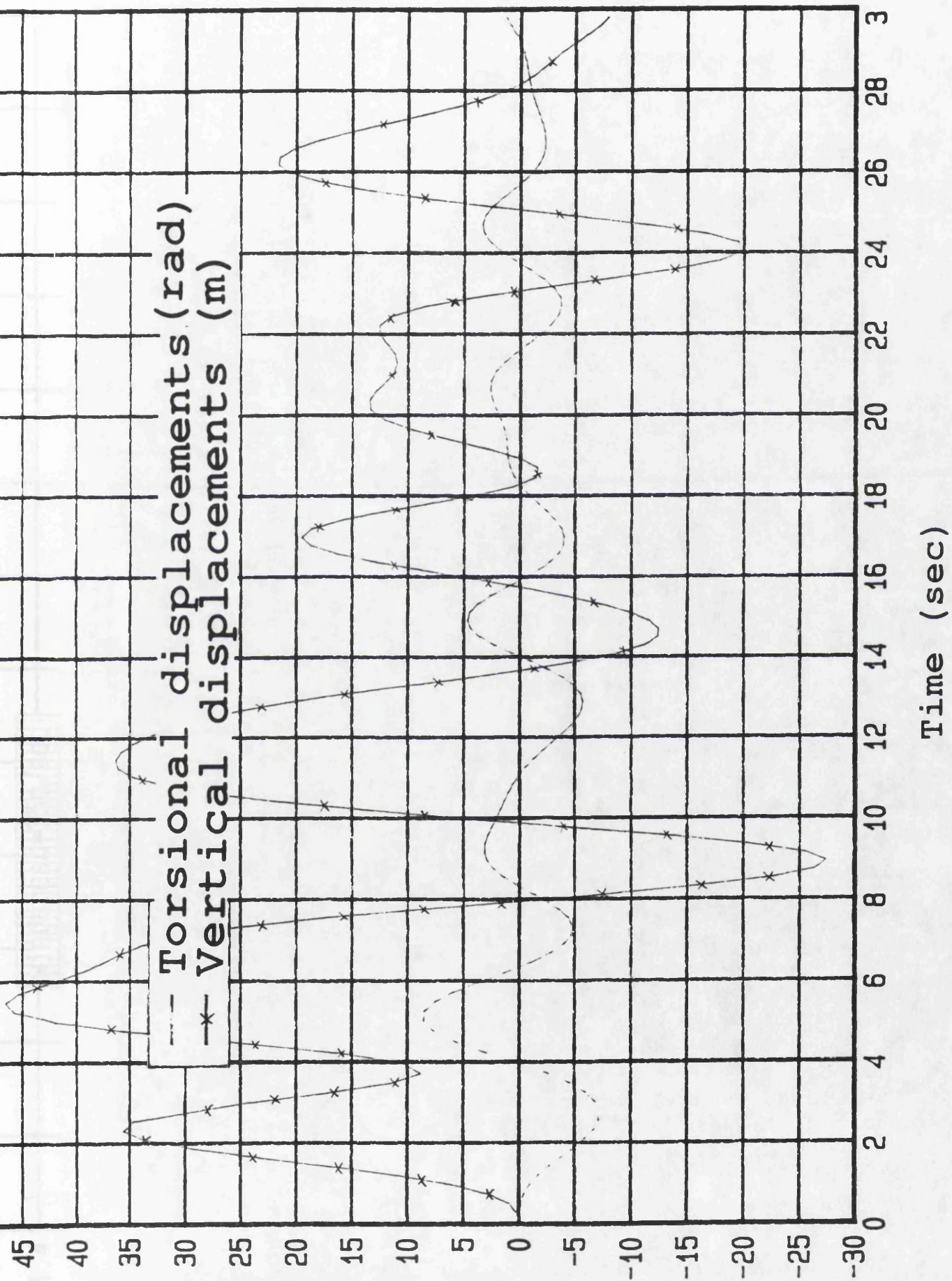


(Fig. 26.b) Oscillations of the centre of a thin flat plate in vertical and torsional motion against time in a windspeed of 33m/sec predicted by ANSUSP2D with the time history method.

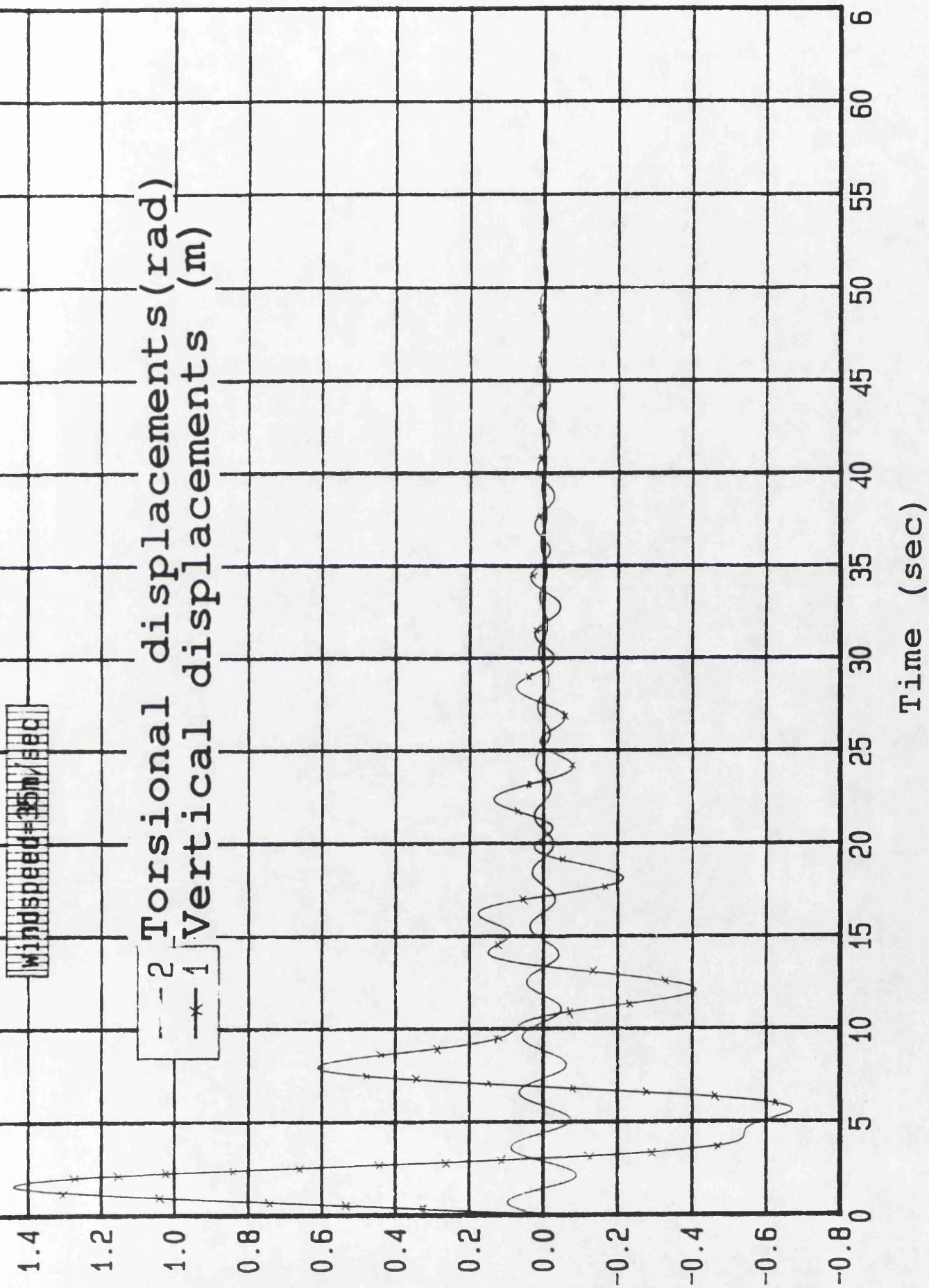


(Fig. 26.c) Oscillation of the centre of a thin flat plate in vertical and torsional motion against time in a windspeed of 35m/sec predicted by ANSUSP2D with the time history method.

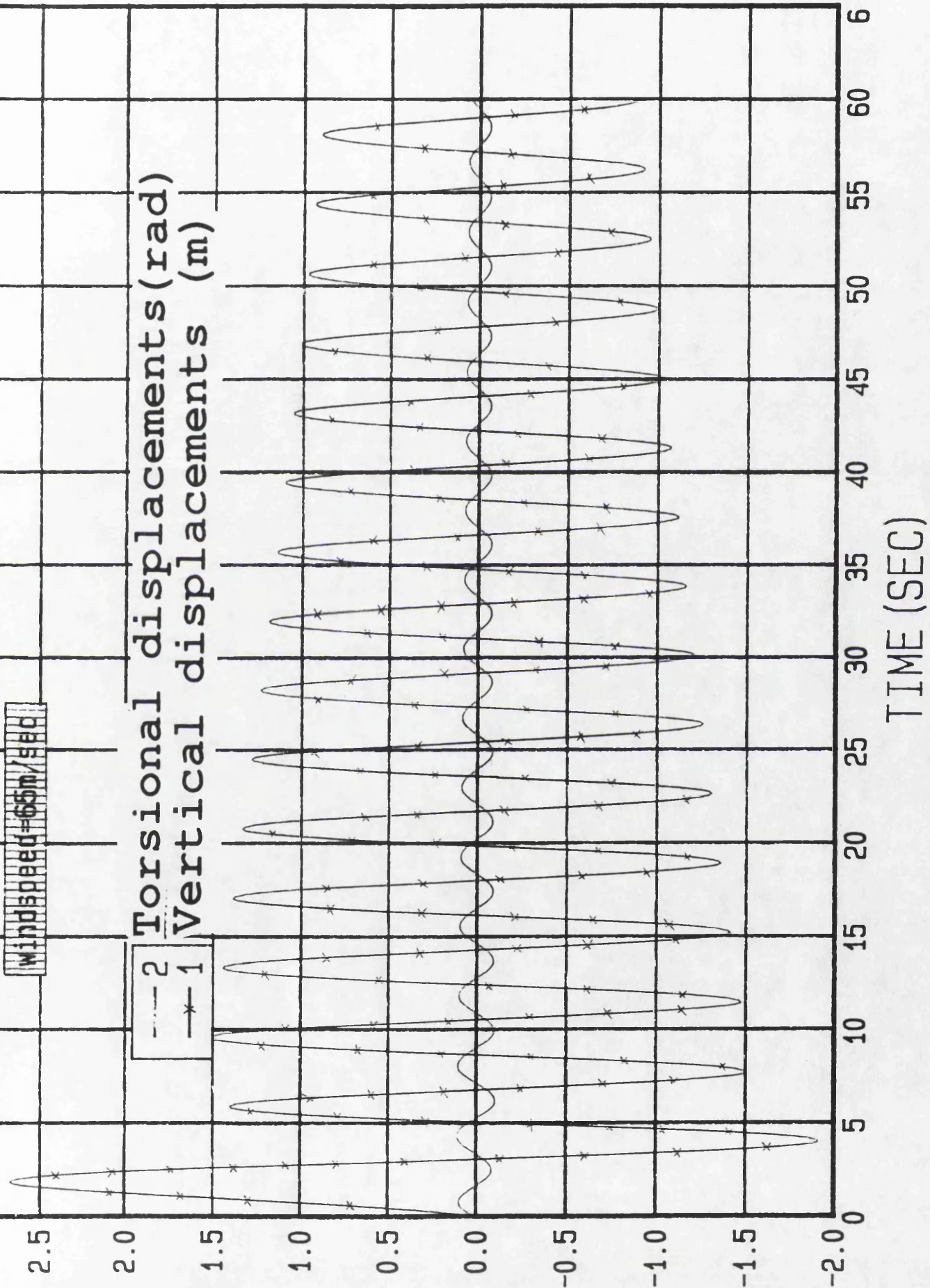


(Fig. 26.d) Oscillation of the centre of a thin flat plate in vertical and torsional motion against time in a windspeed of 65m/sec predicted by ANSUSP2D with the time history method.

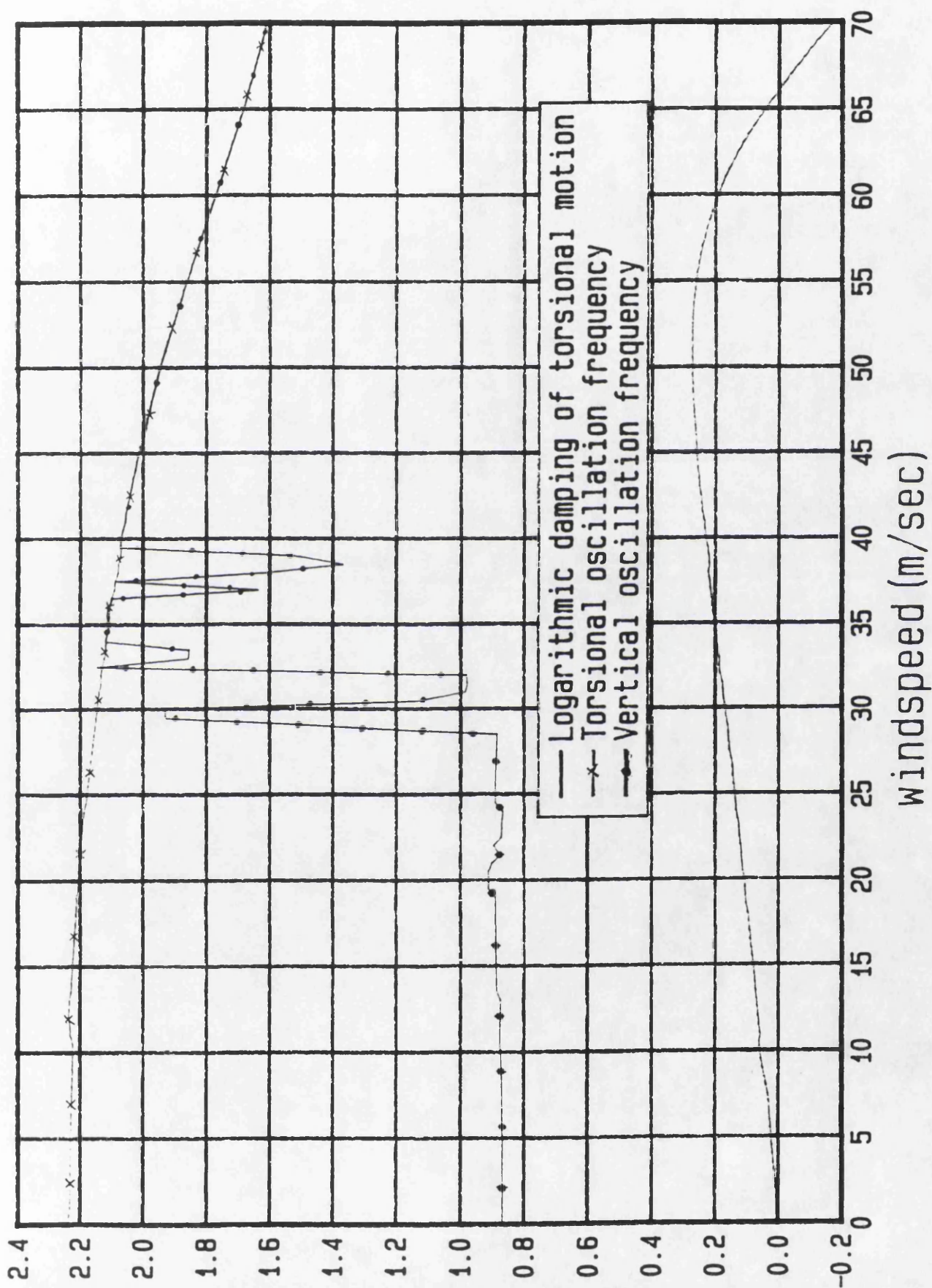


(Fig. 27) Circular frequencies of a 2 degree of freedom system in vertical and rotational motion and damping in rotational motion versus increasing windspeeds, by ANSUSP2D with the time history method.

Newmark β Method - Flow Diagram

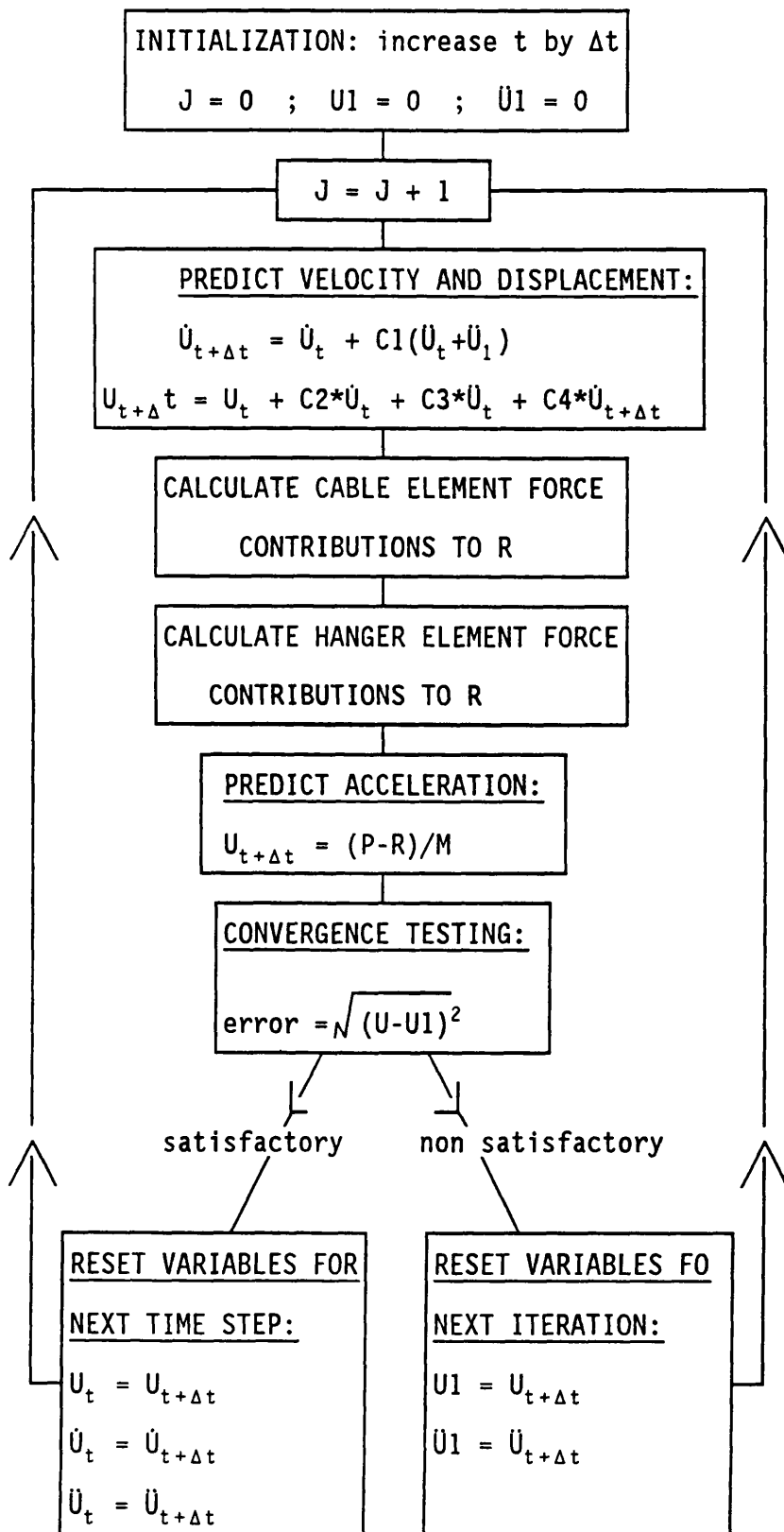
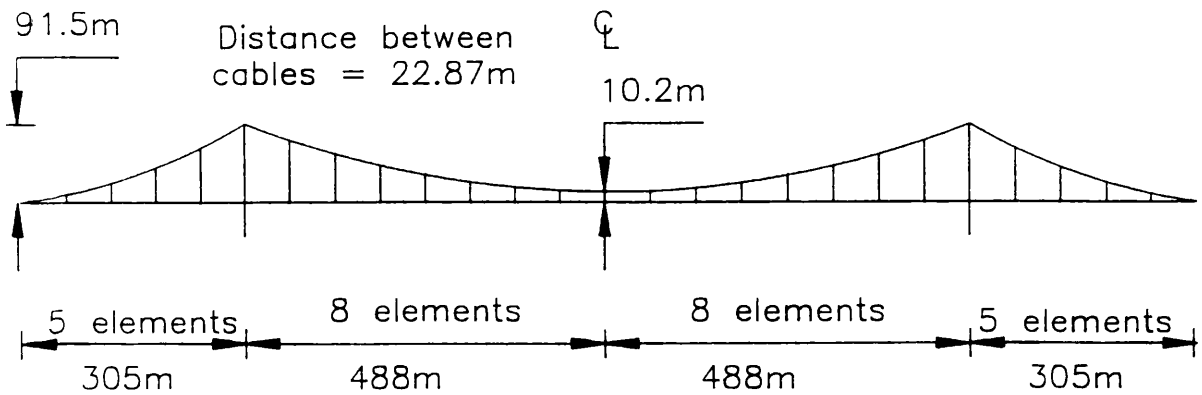


(Fig. 28) Flow chart of the time history method as used in ANSUSP.



Structural Properties

Cables	: CSA	= 1.158 m ²
	Mass	= 1338 kg/m
Hangers	: CSA	= 0.0146 m ²
	Mass	= 124 kg/m
Towers	: I _{long}	= 2.13 m ⁴
	J _{torsion}	= 8.52 m ⁴
	E _{steel}	= 207 · 10 ⁶ kN/m
Deck	: I _{vert}	= 1.079 m ⁴
	J _{torsion}	= 3.995 m ⁴
	Mass	= 10350 kg/m
	Mass moment of inertia	= 696 · 10 ³ kg/m ²
	Overall width	= 31.85 m

(Fig. 29) Nominal properties, geometrical and elastic of the Severn bridge. [14]

Chapter 5

Parametric study using ANSUSP.

A parametric analysis is presented here, the objective being to gain insight into the behaviour of a cable suspended bridge under flutter conditions. Various structural properties of a typical modern suspension bridge are modified and the effect of the modification on the flutter windspeed is examined. It is assumed for all the present parametric studies that the deck behaves aerodynamically as a flat plate so that equations (1) can be applied.

In most of the analysis only as many modes are used as are necessary to include the first two torsional modes - a symmetric and an antisymmetric mode. In the following, only symmetric modes are included when trying to find the symmetric flutter windspeed or alternatively antisymmetric modes when examining the antisymmetric flutter windspeed, ignoring the rest and keeping the workload to a minimum.

The analysis through different windspeeds does not start from zero values, since this was found to be unnecessary, but an analysis should always start at a windspeed where the previous tests were indicating instability should be expected. This was found useful enabling shorter computing times.

The parameters which have been modified can be divided into four major categories which are outlined below.

GEOMETRICAL PROPERTIES: These include the modification of cable sag to span ratio which in design practice usually takes a value between 1/10 to 1/14 [47]. This ratio gives a measure of gravity stiffness of the bridge in the vertical direction. Another factor included in this group is the horizontal separation of the suspension cables. This in combination with the deck torsional stiffness affects the torsional stiffness of the structure [47].

ELASTIC PROPERTIES: These include variations of deck vertical and torsional stiffness and the cable Young's Modulus. These factors strongly influence the vertical or torsional frequencies of the bridge and hence the behaviour of the bridge in its dynamic response.

INERTIAL PROPERTIES: The deck's vertical inertia (mass) and torsional inertia and cable inertia have been modified. These affect the values of the vertical and torsional natural frequencies respectively.

AERODYNAMIC PROPERTIES: Alterations to the aerodynamic width of the deck and the density of the air have been carried out. In this category the modifications do not alter the natural frequencies of the structure, but clearly can influence the magnitude of the aerodynamic forces which ultimately drive the flutter conditions.

Initially numerical tests were carried out using the ANSUSP modal analysis method. This enables a reasonably quick calculation of predictions. A comparison with Selberg's formula is also included where applicable. Having established the most important factors, ANSUSP

time integration method has been used to check the accuracy of the modal analysis results.

5.1 Modal flutter analysis by ANSUSP.

5.1.1 The effect of cable sag [all other bridge properties as nominal (Fig.29)].

Investigation of the effect of cable sag has been carried out for two slightly different types of configurations as indicated in (Fig.30) and (Fig.31).

In the first configuration the distance between cable and deck at the bridge midspan has been kept constant, with the tower height h having to accommodate the variations made in sag. In the second configuration tower height has been held constant while the cable to deck clearance at midspan has been varied to accommodate the variations made in sag.

The variation of natural frequencies caused by varying sag/span ratio between $1/10$ and $1/14$ for the two above described configurations are shown in Graph1 and Graph3 respectively. Comparison of these graphs indicates an insignificant difference in predictions so that the choice of configuration (between Fig.30 and Fig.31) is unimportant. The lower natural mode shapes in vertical flexure and torsion for the nominal bridge properties are shown in (Fig.32). Mode shapes also show no significant change from those corresponding to the nominal properties, over the full range of variation of sag/span ratio considered.

Considering Graph1 and Graph3 in detail it is noted that there is a trend for all the antisymmetric frequencies to slightly reduce, with increasing sag/span ratio. This can be explained as follows:

As sag/span ratio increases the cable length and hence cable mass increases. Also, the antisymmetric vibration modes involve displacements of the cable which is primarily a change in geometry rather than developing an increase in internal cable tension. As such the cable becomes less stiff with increasing sag/span for this type of antisymmetric motion. The increased cable mass and its reduced stiffness compound with each other to reduce the antisymmetric frequencies with increasing sag/span. This is true not only for the vertical frequencies, but also for the fundamental torsional antisymmetric frequency which involves antisymmetric vertical cable motion.

Considering the symmetric frequencies, it can be seen that the two lowest (1-S-F and 2-S-F) also reduce slightly with increasing sag/span, while the 3rd (3-S-F) and the fundamental torsional increase. The mode shapes for 1-S-F and 2-S-F indicate longitudinal tower top motion to accommodate the opposing sense vertical deck displacements in the centre and side spans. This leads primarily to a change in the geometry of the cable rather than increase in internal cable tension. Consequently the effect for the symmetric modes is similar to the effect for the antisymmetric vertical modes.

However it can be seen from the 3-S-F and 1-S-T mode shapes, which involve little or no longitudinal tower top

displacement (cable displacements of the same sense in the centre and side spans), that the cable displacement involves primarily stretching to develop additional internal tensions. The consequence is that the cable is relatively much stiffer than for the previous cases and so the result is an increase in natural frequencies.

Considering now how these changes in natural frequencies affect flutter speed, it would be expected that symmetric mode flutter speed would follow the trend in fundamental torsional frequency i.e. increase with increasing sag/span ratio. This is seen to be predicted in Graph2 with the prediction being significantly larger than the semi-empirical Selberg prediction. The opposite effect would be expected for flutter speed for antisymmetric flutter mode, i.e. reducing flutter wind speed with increasing sag/span. This trend has been produced by the ANSUSP modal predictions. However because the predictions (ranging from 114-128m/sec) are outwith the normal design criteria, the results have not been presented in Graph2.

5.1.2 The effect of cable sag (with deck torsional stiffness reduced to 7% of its nominal value).

Here an investigation similar to the one presented above is repeated on the influence of the sag variation when a major part of the torsional stiffness comes from the cables, the deck torsional stiffness being reduced to 7% of its nominal value. This deck torsional stiffness was chosen so that the fundamental antisymmetric

torsional natural frequency would be lower than the symmetric torsional natural frequency in order to examine if the antisymmetric flutter speed would follow the same pattern as for the natural torsional frequencies and become lower than the symmetric flutter speed.

With a torsionally flexible deck, as cable sag increases, the first torsional symmetric frequency slightly increases following the same trend as in section 5.1.1. In the same way as in the previous analysis the first torsional unsymmetrical frequency slightly reduces. However the flexural natural frequency curves are unchanged in Graph1 and Graph4 since the torsional stiffness of the deck does not affect the vertical oscillations.

The critical windspeeds have decreased considerably with the torsionally flexible deck and so symmetrical and antisymmetric flutter windspeeds are of comparable magnitudes as expected (Graph5). For sag/span ratio equal to 1/12 (as in the original Severn bridge) antisymmetric flutter speed is approximately the same as the symmetric flutter speed. This shows clearly the way in which the natural torsional frequencies affect the oscillation pattern (symmetric or antisymmetric) when flutter occurs.

With reducing sag, antisymmetric flutter windspeed increases marginally, following the same trend as in section 5.1.1, because the torsional antisymmetric natural frequency increases and also because the difference between it and the fundamental antisymmetric

flexural frequency increases. In contrast symmetric flutter windspeed reduces marginally as in section 5.1.1.

5.1.3 The effect of horizontal separation of the cables.

The horizontal separation of the cables is a feature which will affect the torsional stiffness of the bridge, whereas the vertical natural frequencies are not affected by cable spacing.

As the cables are positioned further apart from each other, for a unit of deck torsional deflection the cables have to undergo larger vertical displacements since they will be positioned further from the centre of rotation. This will result in an increase of torsional stiffness of the bridge when the structure oscillates in modes that involve cable stretching. However the increased horizontal separation of the cables increases the torsional inertia of the bridge also. These two effects combine to affect the torsional natural frequencies of the bridge. Considering (Fig.32) we notice that the cables will not have to stretch significantly for torsional antisymmetric oscillations. Consequently the inertial effect is the only factor to affect the antisymmetric torsional frequency. It is therefore expected that the antisymmetric natural frequency will reduce considerably as cable separation increases.

A detailed examination of the effects of the increasing cable separation is presented below:

$$\omega = \sqrt{\frac{K}{M}}$$

$$K = \frac{kb^2}{2}, \quad M = \frac{2mb^2}{4}$$

$$\text{Therefore } \omega = \sqrt{\frac{kb^2}{2mb^2}}$$

where

K = generalized stiffness

M = generalized mass

ω = circular torsional frequency

b = separation of the cables

k = spring stiffness representing cable vertical
stiffness

shows a dependence of the cable torsional stiffening effect being proportional to the square of the cable separation (Fig. 33). Considering that the stiffening effect occurs only in symmetrical modes, at least when the deck is considerably stiffer in rotation it would be expected that increasing cable separation will have much less influence on the torsional symmetric natural frequencies than on the antisymmetric natural frequency.

This agrees with the results of the analysis presented in Graph 6. The antisymmetric torsional frequency reduces significantly as the horizontal

separation of the cables increases, while the symmetric torsional frequency remains at a constant value.

The flutter windspeed of the antisymmetric motion is not presented in Graph7 since it is not the critical curve for this analysis. However it is noted that its trend is decreasing as horizontal separation between cables increases. The symmetric flutter speed versus cable separation curve is the critical curve in the present case and shows an interesting trend increasing initially, but then achieving a constant value. There is a noticeable decrease of the slope of the curve in Graph7 representing a region where the influence of increasing horizontal separation of the cables is limited.

5.1.4 The effect of horizontal separation of the cables (with deck torsional stiffness reduced to 4% of its nominal value).

In this case the same variation of cable separation has been applied to a bridge with reduced deck torsional stiffness of 4% of the nominal value. This reduction of the torsional deck rigidity will be accompanied by reduction of total torsional stiffness of the bridge. The vertical stiffness should not be affected at all and neither will vertical inertia. Therefore we expect the flexural natural frequencies to be constant and to accord with those in section 5.1.3. From (Fig.34) examining closely the 1-S-T and 1-A-T torsional mode shapes, we notice the symmetric mode showing a deformation of both central and side spans indicating a lateral deformation

of the tower tops. The antisymmetric torsional mode shape shows no deformation of the deck at the side spans which implies that the deformation of the deck is accommodated in the main span without any influence at the side spans and so without any need for the tower tops to deflect significantly. Hence the cable does not have to stretch. Considering also a deck with zero torsional stiffness, it can be concluded that when the deck is flexible enough the torsional symmetric natural frequency will become higher than the antisymmetric torsional frequency. Extending this argument it can be said that it is possible to control, (by means of altering the torsional stiffness of the deck), which natural torsional frequency (symmetric or antisymmetric) is the lower. For the present case torsional rigidity of the deck was chosen such that the symmetric torsional natural frequency is higher than the antisymmetric torsional natural frequency.

As the horizontal separation between the cables increases, the two effects referred earlier in section 5.1.3 will be involved here. The inertia influence of the cables will increase with the square of their distance apart and the displacements imposed on the cables due to deck rotation will also increase with the square of the distance from the torsional centre. Hence it would be expected that as the horizontal separation of the cables increases, symmetric natural frequency should also increase because symmetrical torsional stiffness is relying to a greater extent on cable contribution, since

torsional deck stiffness is greatly reduced. This is apparent in Graph8. Inertial effects are of lower importance for lower cable separation but start to influence the symmetric torsional frequency more as the distance of the cables increases. Antisymmetric torsional natural frequency is not related to tower top deformations but only to cable change of geometry. However the further apart the cables are positioned, the larger vertical deformations they will have to undergo, and some stretching of the cables will be needed particularly at the centre of the centre-span. So an increase in torsional antisymmetric natural frequency will be expected, even though the inertial effects of the positioning of the cable mass further apart is bound to become apparent after a certain value. In Graph8 we notice the antisymmetric natural torsional frequency increasing but with reducing slope as cable separation increases.

Flutter speeds are expected to follow the same trend as the torsional natural frequencies. Increase of horizontal cable separation is expected to increase symmetrical flutter speed. A similar pattern is expected for the antisymmetrical flutter speed. Antisymmetrical flutter speed is lower than the symmetrical corresponding closely with the way torsional natural frequencies relate to each other, with the difference between the two natural frequencies increasing as cables are positioned further apart. This indicates that antisymmetrical torsional frequencies are more sensitive to increase in

torsional inertia than the symmetrical torsional frequencies.

5.1.5 The effect of horizontal separation of the cables with tower stiffness increased to 10 times the nominal value.

This case was included in the analysis to clarify the influence of the torsional stiffness of the deck in the overall torsional stiffness of the bridge. Increasing torsional deck stiffness by a factor of ten (within reasonable limits) is going to affect the torsional natural frequencies, without any effect on flexural natural frequencies. Therefore it is expected that the flexural natural frequencies are going to be held exactly the same as in Graph6 where deck torsional stiffness was the nominal value (section 5.1.3).

Considering torsional natural frequencies the contribution of the deck torsional rigidity is expected to affect the torsional rigidity of the whole bridge and in effect to increase the natural torsional symmetric frequency. The antisymmetric natural torsional frequency is also expected to increase in comparison to section 5.1.3. However comparing Graph10 with Graph6 it is interesting to note that only symmetric torsional frequency has increased while antisymmetric torsional frequency is very much the same.

As horizontal separation of the cables is increased, we expect an increase in torsional stiffness coming from the cables. At the same time, the torsional

inertia will affect also the torsional natural frequencies with opposite action. Therefore similar values are expected as in the case with nominal deck rigidity in Graph6 (section 5.1.3). The antisymmetric torsional natural frequency will be reducing for increasing horizontal separation of cables, due to the increase of the torsional inertia of the bridge, being less affected by the increasing cable-related torsional stiffness.

According to the torsional natural frequencies it can be expected that as the horizontal separation of the cables increases, the flutter speed will follow the same trend as for the nominal values for deck stiffness in Graph7, though in this case flutter speeds for symmetrical oscillation should be generally higher than in section 5.1.3. This is predicted in Graph11. Antisymmetrical flutter speeds are expected to be much the same for this case considering the small changes of the antisymmetric torsional frequencies. This also agrees with the results of the flutter analysis in antisymmetric oscillation (110-128m/sec).

5.1.6 The effect of horizontal separation of the cables with tower torsional and flexural stiffness increased to 10,000 times the nominal value.

In this case the stiffness of the towers has been increased by a factor of 10,000 to model the effect of essentially fixing the cables at the tower tops. With the tower tops prevented from moving significantly the cable

will have to develop internal tension or undergo change of geometry in order to accommodate the oscillations that were previously undertaken by the towers (mode 1-S-F in natural tower properties and in the present case). Therefore it is expected that especially the symmetrical frequencies, which correspond to mode shapes that involve cable stretching, will increase in accordance with the symmetrical torsional frequencies.

Considering closely the natural frequency values in the present case and also in the case with nominal tower stiffness and their corresponding mode shapes (Fig.35), it is noticed some increase has occurred in some vertical natural frequencies Graph13 in comparison with the towers with nominal properties. The frequency corresponding to mode 1-A-F is identical with both tower properties since little if any tower deformation is involved in this mode and so the corresponding frequency is not affected at all. On the contrary the 1-S-F frequency has increased by 15% with rigid towers since the cable has had to develop some stretching. The 2-S-F mode has become similar to the 3-S-F mode for the nominal geometry and has also increased since the small deformations that were performed by the towers in (Fig.32) are suppressed in the present case (Fig.35). The 2-A-F mode in the present case corresponds to 3-A-F in the nominal geometry case Graph5 and the corresponding natural frequency has decreased considerably. Mode 3-A-F is similar to mode 2-A-F for nominal values and its corresponding frequency has increased slightly.

The torsional frequencies are also expected to change. The 1-S-T frequency is expected to increase since the cable will not have any freedom of movement at the tower top, while 1-A-T natural frequency will not be affected by the more rigid towers because the mode shape it develops does not involve any cable stretching.

Increasing the horizontal separation of the cables is not expected to affect in any way the flexural natural frequencies, since it will not bring any elastic or inertial change in the vertical sense. However it is to be expected that the torsional frequencies will be affected and particularly 1-S-T frequency will increase more sharply than in the case of Graph6 since the stiffening effect of the cables, being positioned further apart are forced to undergo more stretching even than with nominal tower properties. Hence the cable torsional stiffness contribution is relatively more important in this case than with nominal tower properties will. In contrast the 1-A-T frequency being affected by the increasing torsional inertia, decreases for increasing horizontal separation of the cables. Hence it is expected that the symmetric flutter speed will show a clear increase for increasing separation of the cables and this is demonstrated in Graph13. For the antisymmetrical flutter, a sharp decrease is expected as the horizontal separation of the cables increases as the 1-A-T frequency reduces substantially with increasing cable separation.

5.1.7 The effect of cables' mass per unit length.

The inertia of the cables has shown in previous sections (5.1.3, 5.1.4, 5.1.5) to play an important role in the dynamic response of the bridge. In the present section an investigation of the effects of the cable mass will be carried out. The present analysis is expected to complement the investigation of the effects of changing the material used for the cables.

Altering the mass of the cables per unit length is expected to affect the contribution of the cables in vertical and rotational inertia. It will also affect the tensile forces in the cables, because of variations in overall weight. The vertical natural frequencies both symmetrical and antisymmetrical are not expected to be significantly affected because with increasing cable mass the gravity stiffness increases in parallel with the inertia in vertical motion which are two effects with opposite results. However the torsional frequencies are expected to decrease with increasing cable mass because the increase in rotational inertia will be relatively more important than the increase in gravity stiffness. The vertical symmetrical natural frequencies are shown in Graph14 to decrease slightly (10-15% reduction) for a cable mass increase by a factor of 10. However the antisymmetrical natural frequencies are only marginally reduced. The symmetrical and antisymmetrical torsional frequencies both decrease as cable mass increases by a factor of 10 with the antisymmetrical frequency being

more affected by mass increase than symmetrical frequency.

Consequently, in Graph15 the flutter speed predictions calculated by ANSUSP show the expected reductions with increasing mass and accord with the previous comments. In this graph the results by the Selberg semi-empirical method are included and can be seen to be generally conservative predictions of the flutter speed.

5.1.8 The effect of rotational inertia of the deck.

Study of the variation of deck rotational inertia will supplement the investigation of the effects of rotational inertia caused by different structural elements of the bridge. The rotational deck inertia depends on the cross-sectional distribution of the mass of the deck. As such it can be significantly altered by small changes in mass distribution at the outer transverse edges of the cross section.

The effects are expected to affect only the torsional natural frequencies of the bridge, with the vertical frequencies unaffected. As the rotational inertia of the deck increases both symmetrical and antisymmetrical torsional natural frequencies are expected to decrease considerably in a similar fashion to section 5.1.7 above. The predictions plotted in Graph16 again show sharp reductions in torsional frequencies with increase of rotational inertia by an order of magnitude. Considering the effects the torsional natural frequencies

have on flutter speeds the latter are expected to reduce in the same fashion as the torsional frequencies. Similar trends to section 5.1.7 above in the reduction of flutter speed with increasing deck rotational inertia are evident from Graph17 where sharp reduction of flutter speed occurred. Here the predictions by Selberg are in very close agreement with the predictions by ANSUSP modal analysis.

5.1.9 The effect of deck mass (vertical inertia).

Deck mass is a parameter dependant on the detailed construction of the deck including the type and form of construction and also other non-structural components such as surfacing and finishes. Changing the mass of the deck not only alters the vertical inertia, but also subjects the cables to different vertical static loads which modify the cable tensile forces which influence their gravity stiffness. As the deck mass increases, both the symmetrical and antisymmetrical vertical natural frequencies are expected to reduce slightly because of increase in inertia. Increasing deck mass is expected to affect the tensile forces in the cables and consequently their contribution to the torsional stiffness of the bridge. As a result higher torsional frequencies are to be expected.

According to ANSUSP results shown in Graph18 all vertical symmetrical flexural frequencies reduce with increasing deck mass. The 1-A-F frequency alone is constant for deck mass varying in the range of 0.1 to a

factor of 10 times the nominal deck mass while the natural frequencies 2-A-F and 3-A-F reduce for increasing deck mass. Natural frequency 3-S-F reduces sharply as deck mass increases because in this mode of oscillation all three spans of the deck oscillate in the same sense. Both symmetrical and antisymmetrical torsional natural frequencies increase considerably with increasing deck mass.

Flutter speeds are expected to follow the trend indicated by the torsional natural frequencies. Both symmetrical and antisymmetrical flutter speeds should increase considerably for increasing deck mass. This is expected because with increasing deck mass torsional frequencies increase while flexural frequencies decrease. In Graph19 ANSUSP flutter speeds and Selberg predictions are included. Their comparison shows considerable disagreement between the two methods. The predictions by Selberg's semi-empirical formula are in line with the alterations of the natural frequencies. It can be concluded that Selberg's predictions rely very much on the vertical to torsional frequency ratio. When this ratio decreases, Selberg's predictions decrease accordingly.

5.1.10 The effect of the deck torsional stiffness.

Tests including the modification of the deck torsional stiffness, have been already carried out in combination with other parameters (cable separation, cable sag). In this section the torsional stiffness of

the deck has been altered while all other parameters have been held constant so that the importance of this factor on the wind stability of the cable suspended bridge can be measured. According to section 5.1.4 and 5.1.6 it is expected that for increasing deck torsional stiffness the natural torsional frequencies, both symmetrical and antisymmetrical, should increase sharply. The vertical natural frequencies should not change since neither cable stiffness nor inertia in vertical motion will be affected.

In Graph 19 can be seen that the symmetrical and antisymmetrical torsional frequencies increase with increasing rate as deck torsional stiffness increases from the nominal value while they also move further apart from each other with the antisymmetrical flutter frequency being the lower of the fundamental torsional cases. For decreasing deck rotational stiffness, antisymmetric torsional natural frequency becomes equal with the symmetrical when the torsional stiffness has a factor of 0.07 times the nominal deck torsional stiffness with the rest properties being the same as for the nominal bridge (Fig.29). For a deck torsional stiffness multiplied by a factor of 0.1 to 0.7 the antisymmetric torsional fundamental frequency is lower than the symmetrical torsional frequency. It should be emphasised that the natural frequencies become less affected by the deck torsional stiffness when this takes very small values. This happens because the contribution of the

cables as part of the bridge torsional stiffness increases as the torsional deck stiffness is reduced.

Considering the flutter speeds, they are expected to follow the same trend with the torsional frequencies increasing with increasing torsional deck stiffness. Flutter speeds illustrated in Graph21 show that with increasing torsional deck stiffness both symmetrical and antisymmetrical flutter speeds increase sharply with the symmetric flutter being the critical case. With reducing deck torsional stiffness antisymmetrical flutter speed becomes the critical flutter case. It can be seen that the Selberg predictions and the ANSUSP predictions are in close accordance.

5.1.11 The effect of deck vertical stiffness.

The effect of deck vertical stiffness has often been investigated in the study of cable suspended bridges as reported in [28]. Deep truss girders were commonly used, in order to suppress excessive oscillation amplitudes. The increase of the vertical stiffness of the deck is expected to affect all the vertical modes/frequencies but not the torsional ones. The vertical natural frequencies should increase as deck vertical rigidity increases, approaching the torsional natural frequencies, which are expected to remain unchanged. In Graph22 the natural frequencies are plotted against deck vertical stiffness where vertical frequencies are seen to increase with increase in deck stiffness. As vertical deck stiffness increases from the nominal value the flexural natural

frequencies are seen to increase with increasing rate with the higher frequencies increasing with higher rate. This is because the higher frequencies are more affected by higher deck flexural stiffness. Only the 3-S-F increases less sharply. Close observation of the mode shapes shows that the 3-S-F mode involves smaller deflections of the deck than the rest modes and so is less affected by increase in vertical deck stiffness.

Considering the flutter windspeeds, both symmetrical and antisymmetrical are expected to decrease with deck vertical stiffness increase since as the vertical frequencies approach the torsional so aerodynamic coupling between them becomes easier. However in Graph23 only the symmetrical flutter speeds show a significant reduction as deck vertical stiffness increases. Antisymmetric flutter speeds are affected only very slightly. The predictions by ANSUSP and Selberg's formula are included in Graph23. The symmetrical flutter speed curve by Selberg shows a slight reduction for increasing vertical deck stiffness, which does not agree with the results by ANSUSP. The predictions for antisymmetrical flutter speeds though by ANSUSP and Selberg's equation agree quite closely.

5.1.12 The effect of the Young's Modulus of the cables .

In this section the possible effects of using different materials for the cables are examined. Such materials might be in practise be kevlar fibres, graphite

fibres or carbon fibres in the composition of the main suspension cables.

The use of stiffer material for the cables is expected to affect the natural frequencies of the bridge depending on the type of mode of oscillation involved in the motion. In general the frequencies that correspond to modes which involve cable stretching are expected to increase. Examining closely the symmetrical vertical mode shapes of the bridge (Fig. 32), it is noticed that the 1-S-F mode involves some cable stretching and therefore 1-S-F frequency is expected to increase with increasing cable Young's modulus. Mode 3-S-F is the mode which involves more cable stretching than any other mode consequently cable Young's modulus is expected to affect the 3-S-F frequency considerably. The antisymmetric vertical modes involve mostly geometrical changes in cable shape rather than changes in internal cable force. Consequently no effect would be expected on these natural frequencies by increasing the Young's modulus of the cables, but is expected to reduce as E_{cable} is reduced by a factor of approximately 10 from its nominal (steel) value. For the same reasons, the 1-S-T frequency is expected to increase considerably, since its mode involves similar cable stretching as the 1-S-F mode while 1-A-T frequency is not affected. Those effects are presented in Graph24. The predictions by ANSUSP are in accordance with the previous comments as can be seen in Graph24.

Flutter windspeeds are expected to follow a similar pattern to that of torsional natural frequencies. Symmetrical flutter speed should increase considerably as cable Young's modulus increases. Antisymmetrical flutter speed is also expected to be affected, reducing slightly. Graph25 includes the flutter speeds predicted by ANSUSP and those predicted by Selberg. The curve for symmetrical flutter is increasing as cable Young's modulus increases in the same fashion with Selberg results. Antisymmetrical flutter speeds are also agreeing closely to the results by Selberg, except for a small spectrum of very low values of Young's modulus.

5.1.13 Effects of air density.

Environmental conditions could play some part in the stability of the bridge. The factor ρ which symbolises for air density relates to temperature and humidity conditions and is included in the aerodynamic force expressions as a multiplication factor. The values of air density ranging from 1.029kg/m^3 to 1.779kg/m^3 are related to temperatures of -70°C to $+70^\circ\text{C}$ respectively. Therefore the aerodynamic forces are related to the environmental conditions. Thus it is expected that flutter windspeeds will relate to air-density in both symmetric and antisymmetric modes. As the air density increases the wind induced forces increase in direct proportion to the factor ρ and so the flutter windspeed might be expected to decrease.

Graph26 with the ANSUSP prediction show the reductions expected with increasing ρ . Close agreement in trend is observed between Selberg and the ANSUSP results.

5.1.14 The effect of full aerodynamic width.

The aerodynamic width of the deck is a factor included in Theodorsen's aerodynamic expressions. As the deck aerodynamic width increases (Fig.36), the aerodynamic forces (1) change significantly since in the expressions for lift force and moment they appear as B^3 and B^4 respectively. Changing B also changes reduced frequency $k = \frac{\omega b}{V}$. Here it should be emphasized that the aerodynamic forces include also the aerodynamic damping so the response of the system is expected to be complicated. In Graph27 as aerodynamic width B increases from the nominal value (31.87m) the symmetric flutter windspeed initially decreases reaching to a minimum value for approximately 40m width. For every further increase of aerodynamic width symmetrical flutter speed increases.

5.2 3-D Time-history method.

So far modal analysis has been used to provide an insight into how some of the most important factors influence the aerodynamic flutter behaviour of the cable suspended bridge. The results already reported in section 5.1 above using modal analysis will now be compared with predictions produced by the time history method in

ANSUSP. A comparison of predictions by time history and modal analysis methods will hopefully result in the enhancement of confidence of numerical methods. However it should be noted that there is a large difference in the computation required for each of these two methods. The modal analysis method requires significantly less computations than the time history method; speaking in terms of overall operation time this refers to a factor of 60.

Because of the large amount of computation involved, not all the studies using modal analysis have been repeated using the time history method; only a selection of the more interesting trends have been investigated and only for the critical symmetrical oscillation case and the results are reported below.

5.2.1 The effect of horizontal separation of the cables.

Following the same procedures as in section 5.1.5, the cables have been positioned at various separation distances. The two ANSUSP numerical results for flutter speed agree very closely, as shown in Graph28 indicating that the much faster modal method produces results consistent with the full non-linear treatment but at a much reduced computational cost.

While these two methods are in good agreement, there is a sizeable discrepancy (approximately 15%) for a wide range of aerodynamic widths in the flutter speed predictions obtained by Selberg's formula.

5.2.2 The effect of deck mass factor.

The mass of the deck is altered following a similar procedure to this of section 5.2.11. As the mass of the deck increases the symmetrical natural flexural frequencies in general decrease while the symmetrical torsional frequencies increase (Graph18). Since the symmetrical flexural and torsional frequencies become more separated with increasing deck mass, it is expected that flutter speed will increase. In Graph29 flutter speed initially decreases slightly as deck mass increases, but for the deck mass factor range in the range between 2 and 10 flutter speed increases very slightly. The time history method results are in line with the modal analysis method.

The results acquired with Selberg's formula show a significant disagreement in fashion and in values. For the nominal Severn value of deck mass the disagreement is very small but as deck mass increases by a factor of 3 the difference between ANSUSP and Selberg results grows rapidly. For decreasing deck mass from the nominal Severn value the disagreement of ANSUSP and Selberg also increases.

5.2.3 The effect of deck torsional stiffness.

The deck torsional stiffness is one of the most important properties of the bridge for dynamic oscillations affecting significantly the aerodynamic

behaviour of the bridge. As deck torsional stiffness increases torsional natural frequencies increase both symmetrical and antisymmetrical. Considering the relation between torsional frequency and flutter speed, it is expected that as torsional deck stiffness increases symmetrical flutter speeds will increase also in the same fashion as the symmetric torsional natural frequency. The steep slope of the flutter windspeed curve acquired by modal analysis is closely followed by the results of time step analysis with increasing deck torsional stiffness from the nominal value. The slope of the flutter speed reduces as deck torsional stiffness reduces from the nominal value. The results show close agreement between the two numerical methods as is displayed in Graph30. The results by Selberg's method show reasonably close agreement with the numerical results by ANSUSP.

5.2.4 The effect of full aerodynamic width of the deck.

The aerodynamic forces are related to the aerodynamic width of the deck. Therefore it is expected that the flutter speeds will be largely affected with increasing aerodynamic width. The results by time step analysis lay in a slight curve with a local minimum. The results by the two numerical methods used in ANSUSP agree closely with each other. A similar pattern to this of section 5.2.2 indicates a spectrum of values of aerodynamic width which correspond to particularly low symmetrical flutter speed (Graph30). Selberg predictions

are significantly lower from the ANSUSP results by 12-13% for aerodynamic width values lower than the nominal Severn value. For aerodynamic width larger than the nominal Severn value Selberg flutter speed predictions continue to reduce and their difference from ANSUSP results increases.

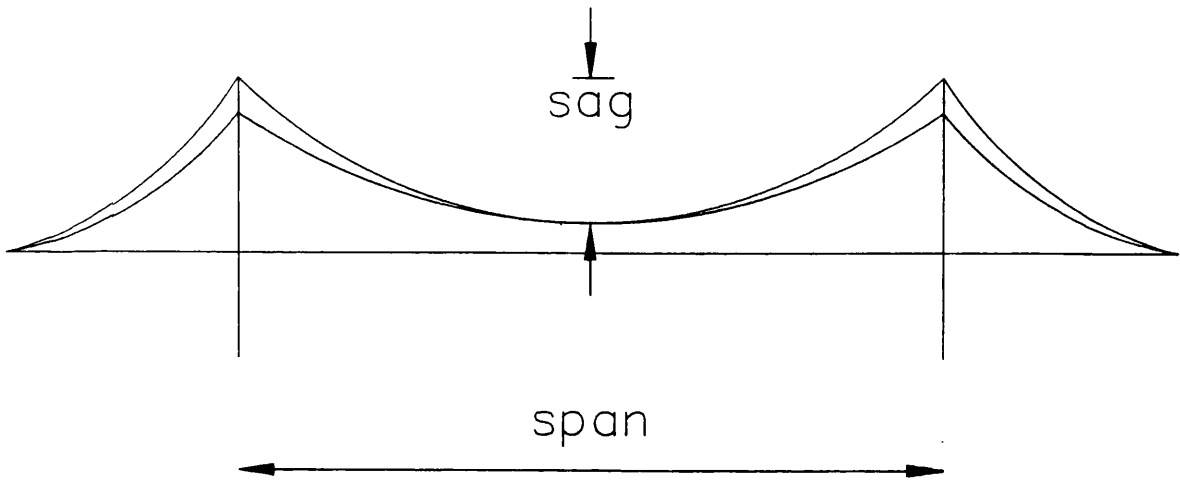


(Fig. 30) Alteration of the cable sag modifying the tower height.

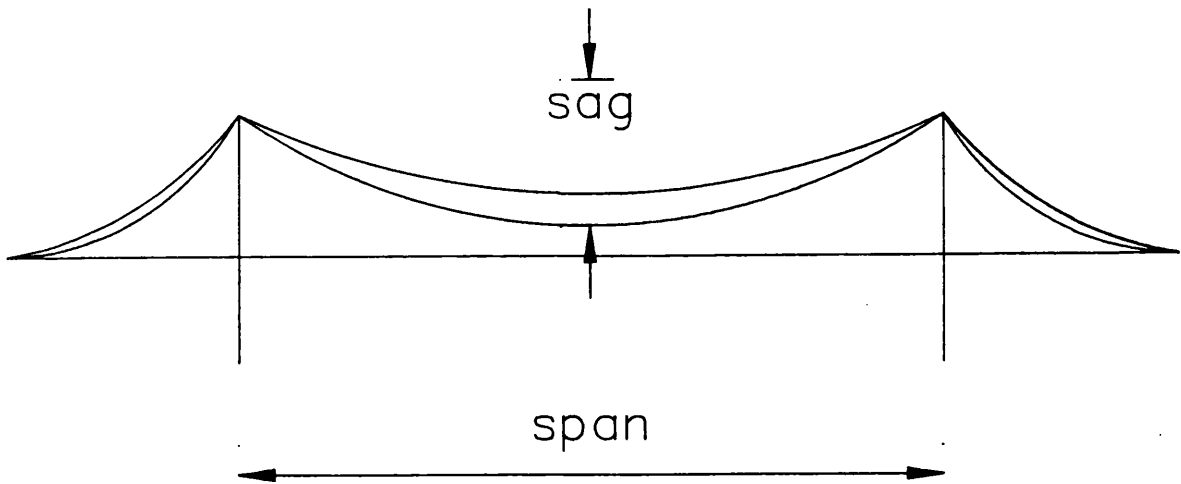


(Fig. 31) Alteration of the cable sag without modifying the tower height.

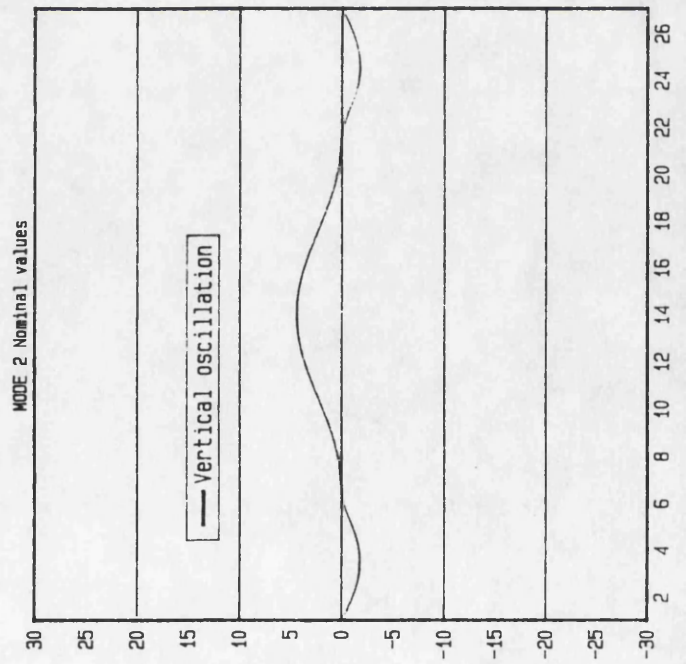
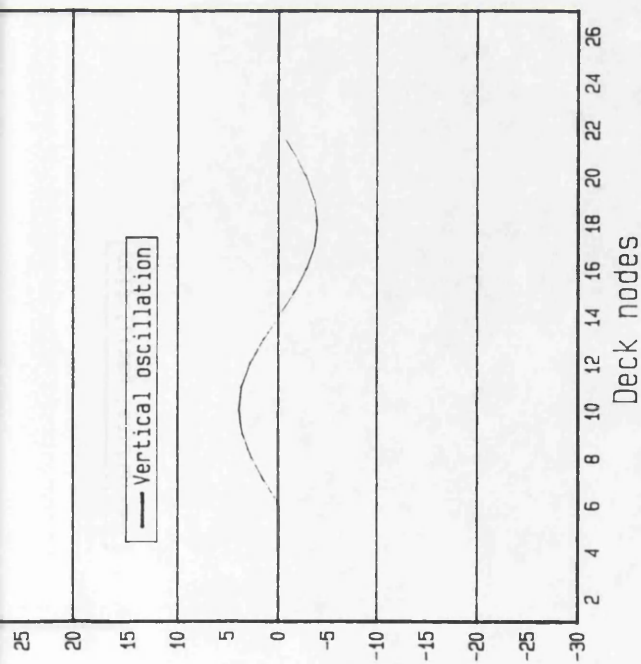
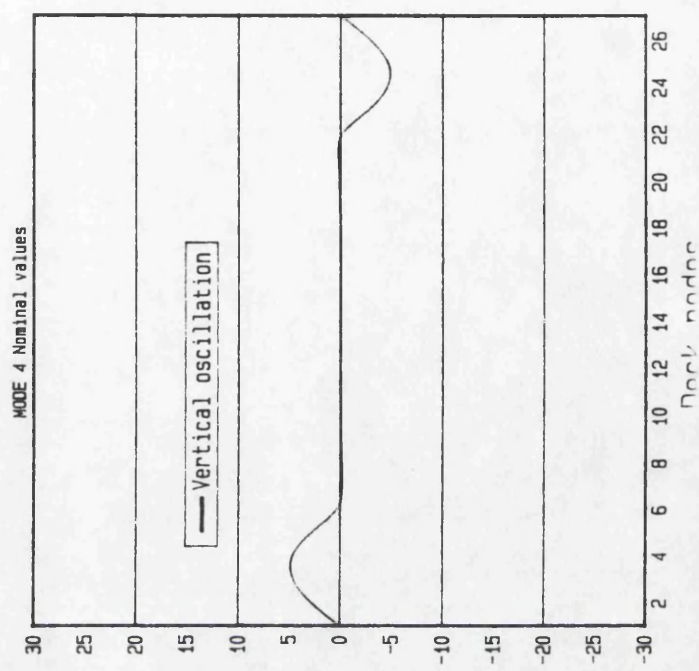
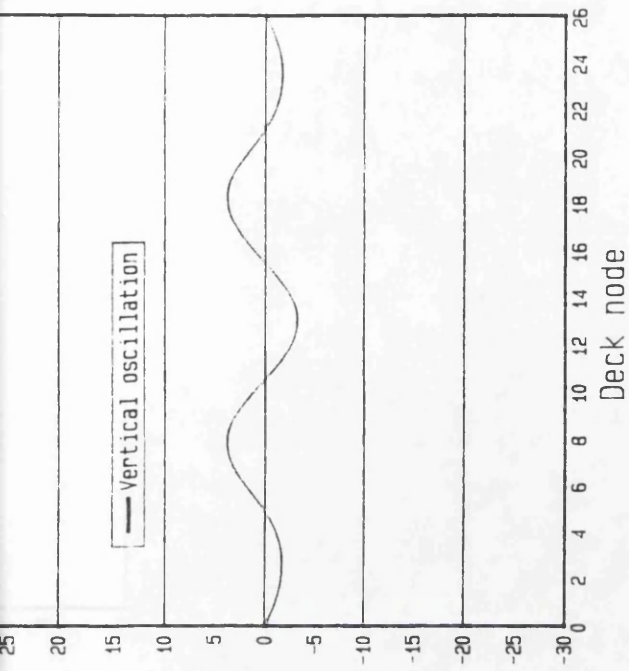


(Fig. 32.a) Natural mode shapes of the bridge numerical model with Severn nominal values.

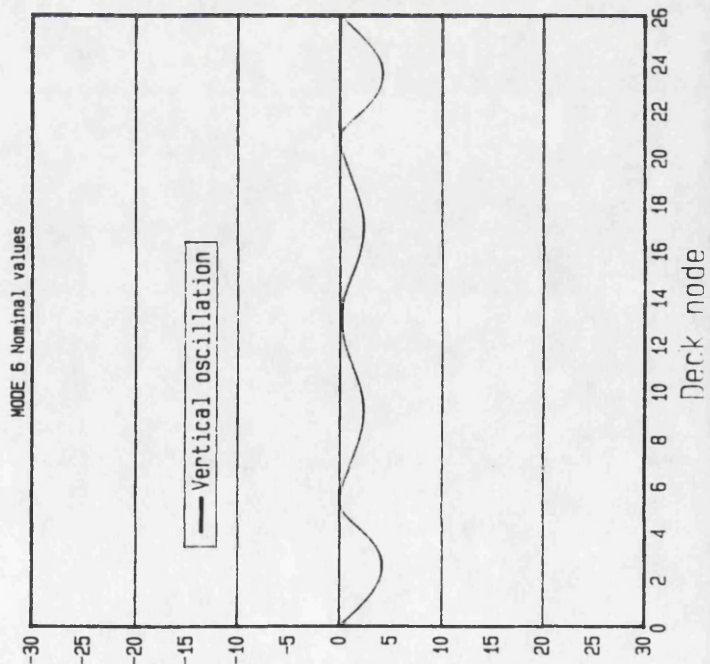
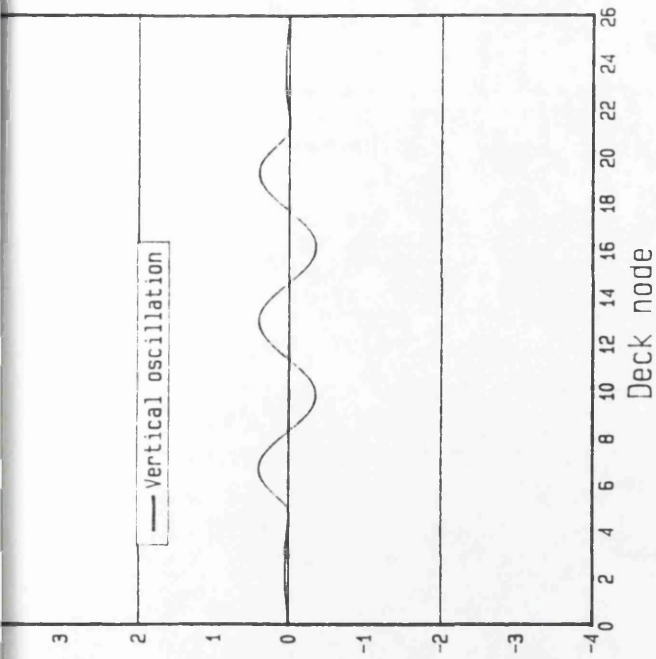
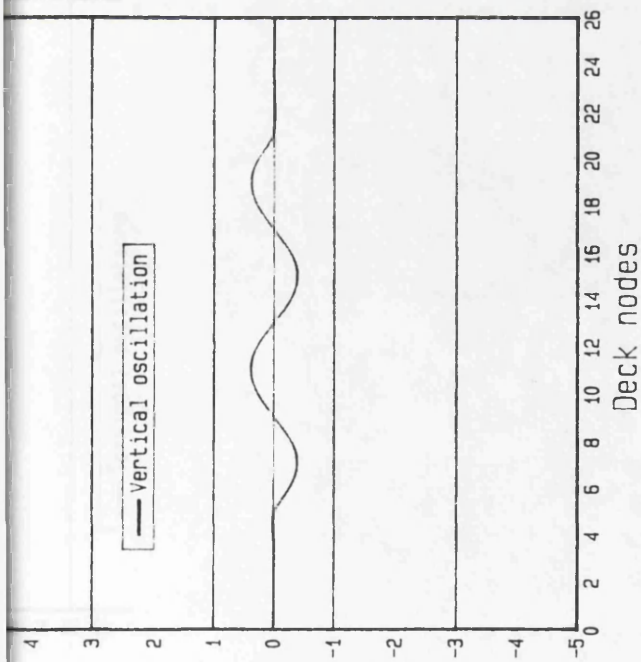


Fig. 32.b) Natural mode shapes of the bridge numerical model with Severn nominal values.

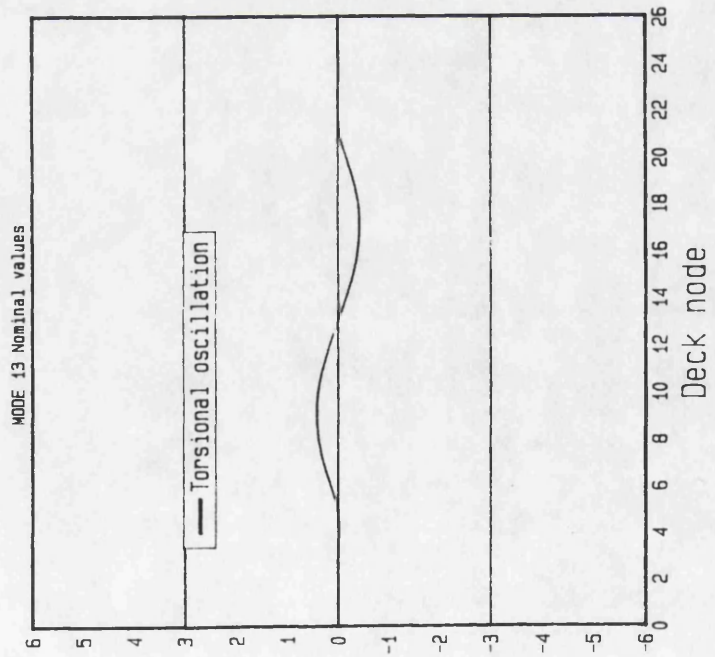
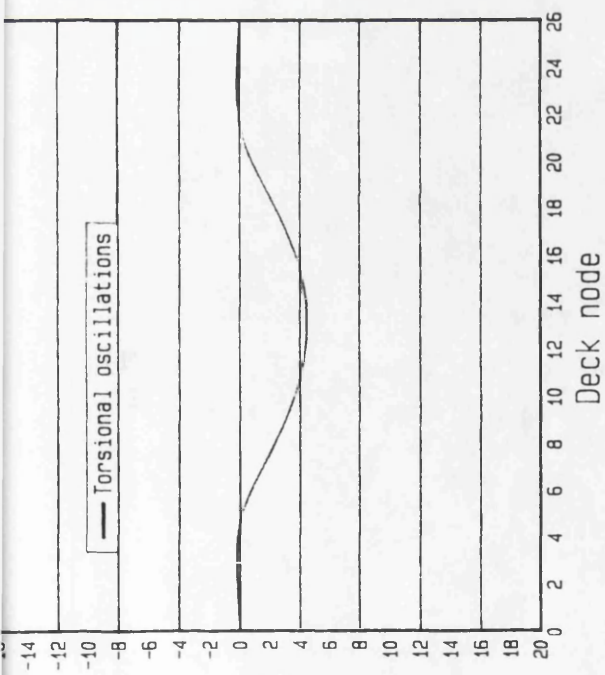
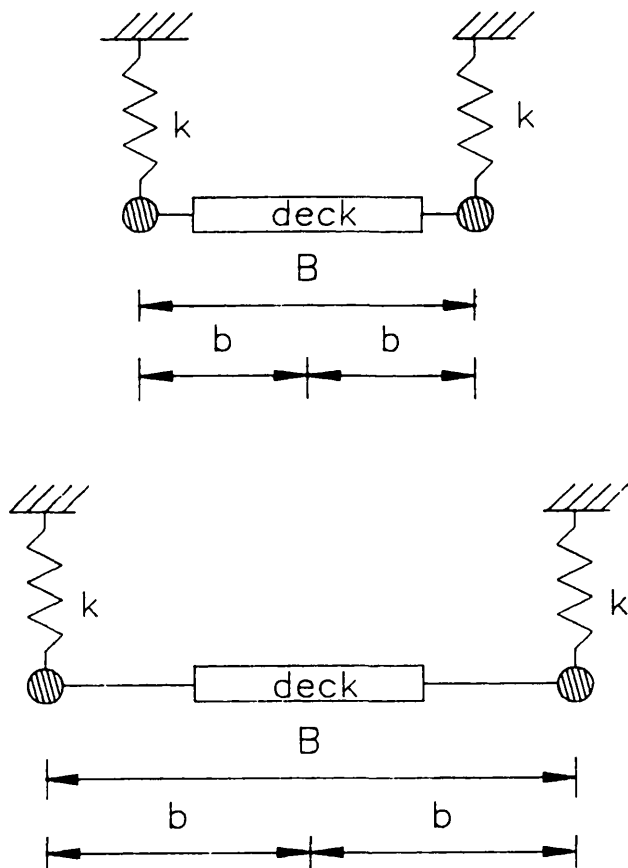


Fig. 32.c) Natural mode shapes of the bridge numerical model with Severn nominal values.



(Fig. 33) Torsional stiffness contribution of the cables proportional to the square of the cable separation B .

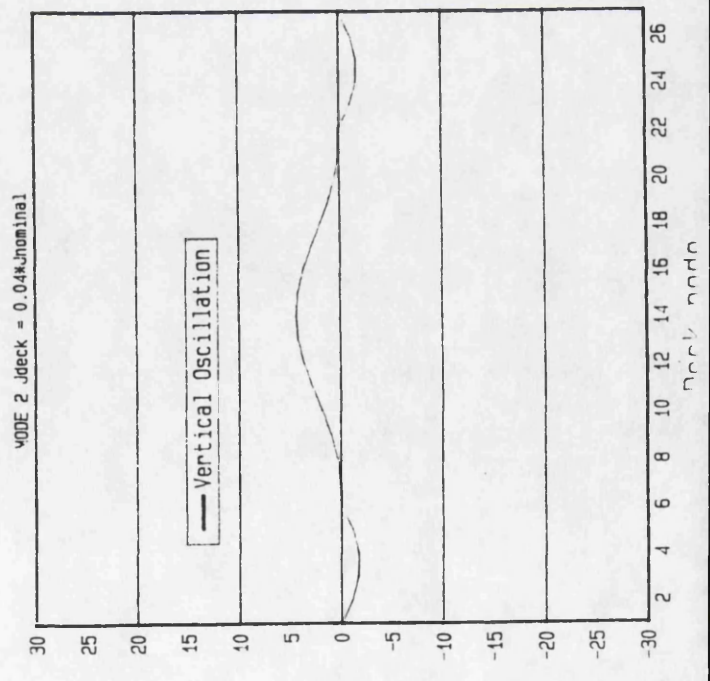
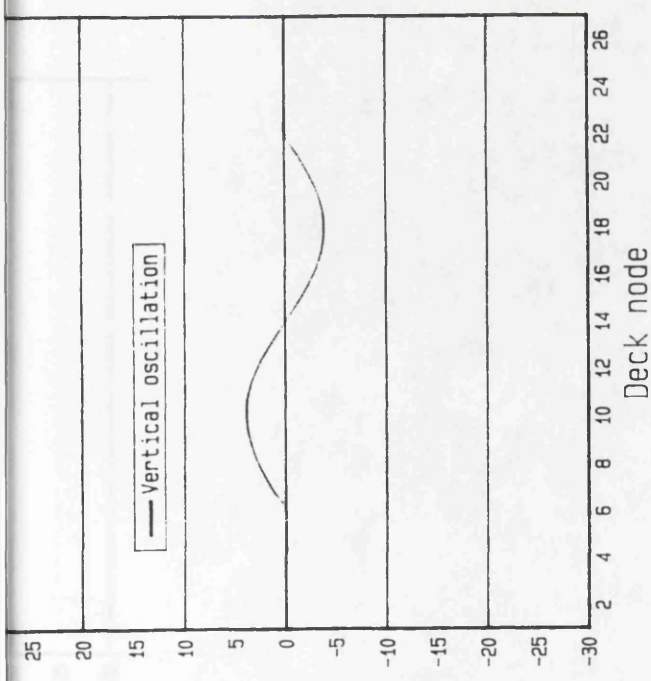
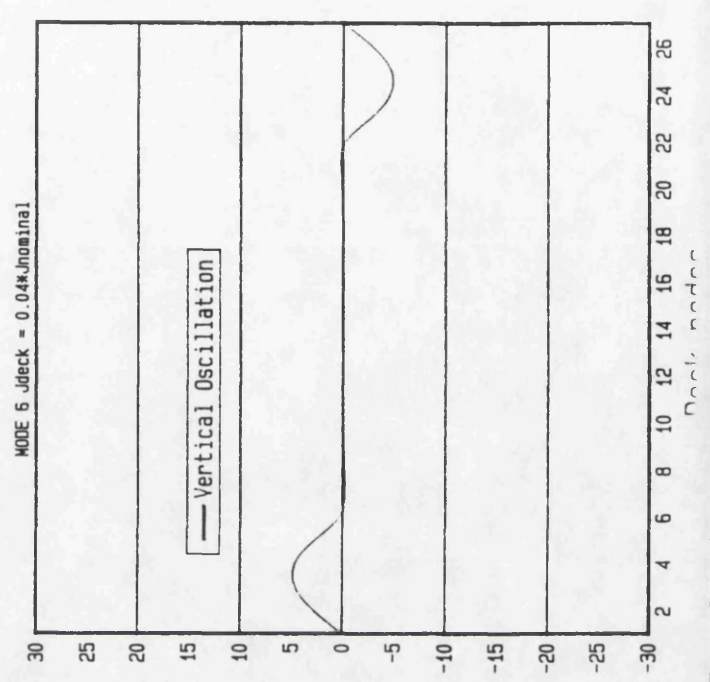
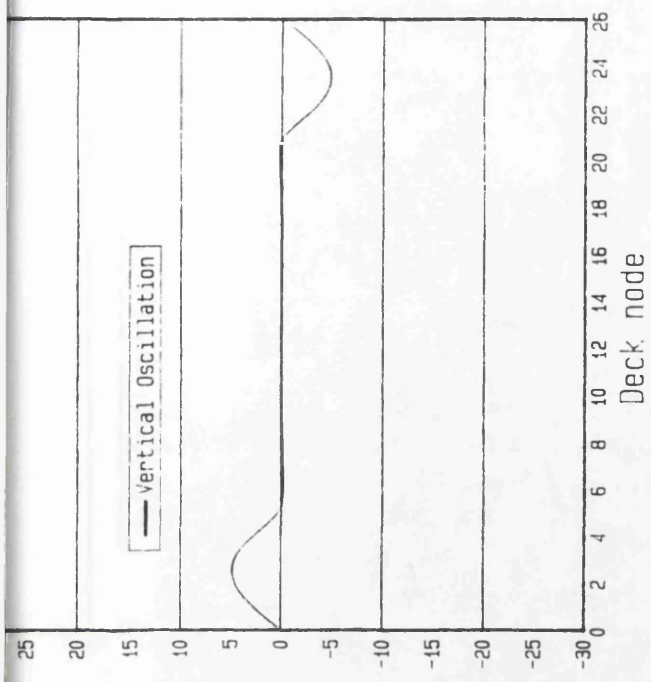
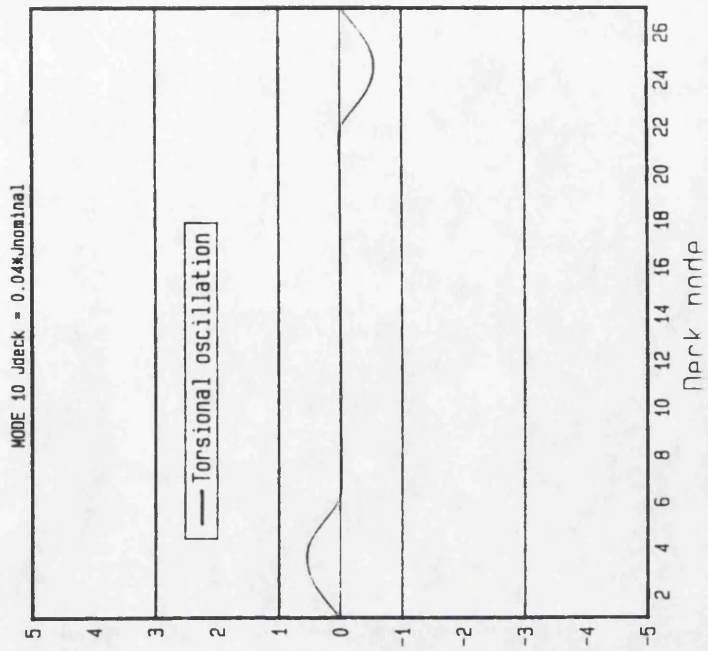
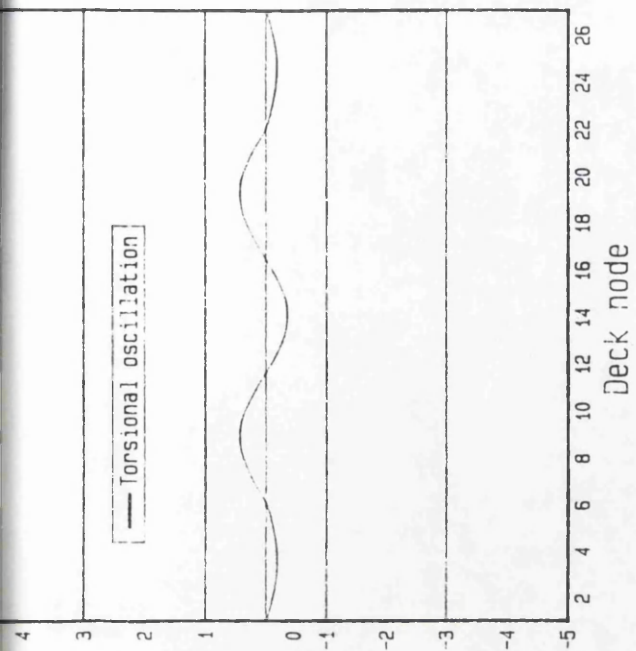
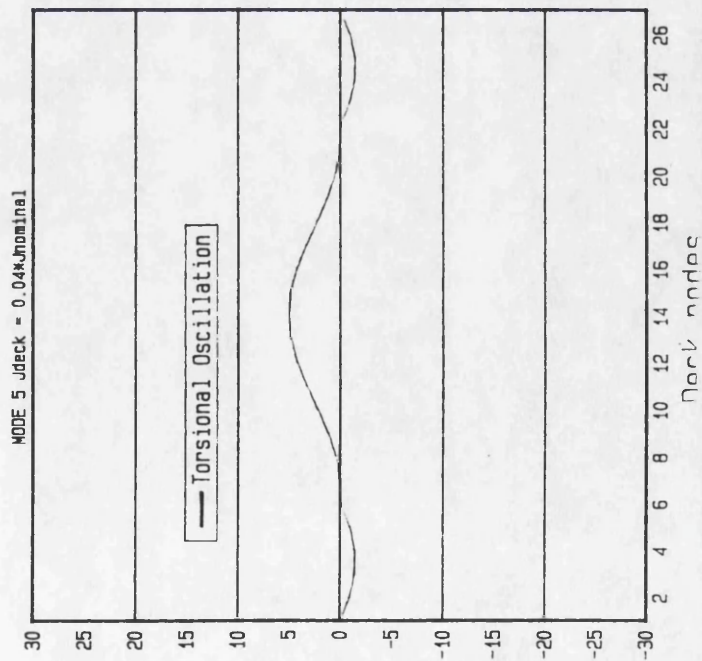
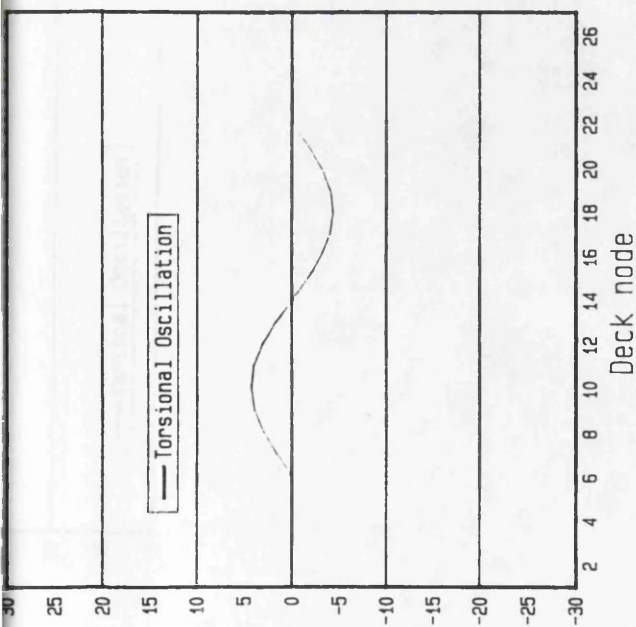
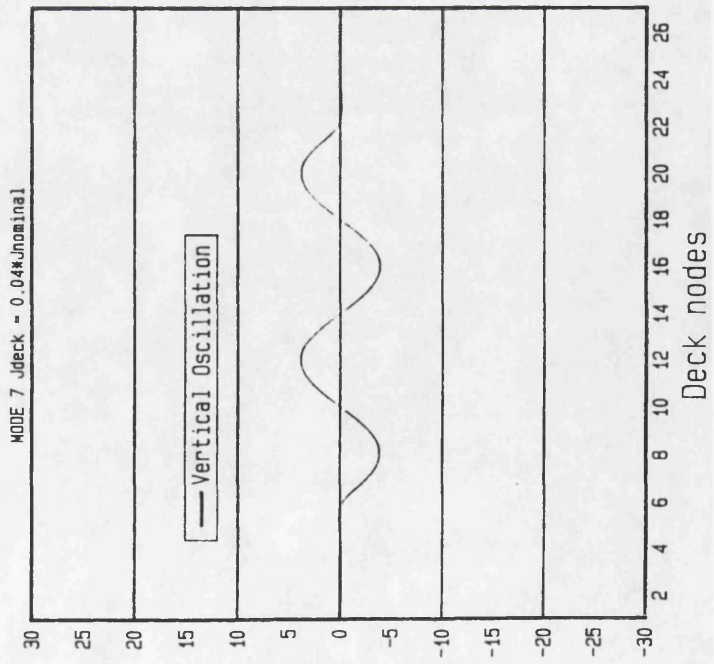
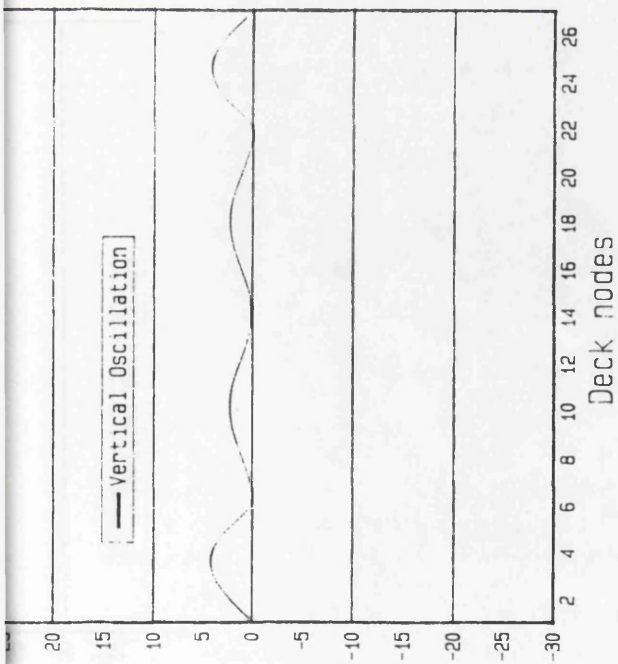


Fig. 34.a) Natural mode shapes of the bridge numerical model with torsional deck stiffness reduced by a factor of 0.04.



(Fig. 34.b) Natural mode shapes of the bridge numerical model with torsional deck stiffness reduced by a factor of 0.04.



(Fig. 34.c) Natural mode shapes of the bridge numerical model with torsional deck stiffness reduced by a factor of 0.04.

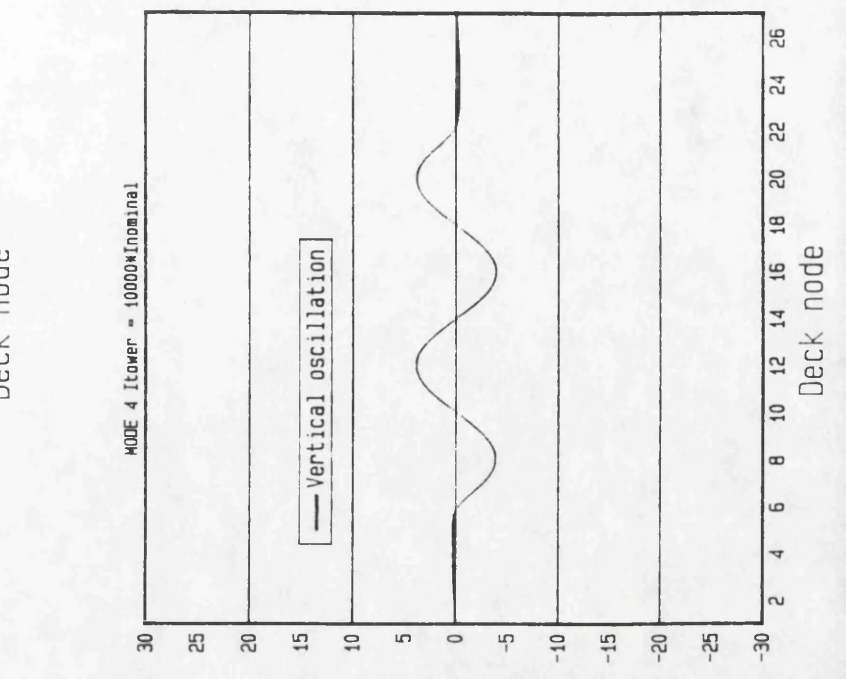
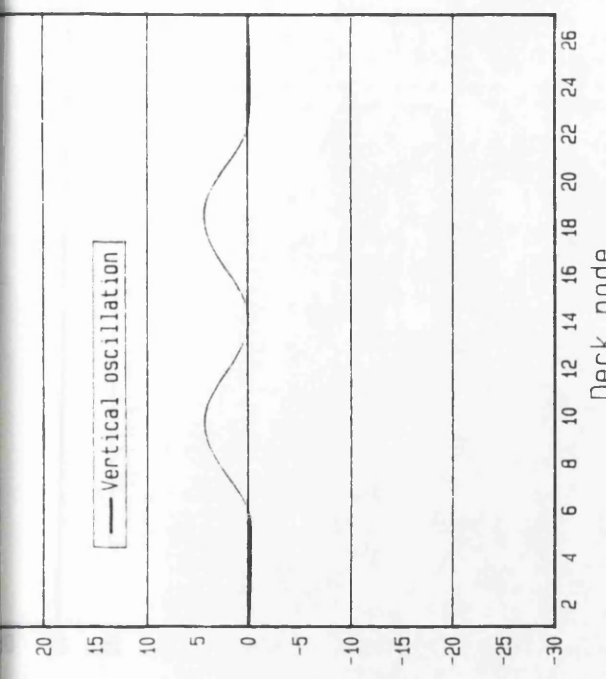
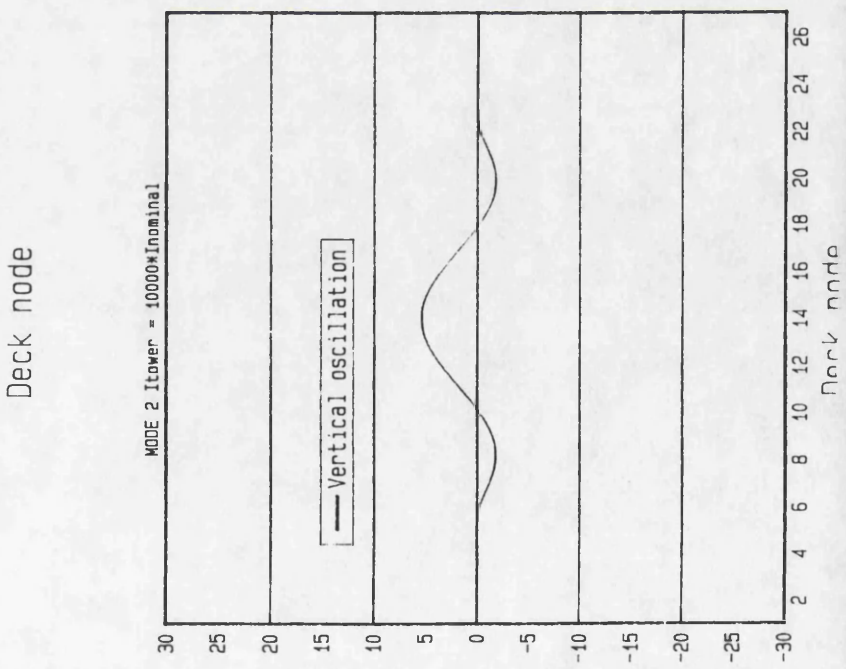
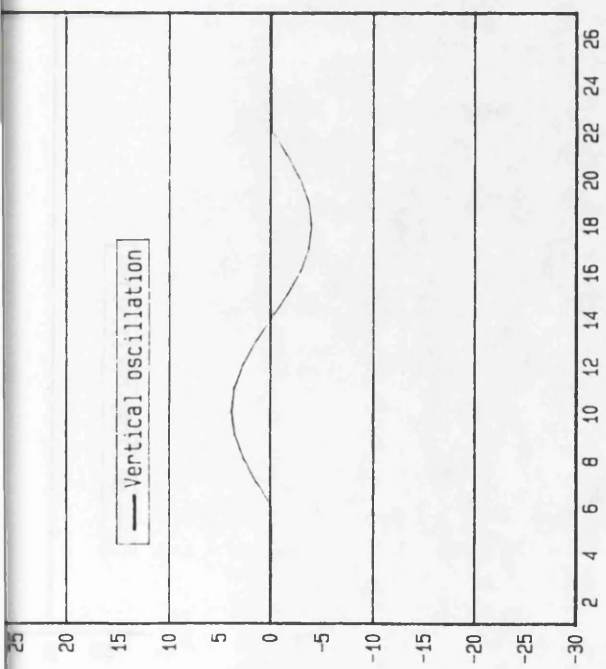


Fig. 35.a) Natural mode shapes of the bridge numerical model with tower stiffness (both in bending and in torsion) increased by a factor of 10,000.

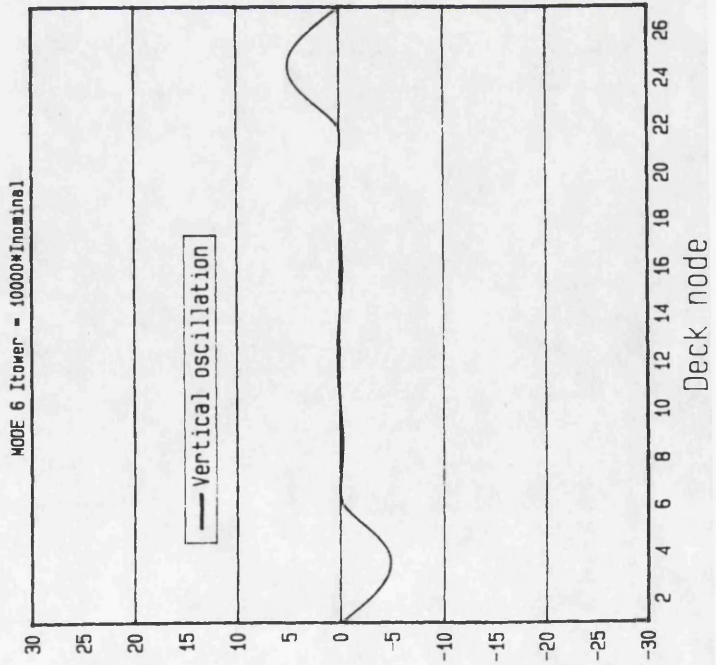
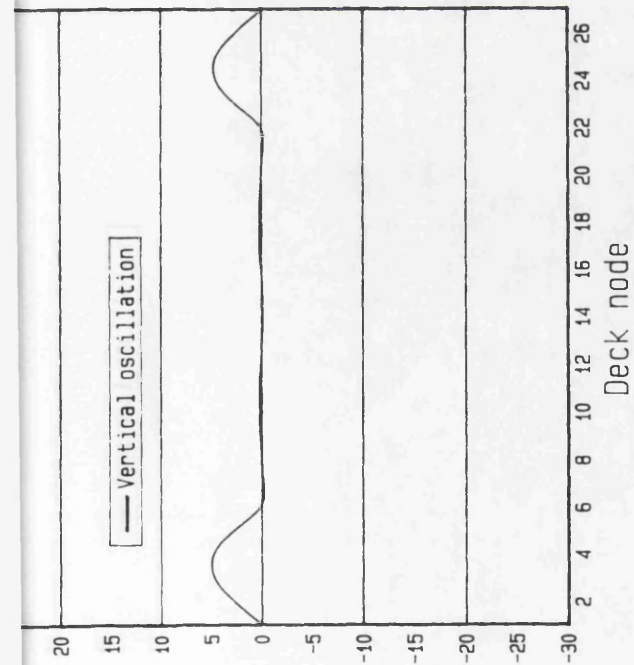
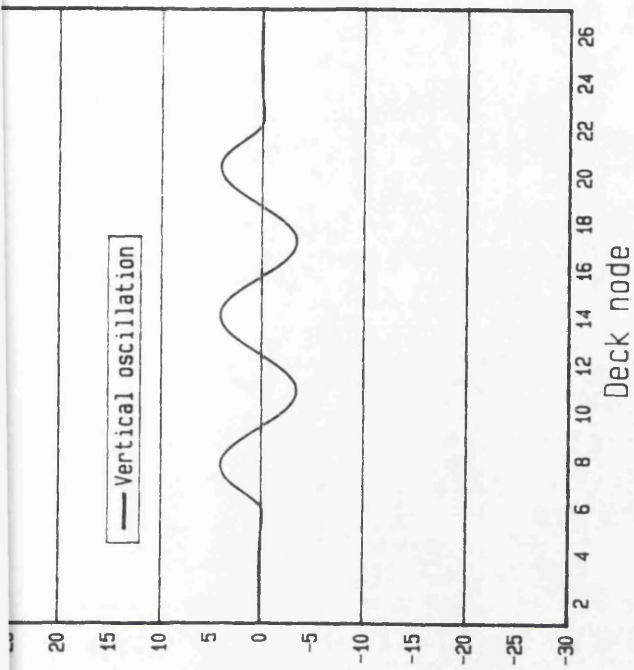


Fig. 35.b) Natural mode shapes of the bridge numerical model with tower stiffness (both in bending and in torsion) increased by a factor of 10,000.

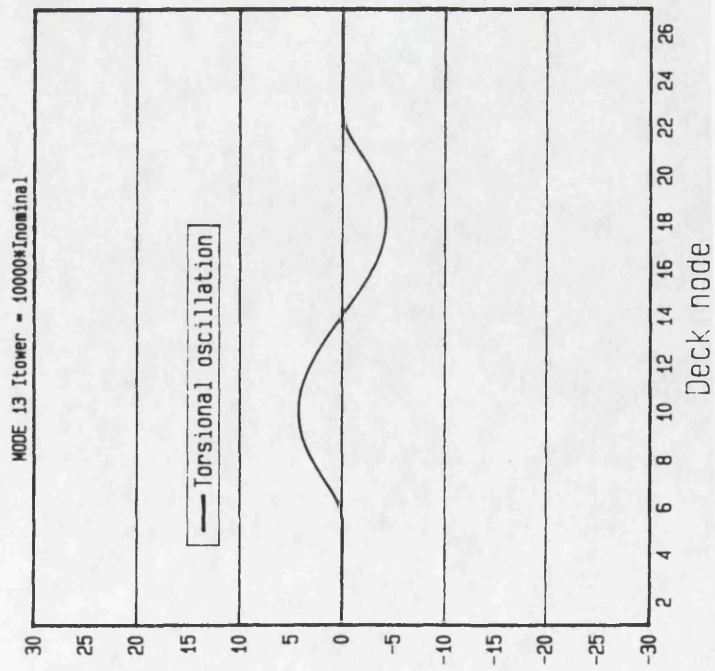
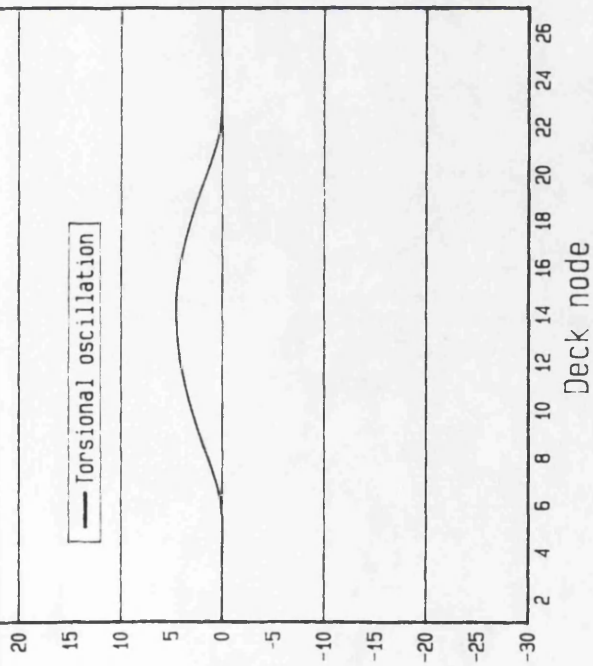
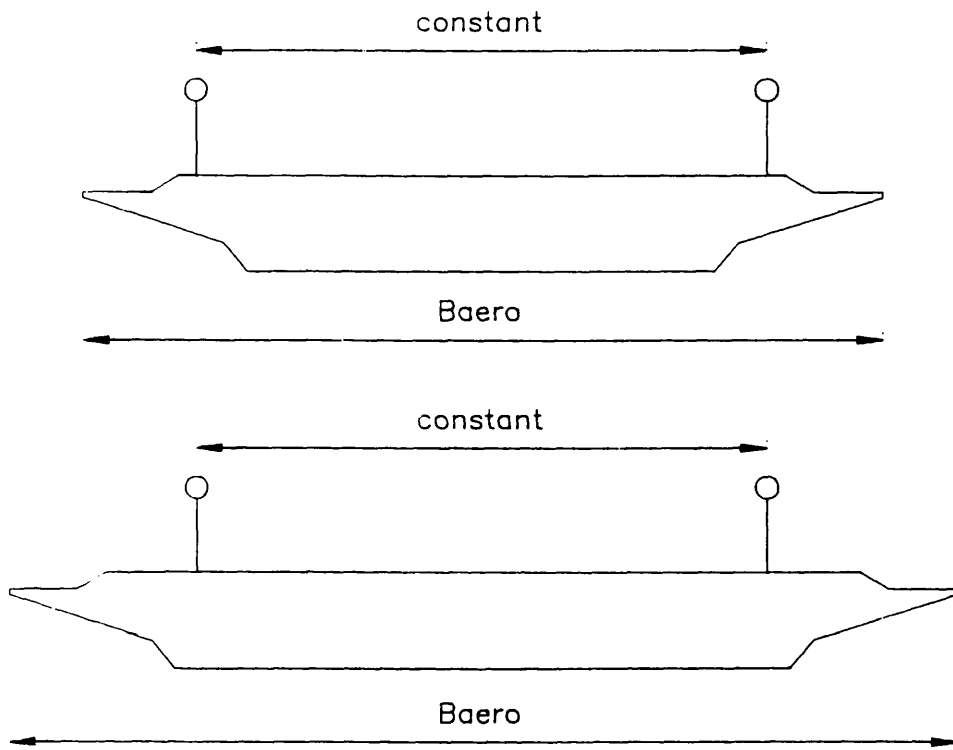
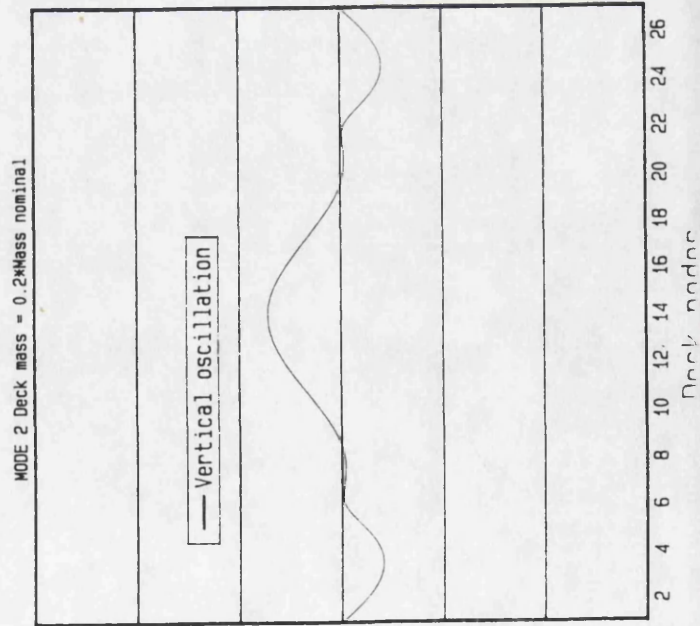
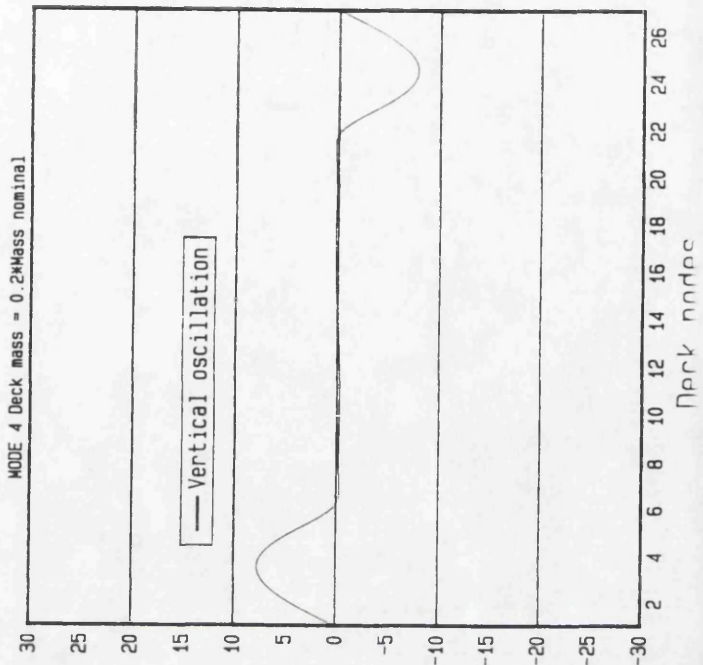
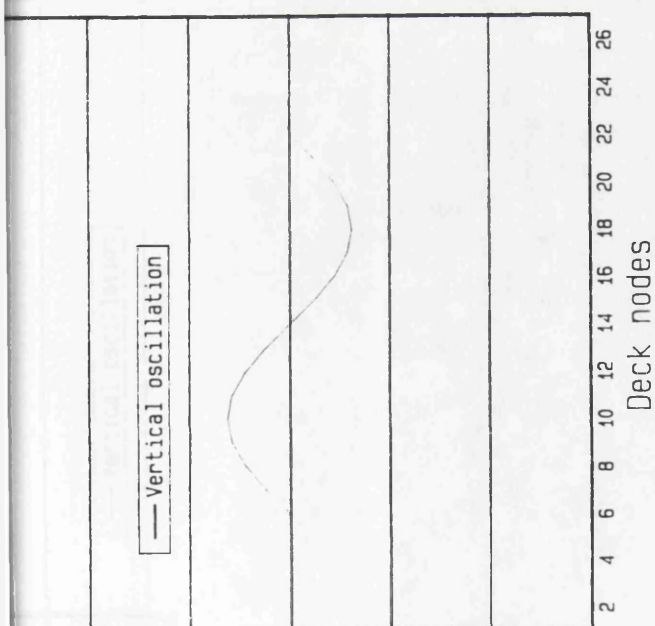
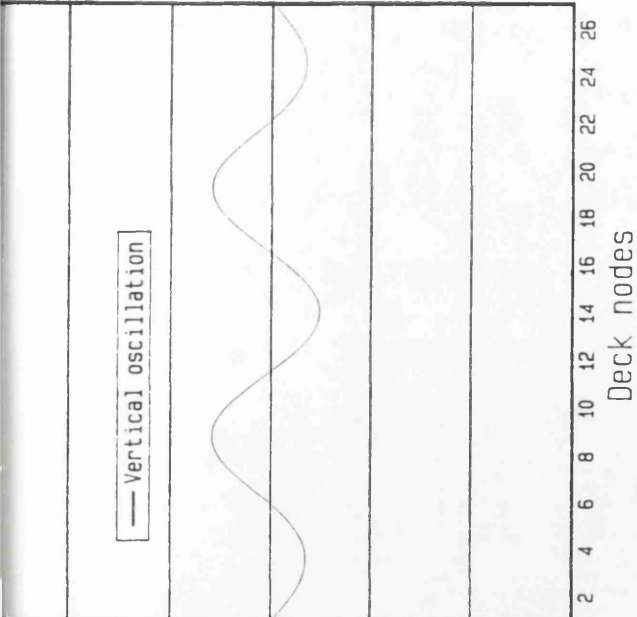


Fig. 35.c) Natural mode shapes of the bridge numerical model with tower stiffness (both in bending and in torsion) increased by a factor of 10,000.



(Fig. 36) Altering aerodynamic width of the deck B_{aero} .



(Fig. 37.a) Natural mode shapes of the bridge numerical model with deck mass reduced to 20% the nominal value.

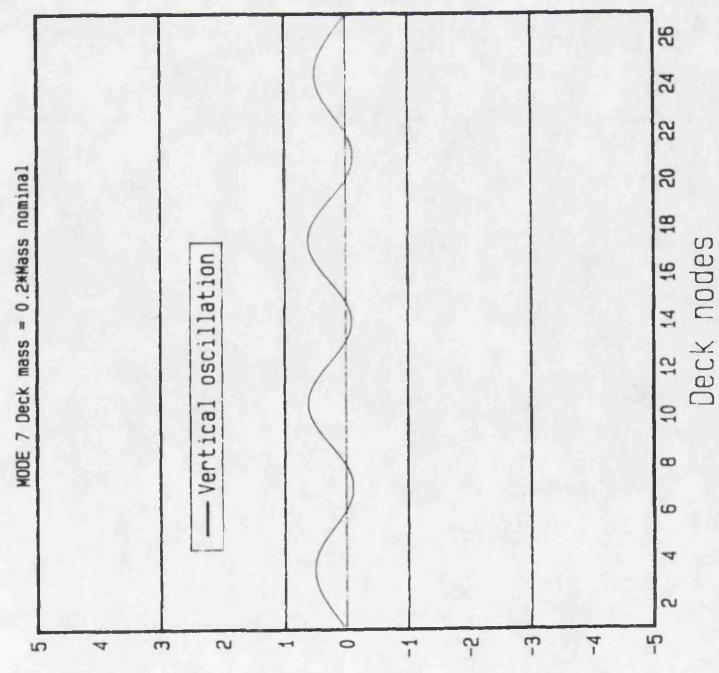
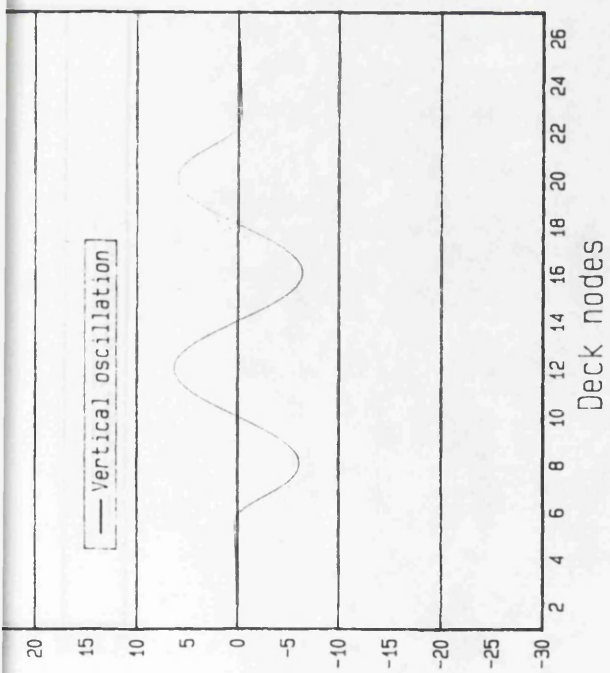


(Fig. 37.b) Natural mode shapes of the bridge numerical model with deck mass reduced to 20% the nominal value.

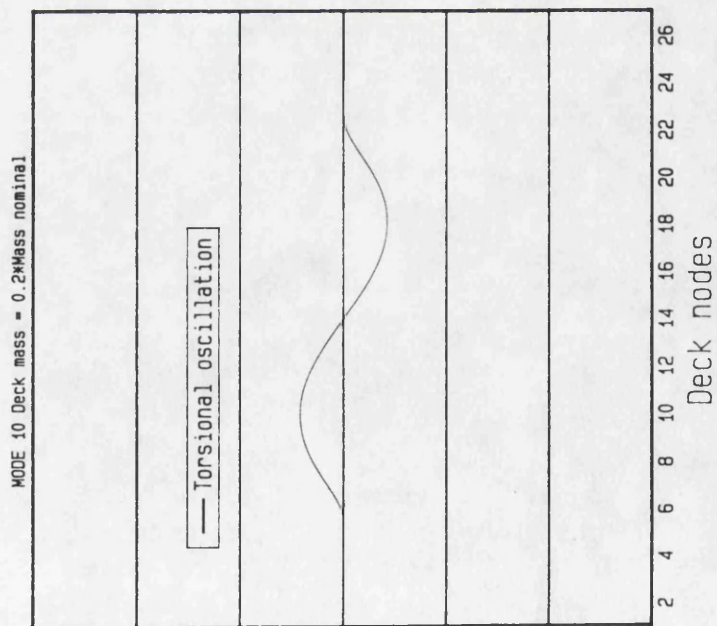
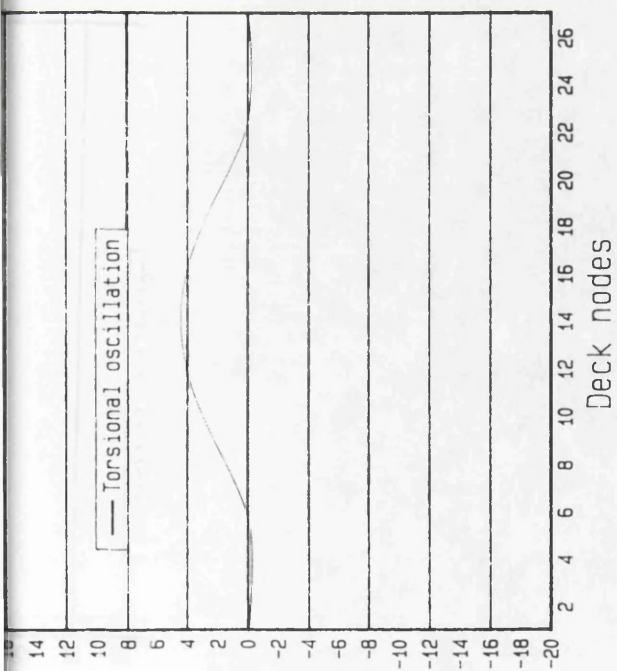
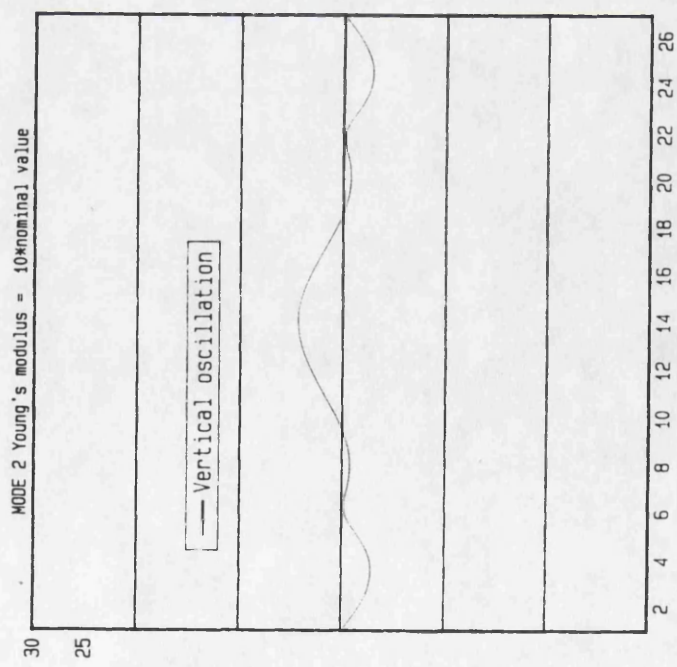
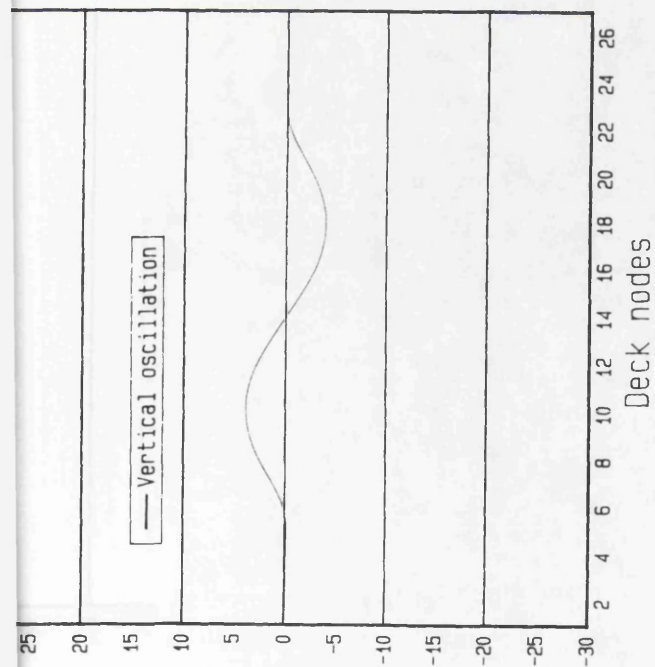
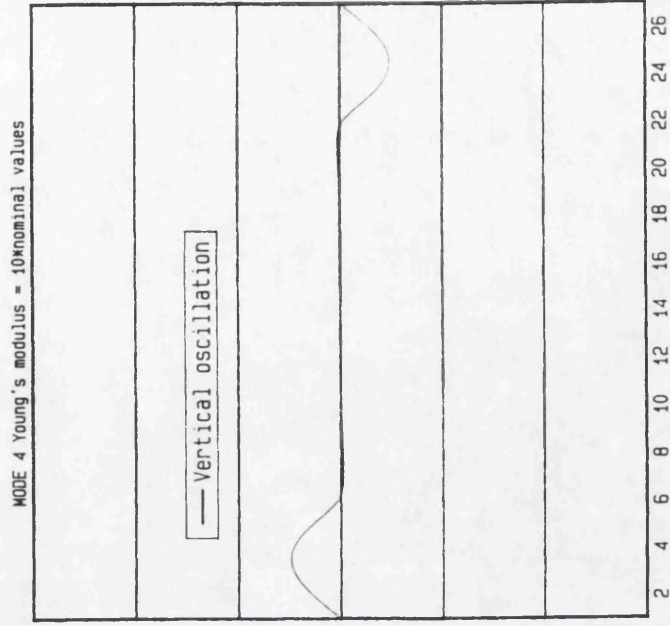
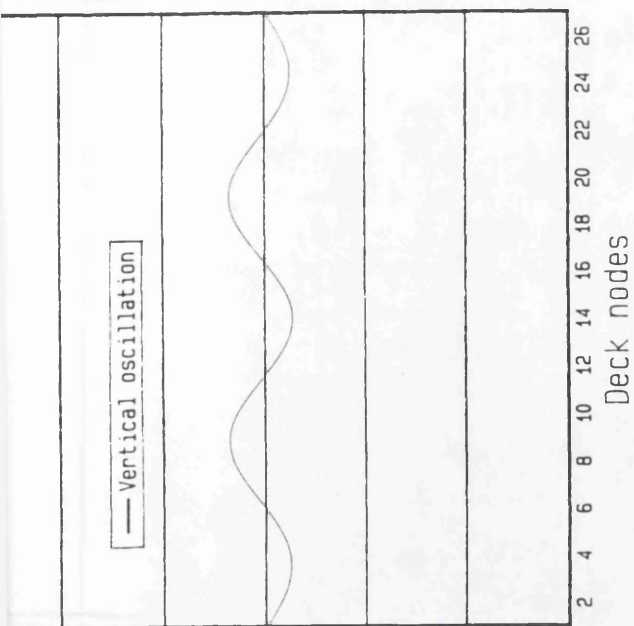
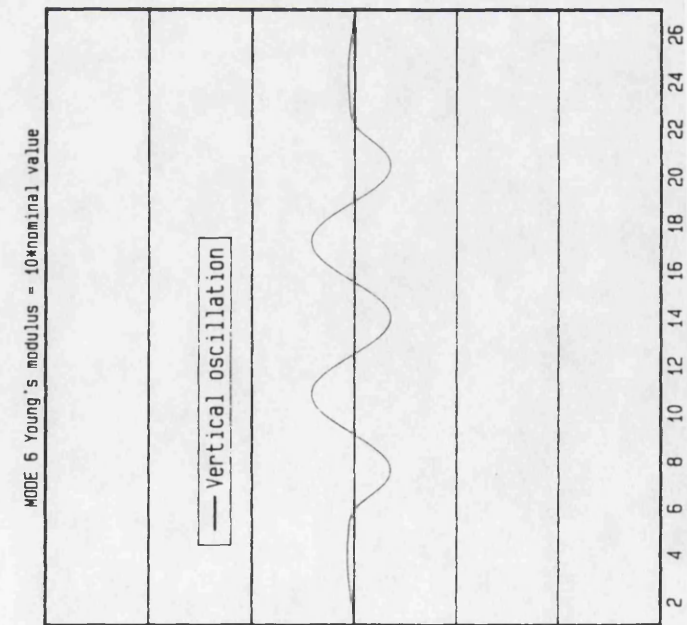
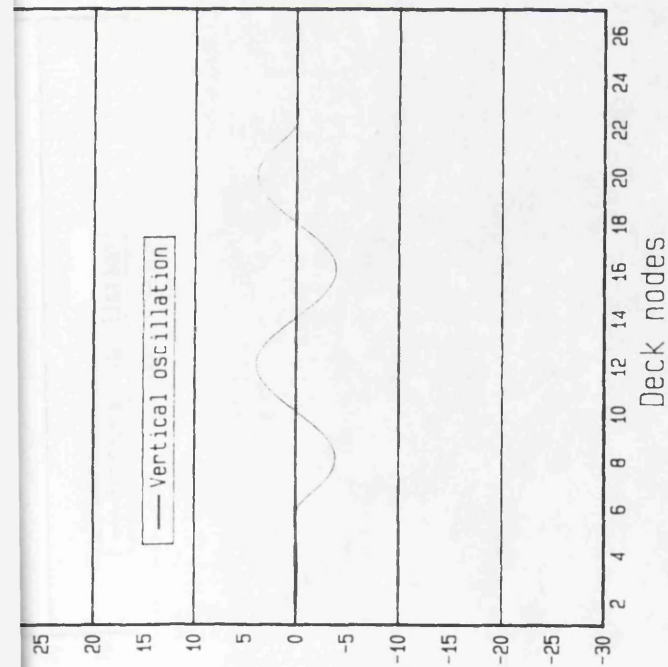
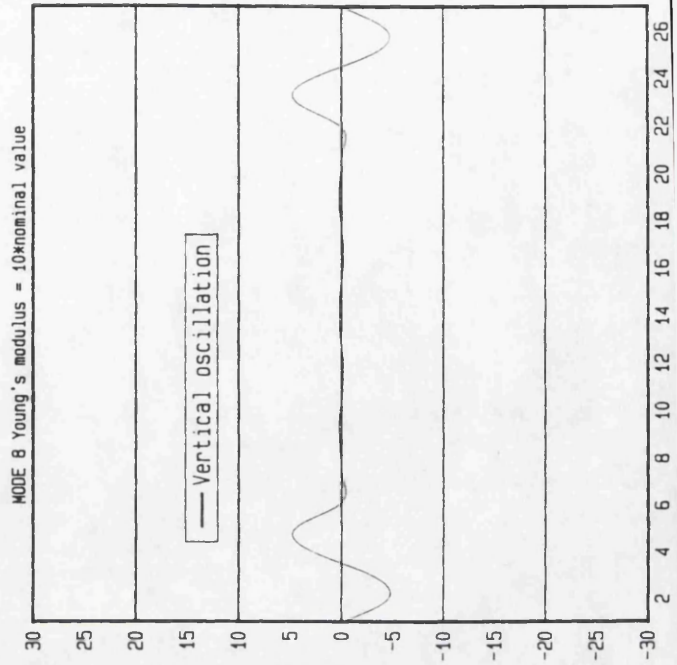
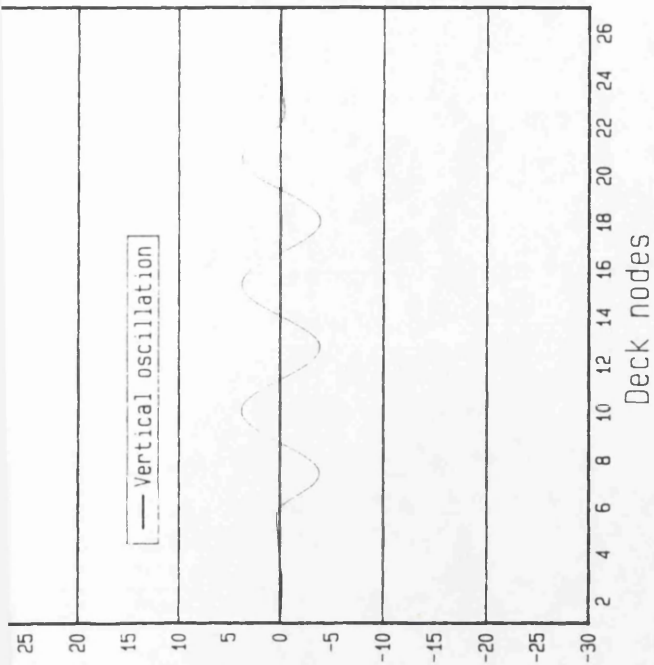


fig. 37.c) Natural mode shapes of the bridge numerical model with deck mass reduced to 20% the nominal value.



(Fig. 38.a) Natural mode shapes of the bridge numerical model with cables Young's modulus increased 10 times the nominal value.



(Fig. 38.b) Natural mode shapes of the bridge numerical model with cables Young's modulus increased 10 times the nominal value.

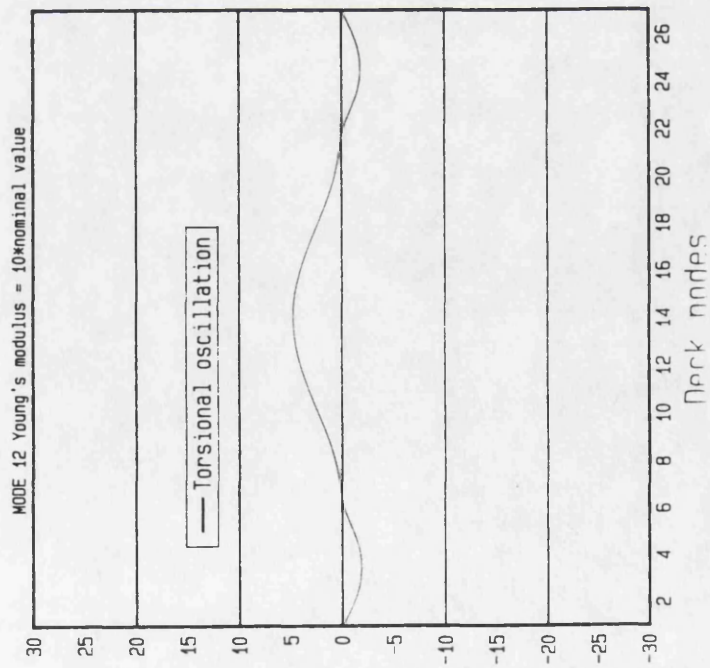
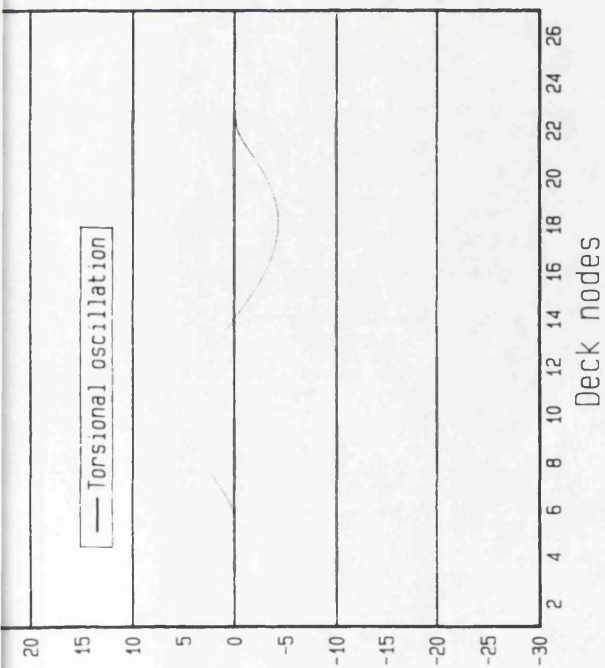
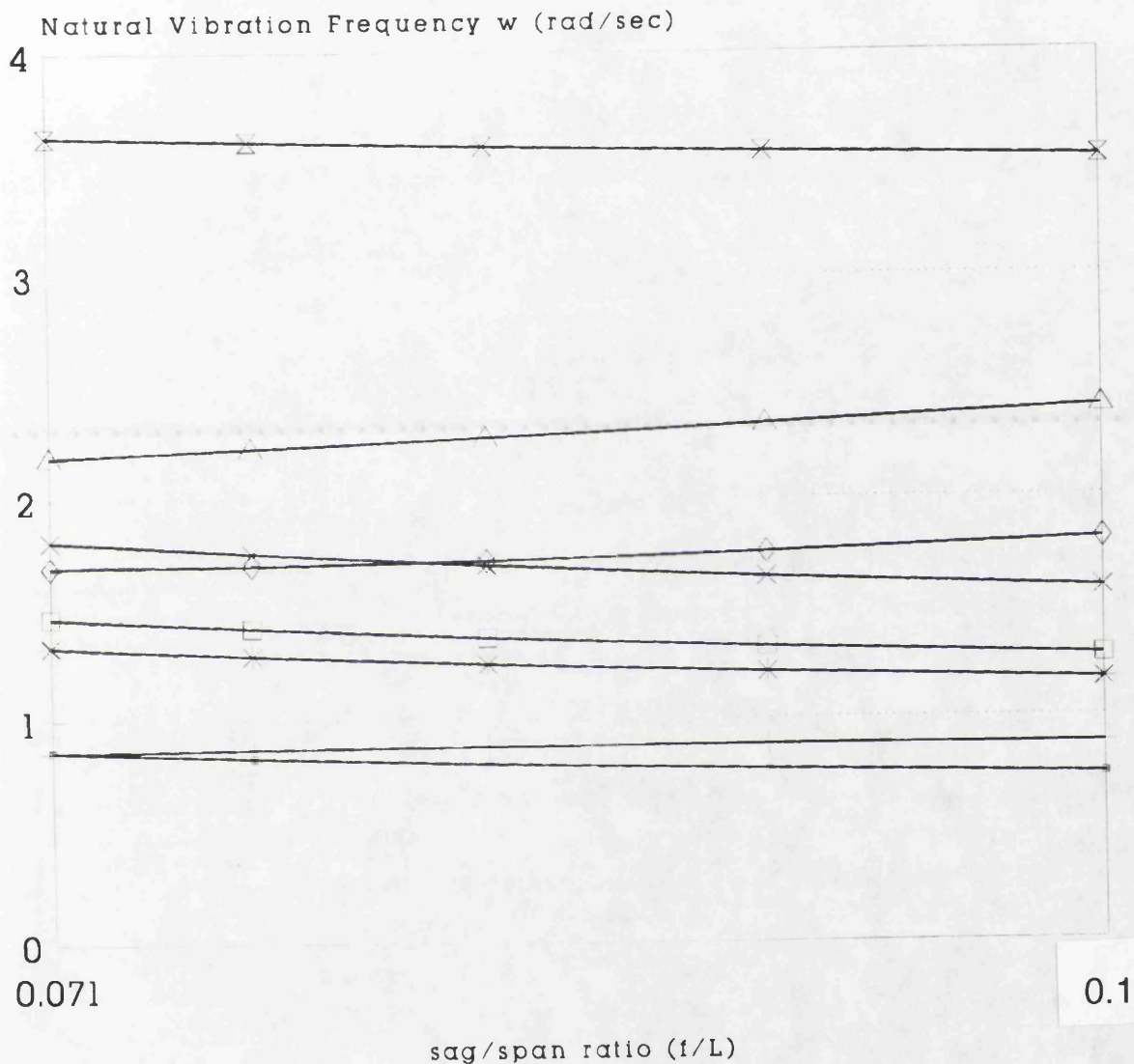


(Fig. 38.c) Natural mode shapes of the bridge numerical model with cables Young's modulus increased 10 times the nominal value.

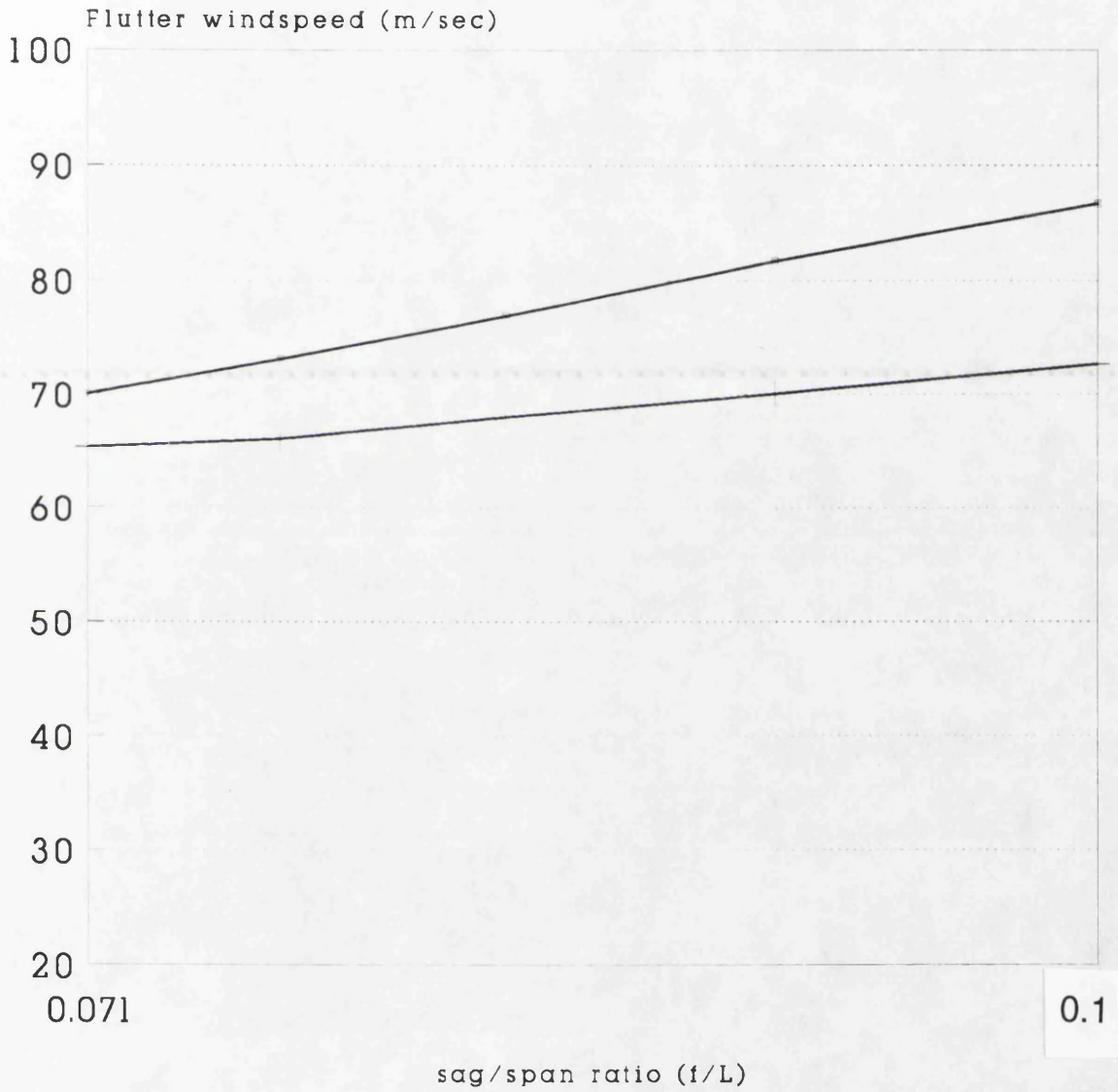
Natural Frequencies calculated by ANSUSP



- | | | | |
|---------|-----------|-----------|-----------|
| — 1-A-F | — 1-S-F | — 2-S-F | —□— 2-A-F |
| — 3-A-F | —◇— 3-S-F | —△— 1-S-T | —×— 2-A-T |

Graph 1 Effect on natural frequencies of varying sag/span ratio keeping $h-f=const$
All other properties as in (Fig.29)

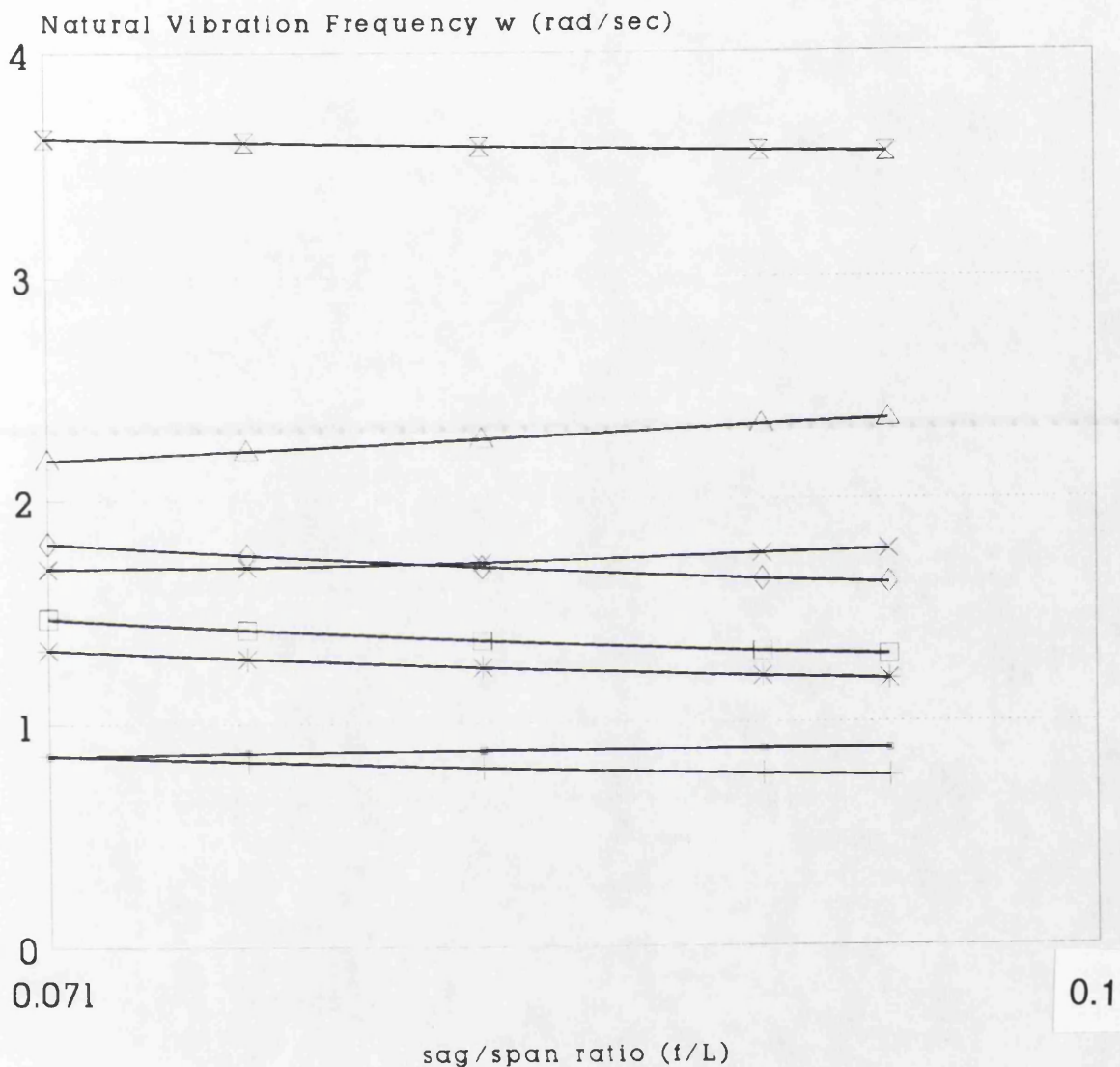
Flutter windspeeds calculated by ANSUSP
Modal flutter analysis including only
symmetric modes.



— ANSUSP Modal Symm. — Selberg

Graph2 Effect on flutter windspeed of
varying sag/span ratio keeping $h-f=\text{const}$
All other properties as in (Fig.29)

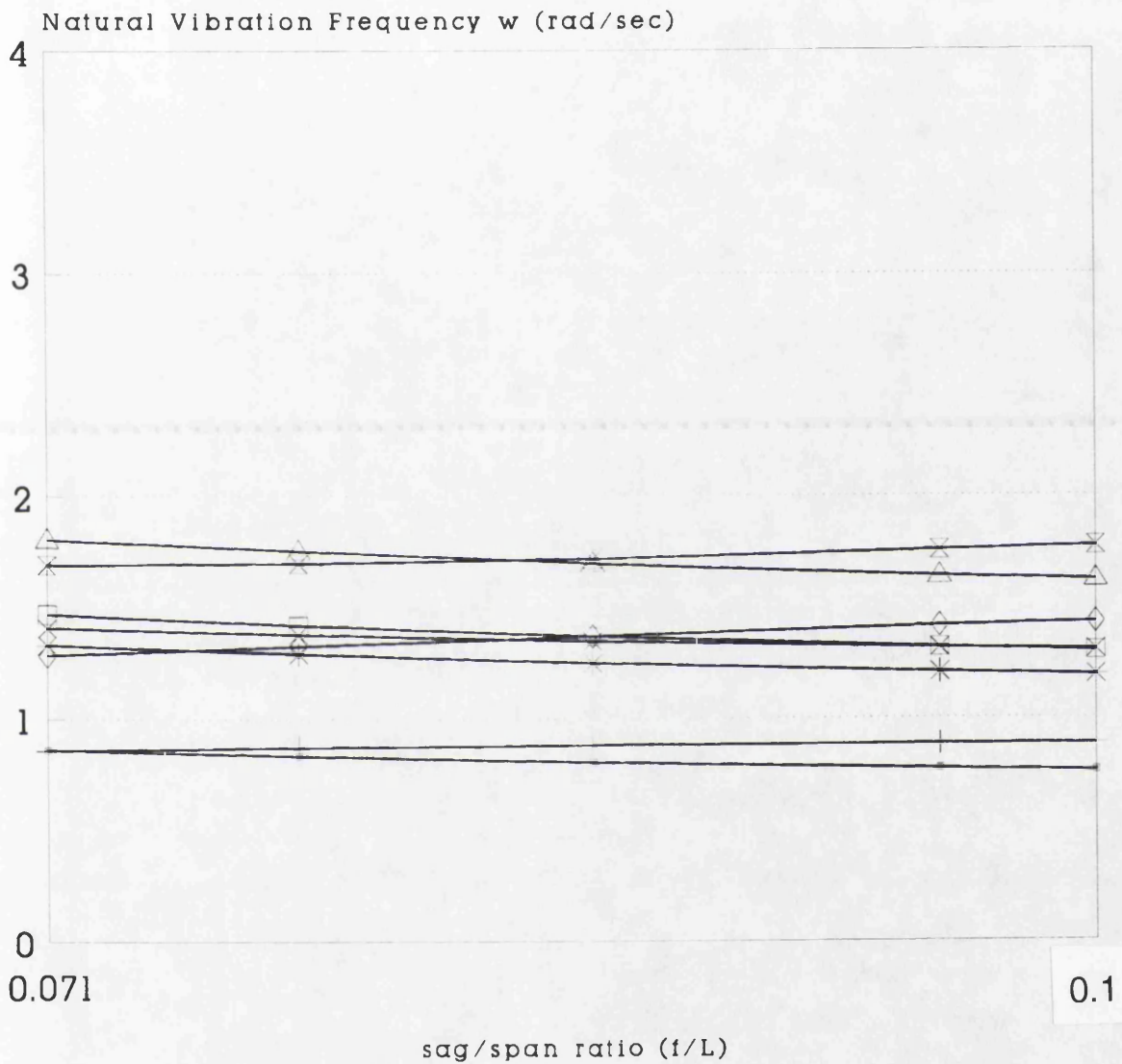
Natural Frequencies calculated by ANSUSP



- | | | | |
|-----------|-----------|-----------|-----------|
| —●— 1-S-F | —+— 1-A-F | —x— 2-S-F | —□— 2-A-F |
| —*— 3-S-F | —◇— 3-A-F | —△— 1-S-T | —x— 1-A-T |

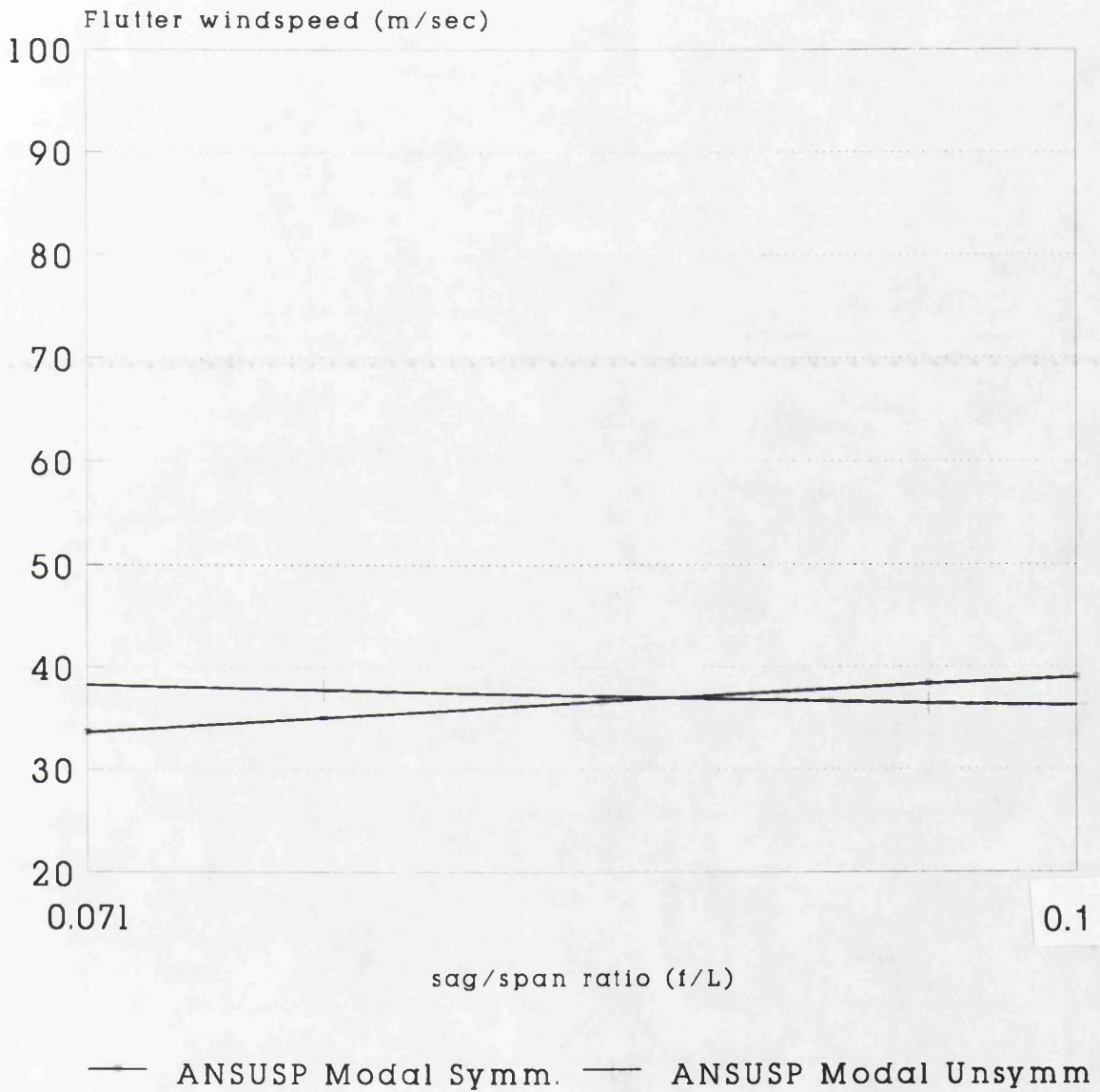
Graph3 Effect on natural frequencies of varying sag/span ratio keeping h =const. All other properties as in (Fig.29)

Natural frequencies calculated by ANSUSP



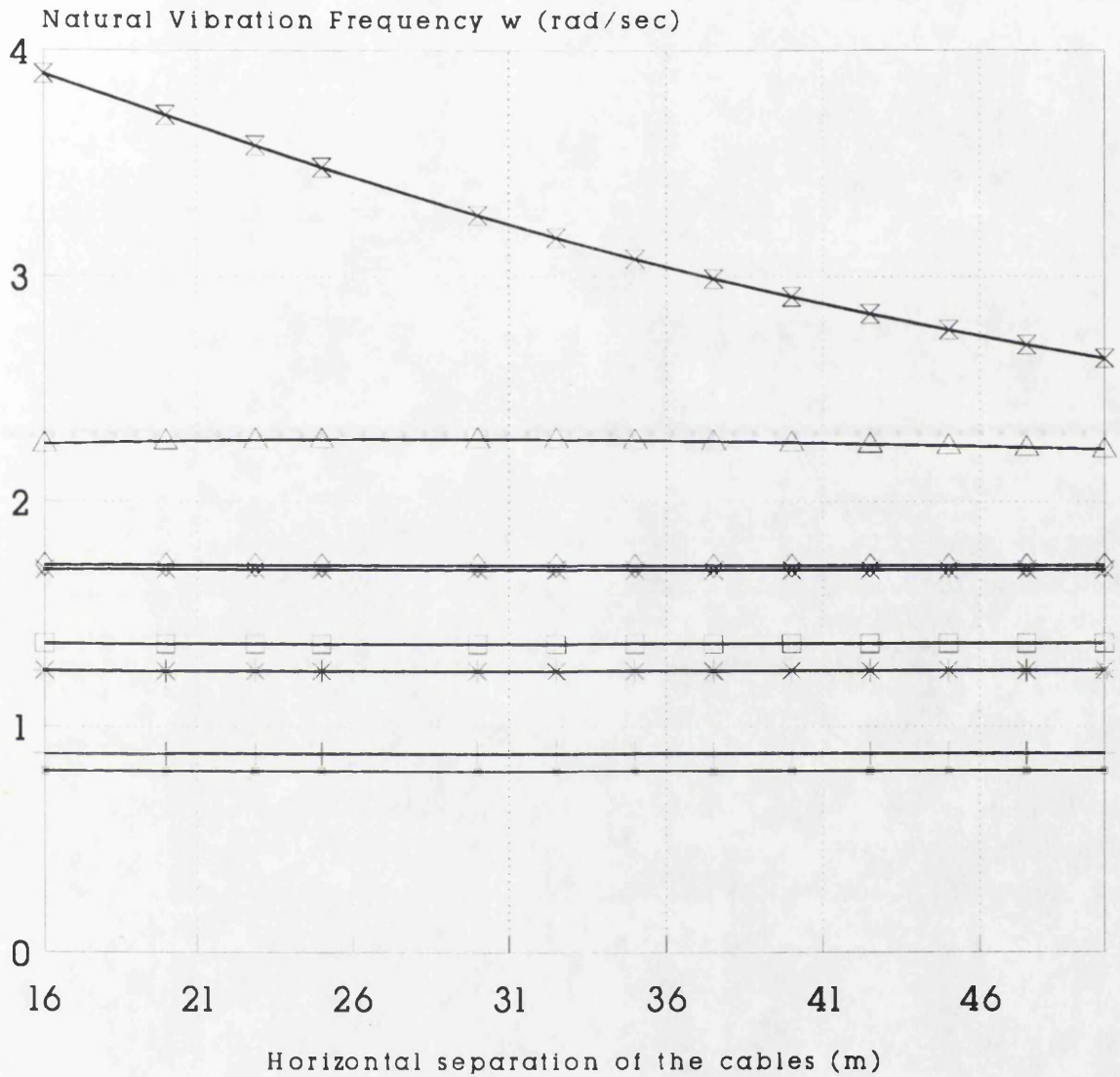
Graph4 Effect on natural frequencies of varying sag/span ratio, $J_{deck}=0.07 \cdot J_{nom}$. All other properties as in (Fig.29)

Flutter windspeeds calculated by ANSUSP
Modal flutter analysis including only
symmetric and only antisymmetric modes



Graph5 Effect on flutter windspeed of
varying sag/span ratio, $J_{deck}=0.07J_{nom}$.
All other properties as in (Fig.29)

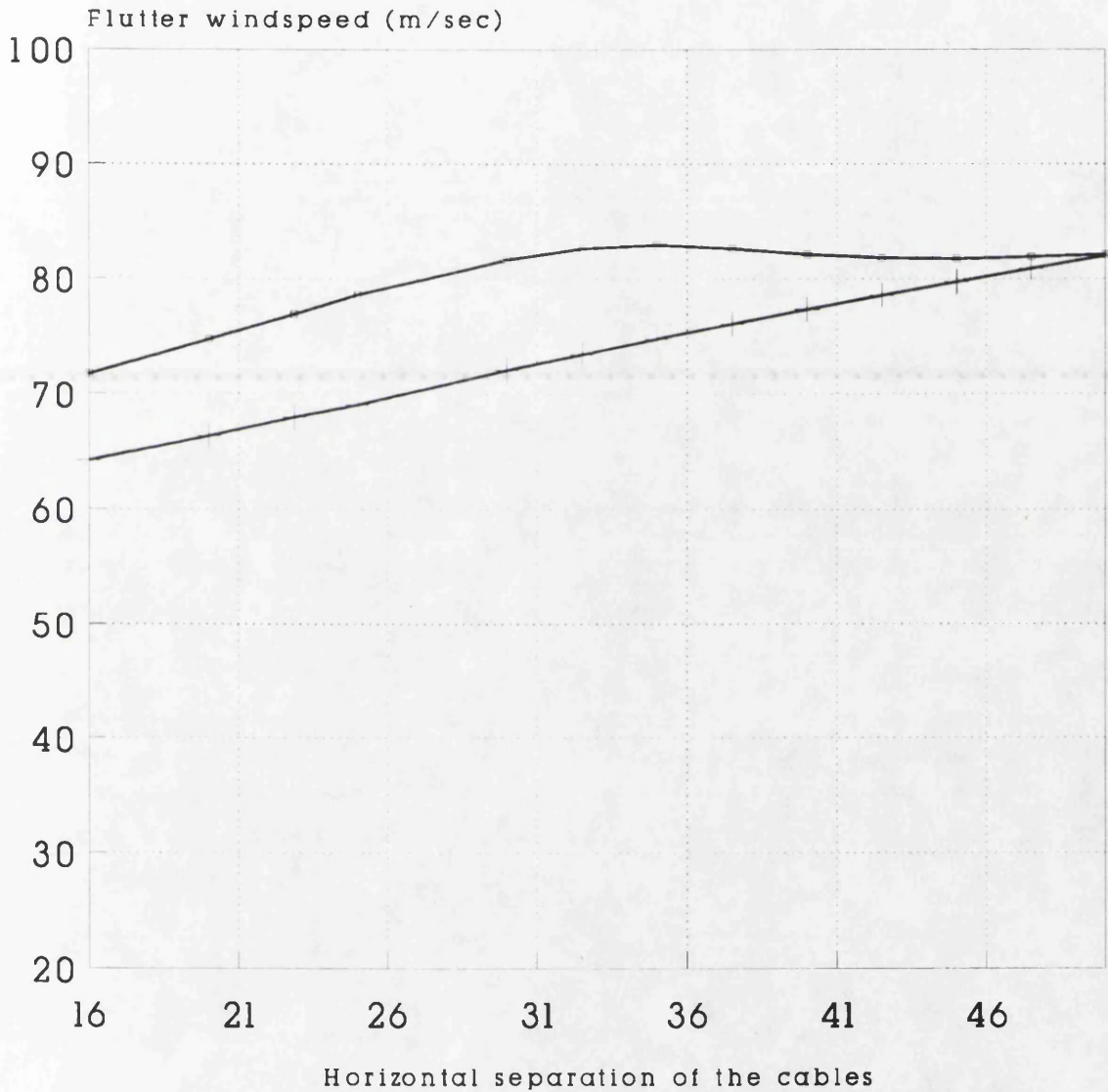
Natural frequencies calculated by ANSUSP



- | | | | |
|-----------|-----------|-----------|-----------|
| —●— 1-A-F | —+— 1-S-F | —×— 2-S-F | —□— 2-A-F |
| —×— 3-A-F | —◇— 3-S-F | —△— 1-S-T | —⊗— 1-A-T |

Graph 6 Effect on natural frequencies on varying horizontal separation of cables
All other properties as in (Fig.29)

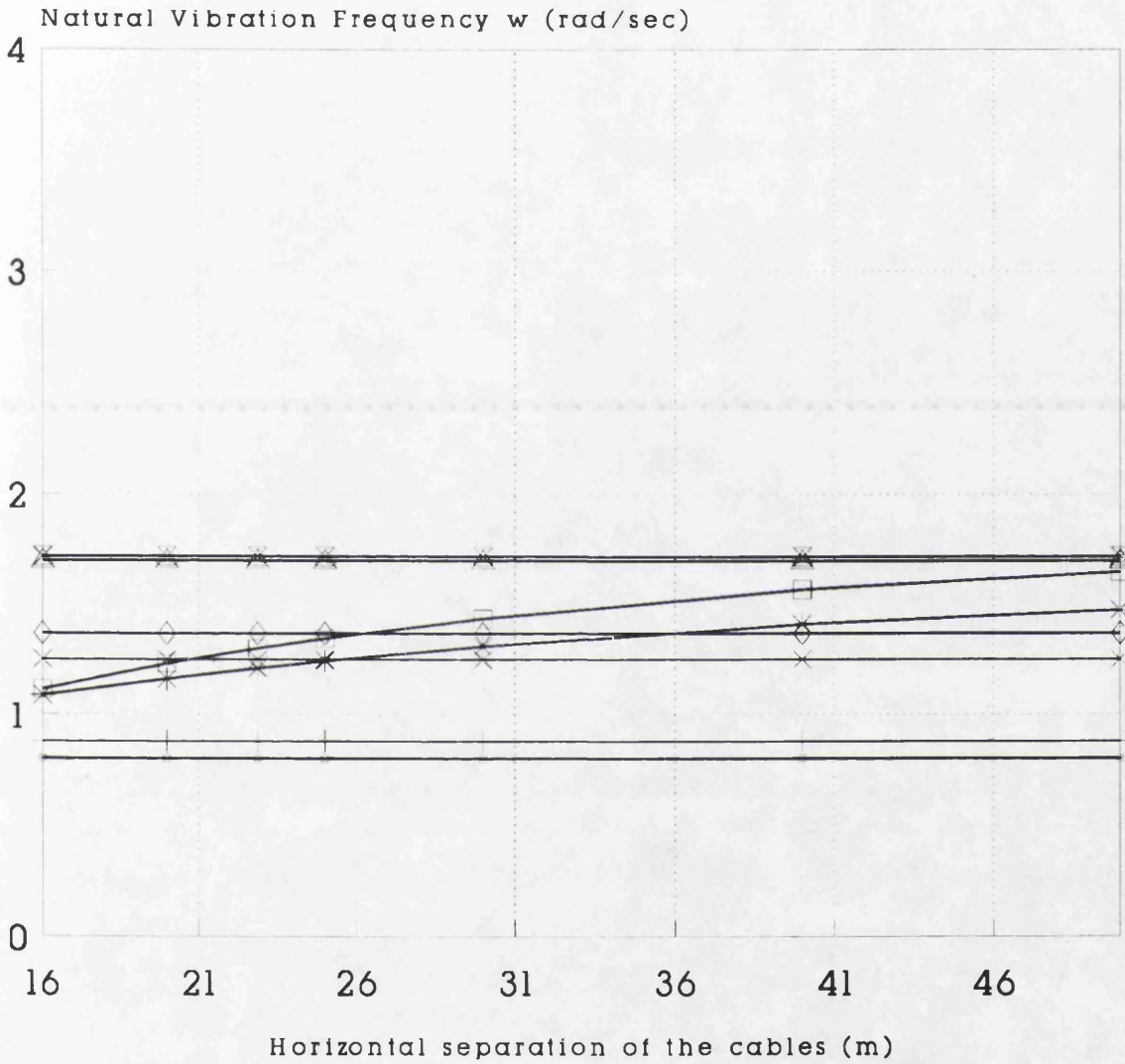
Flutter windspeeds calculated by ANSUSP
Modal flutter analysis including only
symmetric modes



— ANSUSP Modal Symm. — Selberg

Graph7 Effect on flutter windspeed of
varying horizontal separation of cables
All other properties as in (Fig.29)

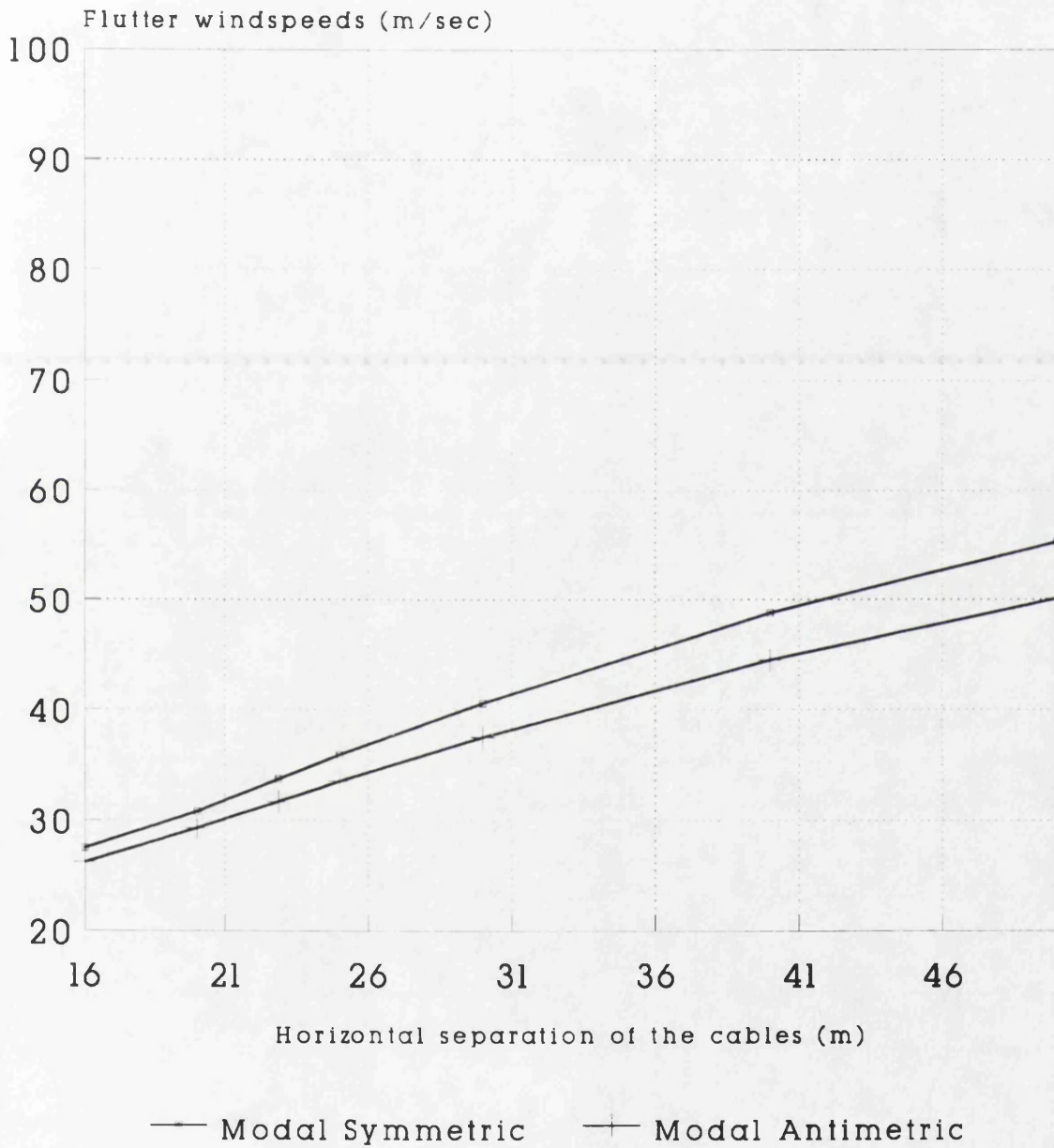
Natural frequencies calculated by ANSUSP
 Deck torsional stiffness $J_{deck} = 0.04 \cdot J_{nom}$



- 1-A-F — 1-S-F — x — 1-A-T — □ — 1-S-T
- x — 2-S-F — ◇ — 2-A-F — △ — 3-A-F — x — 3-S-F

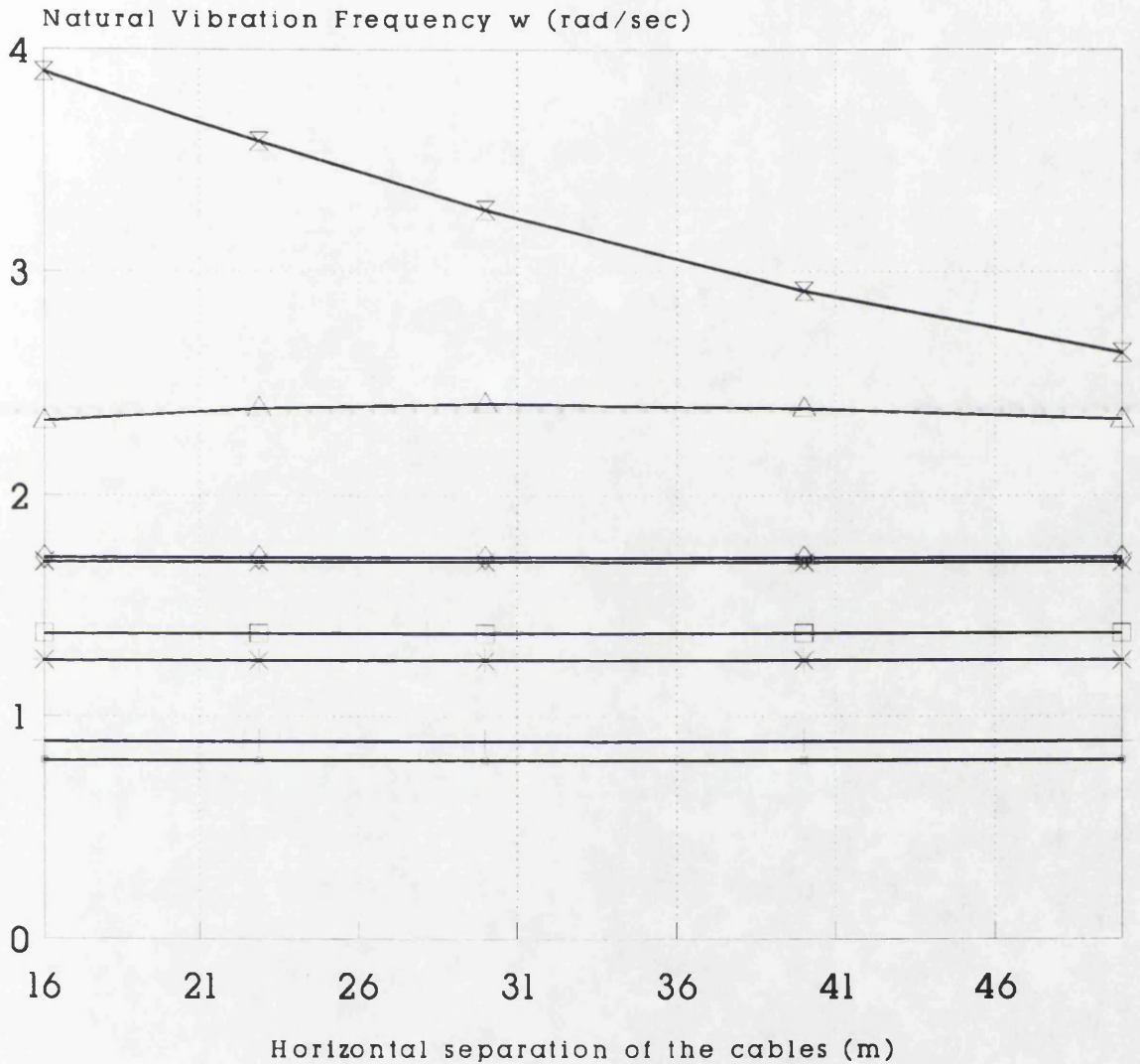
Graph8 Effect on natural frequencies of varying horizontal separation of cables
 All other properties as in (Fig.29)

Flutter windspeeds calculated by ANSUSP
Modal flutter analysis
Deck torsional stiffness $J_{deck} = 0.04 \cdot J_{nom}$



Graph9 Effect on flutter windspeed of varying horizontal separation of cables
All other properties as in (Fig.29)

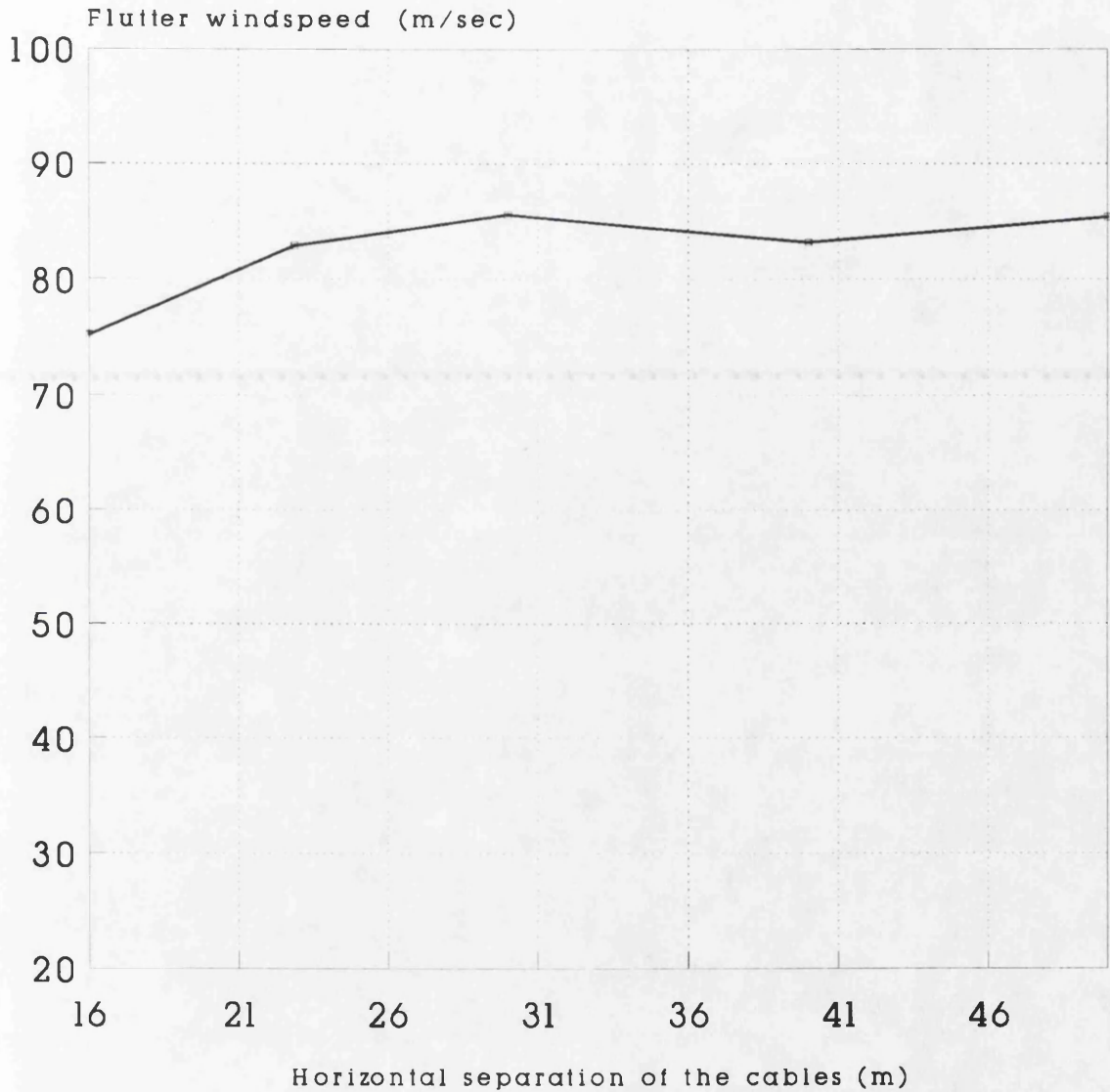
Natural frequencies calculated by ANSUSP
 Torsional deck stiffness $I_{tower} = 10 \cdot I_{nom}$.



— 1-A-F	—+— 1-S-F	—x— 2-S-F	—□— 2-A-F
—x— 3-A-F	—◇— 3-S-F	—△— 1-S-T	—x— 1-A-T

Graph 10 Effect on natural frequencies of
 varying horizontal separation of cables
 All other properties as in (Fig.29)

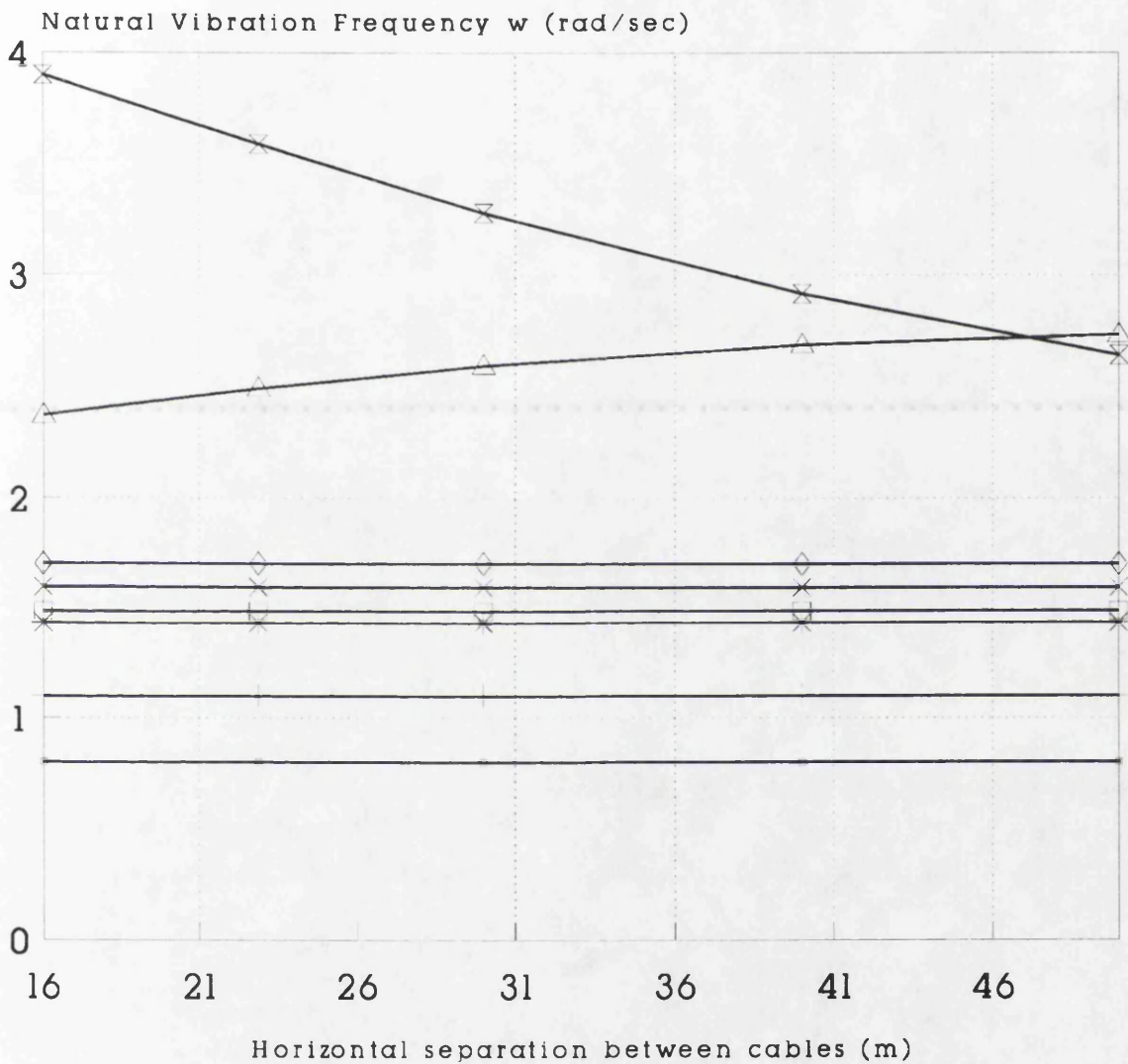
Flutter windspeeds calculated by ANSUSP
Modal flutter analysis including only
symmetric modes, $\theta_{tower}=10^\circ$ in nominal



— ANSUSP Modal Symm.

Graph 11 Effect on flutter windspeed of
varying horizontal separation of cables
All other properties as in (Fig.29)

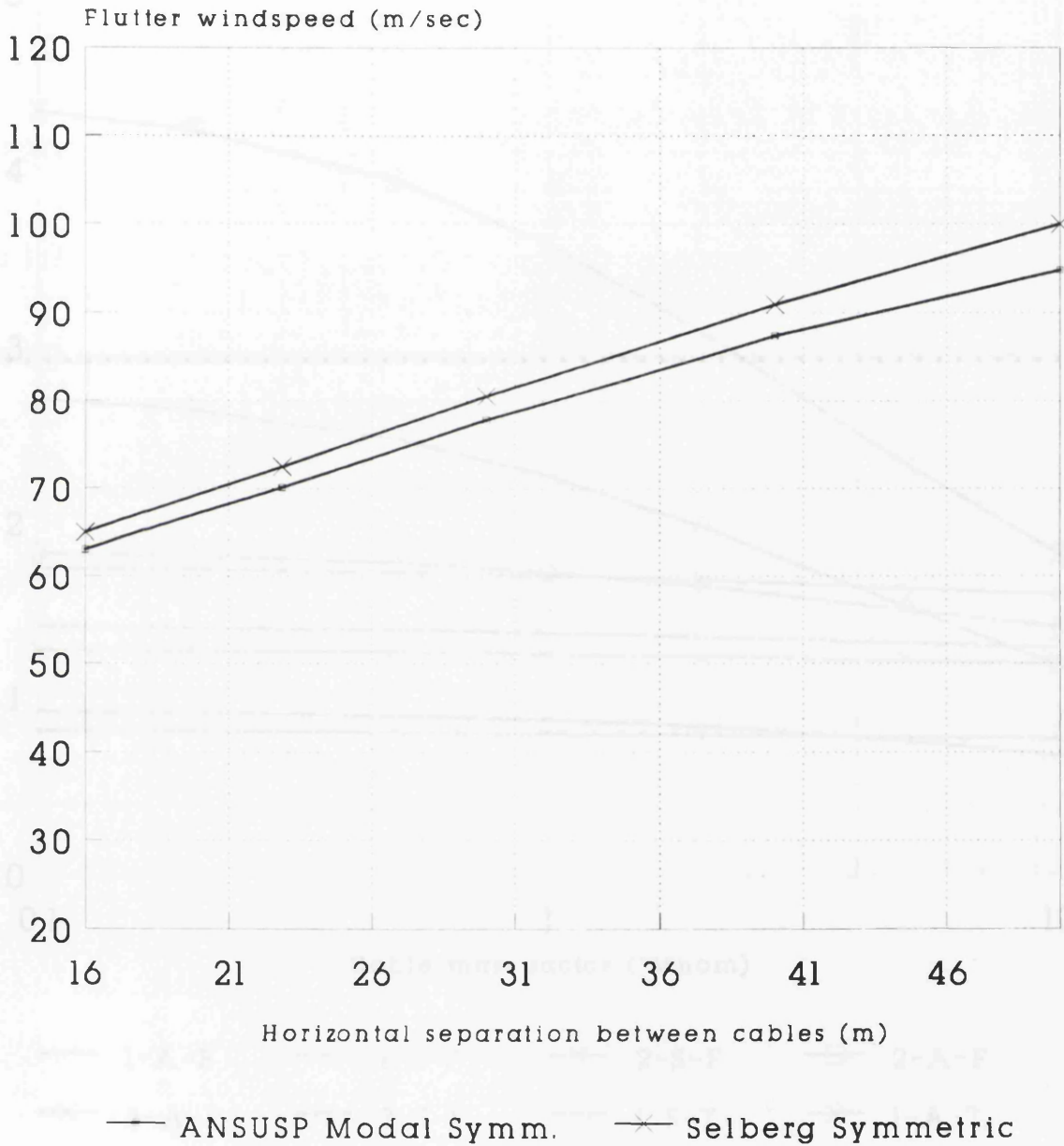
Natural frequencies calculated by ANSUSP
 Tower stiffness $I_{tower} = 10000 \cdot I_{nominal}$



- | | | | | | | | |
|----|-------|----|-------|----|-------|----|-------|
| — | 1-A-F | — | 1-S-F | —x | 2-S-F | —□ | 2-A-F |
| —x | 3-S-F | —◇ | 3-A-F | —x | 1-S-T | —x | 1-A-T |

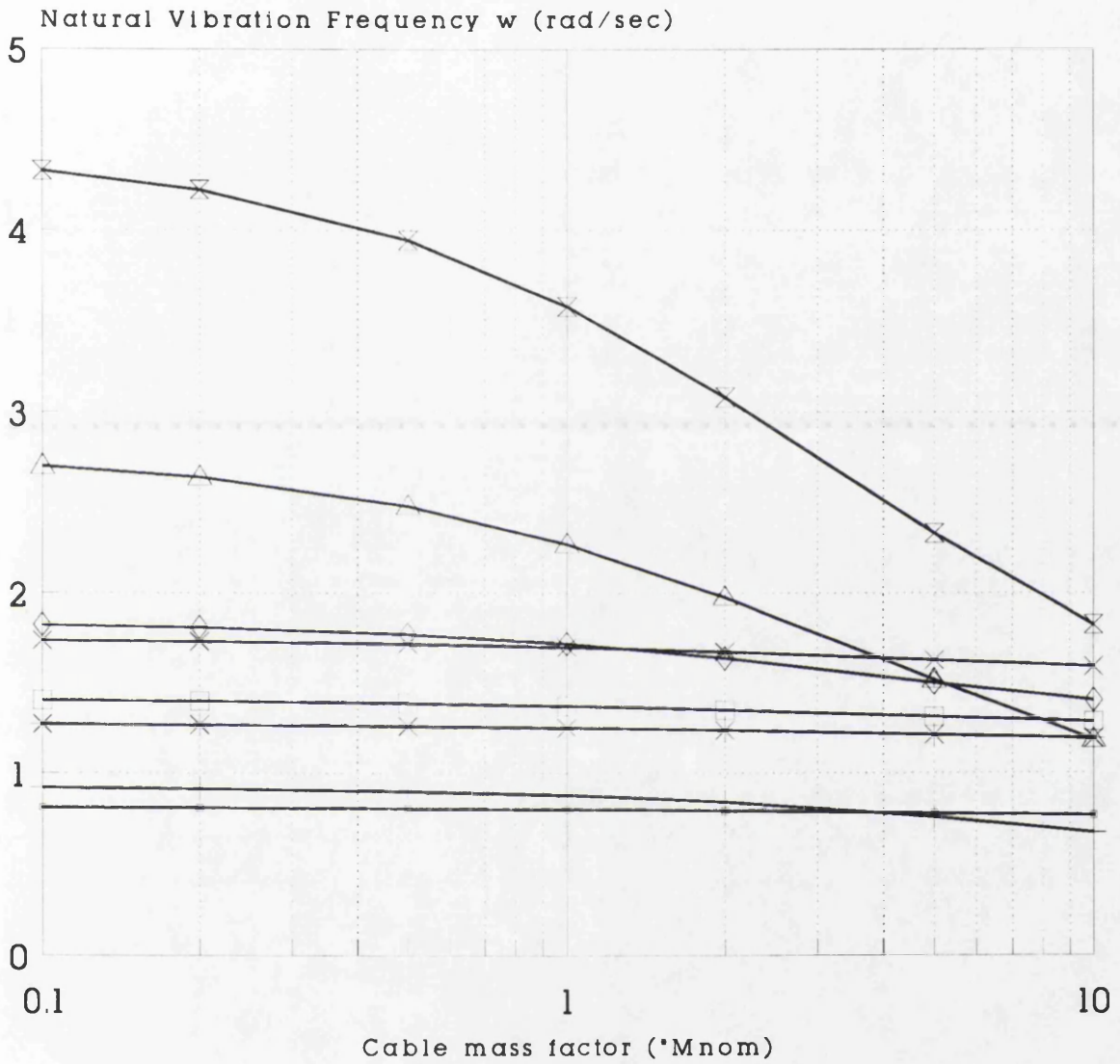
Graph 12 Effect on natural frequencies of varying horizontal separation of cables
 All other properties as in (Fig.29)

Flutter windspeeds calculated by ANSUSP
Modal flutter analysis including only
symmetric modes, $I_{tower}=10000 \cdot I_{nominal}$



Graph13 Effect on flutter windspeed of
varying horizontal separation of cables
All other properties as in (Fig.29)

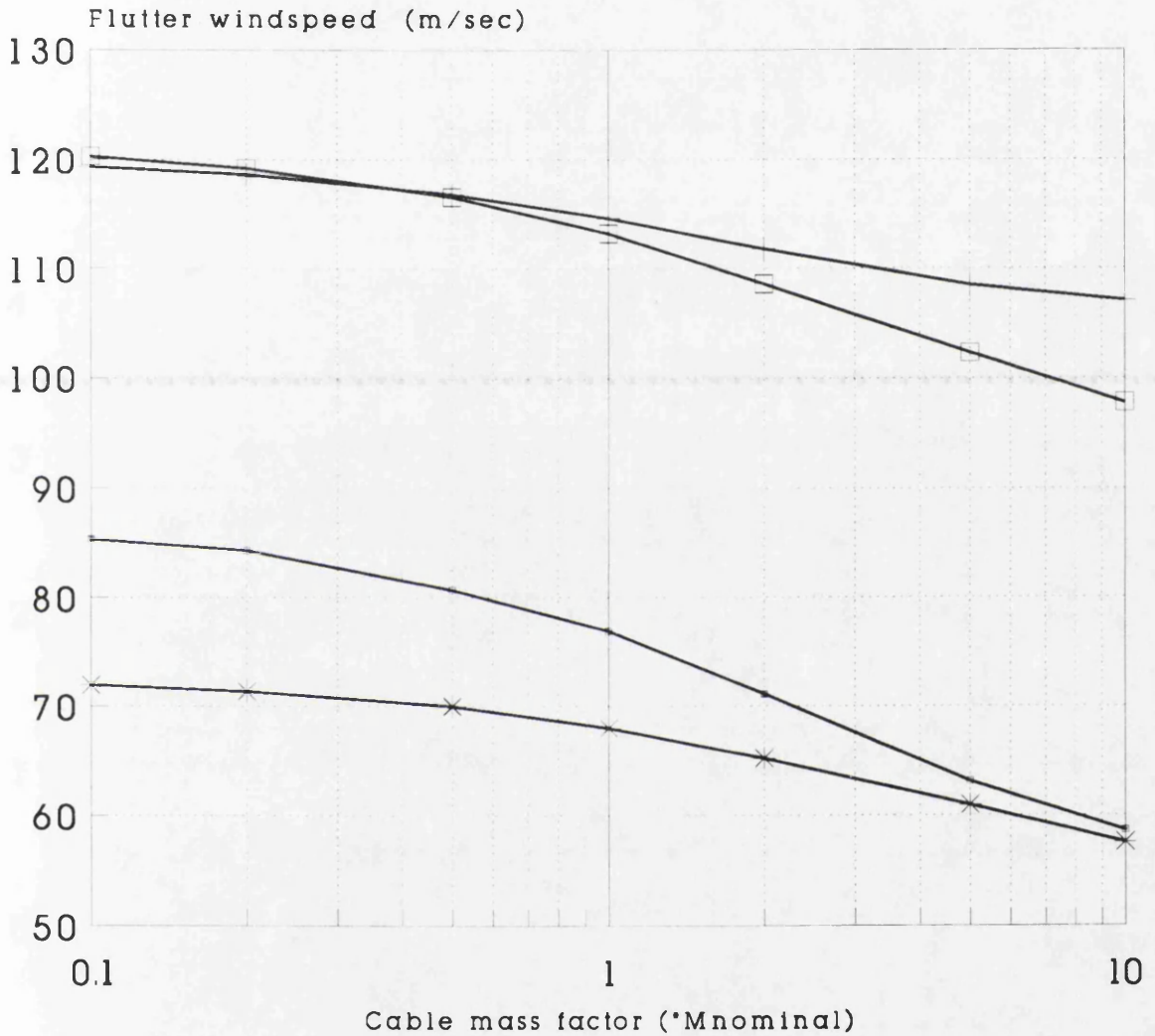
Natural frequencies calculated by ANSUSP



- | | | | |
|---------|---------|---------|---------|
| — 1-A-F | + 1-S-F | × 2-S-F | □ 2-A-F |
| × 3-A-F | ◇ 3-S-F | △ 1-S-T | ⊗ 1-A-T |

Graph 14 Effect on natural frequencies
varying cable mass per unit length
All other properties as in (Fig.29)

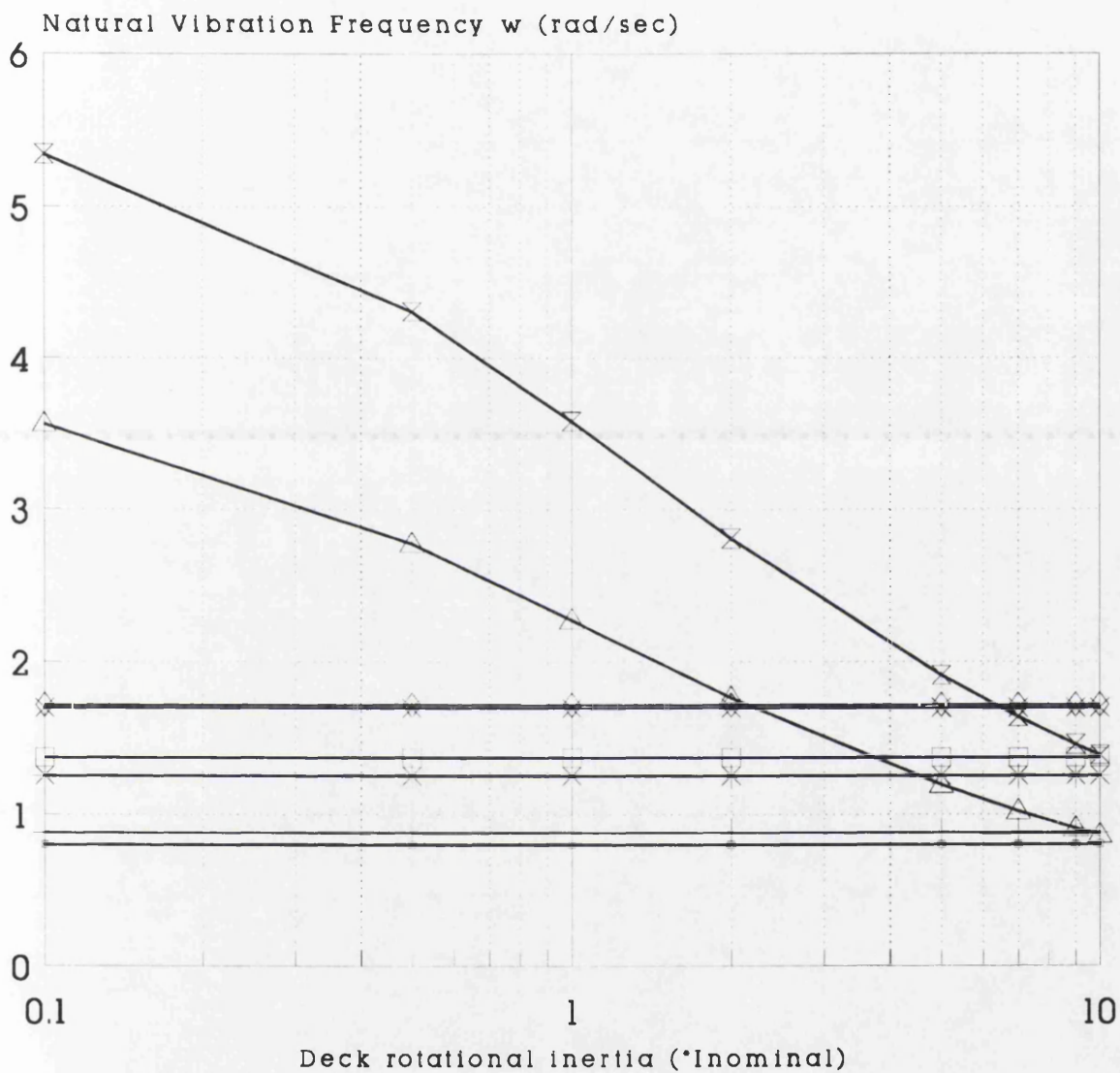
Flutter windspeed calculated by ANSUSP
 Modal flutter analysis including only
 symmetric and only unsymmetric modes



— ANSUSP Modal Symm. — ANSUSP Modal Unsymm.
 * Selberg Symmetric — Selberg Unsymm.

Graph15 Effect on flutter windspeed of
 varying cable mass per unit length
 All other properties are as in (Fig.29)

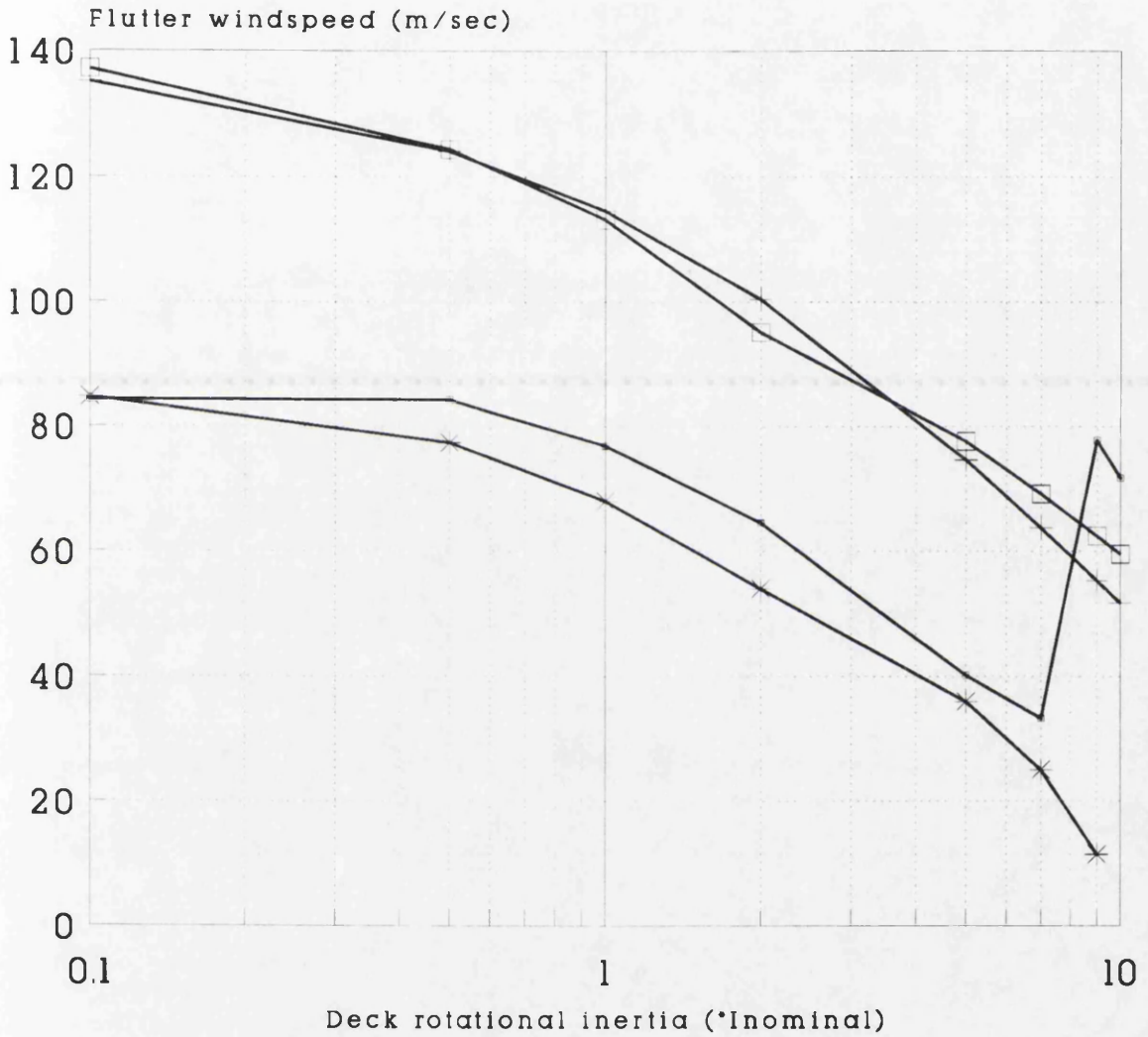
Natural frequencies calculated by ANSUSP



- | | | | |
|---------|---------|---------|---------|
| — 1-A-F | — 1-S-F | — 2-S-F | — 2-A-F |
| — 3-A-F | — 3-S-F | — 1-S-T | — 1-A-T |

Graph 16 Effect on natural frequencies of varying deck rotational inertia
All other properties as in (Fig.29)

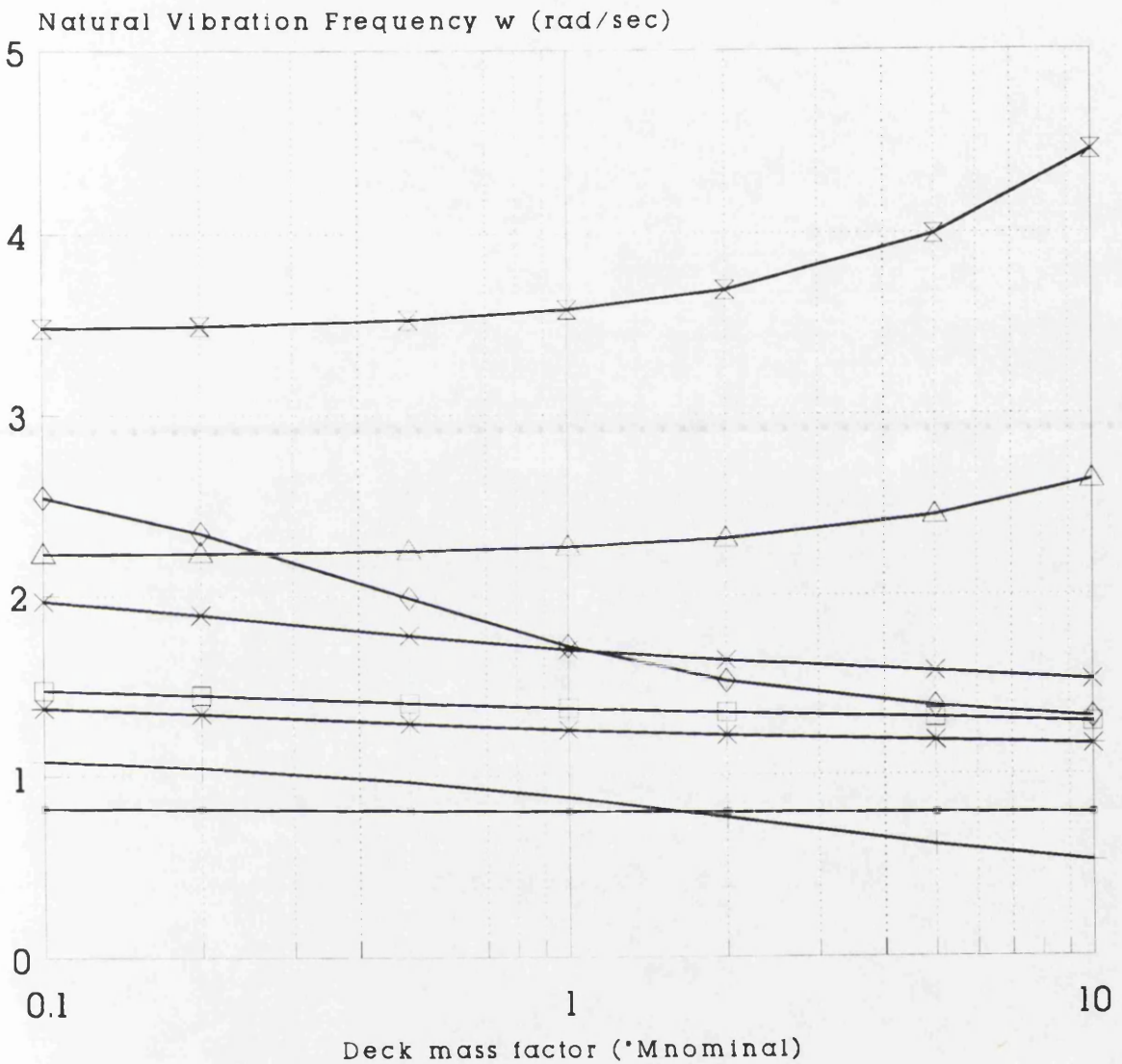
Futter windspeed calculated by ANSUSP
 Modal flutter analysis including only
 symmetric or only unsymmetric modes.



— ANSUSP Modal Symm. — ANSUSP Modal Unsymm.
 * Selberg Symmetric — Selberg Unsymmetric

Graph17 Effect on flutter windspeed of
 varying deck rotational inertia
 All other properties as in (Fig.29)

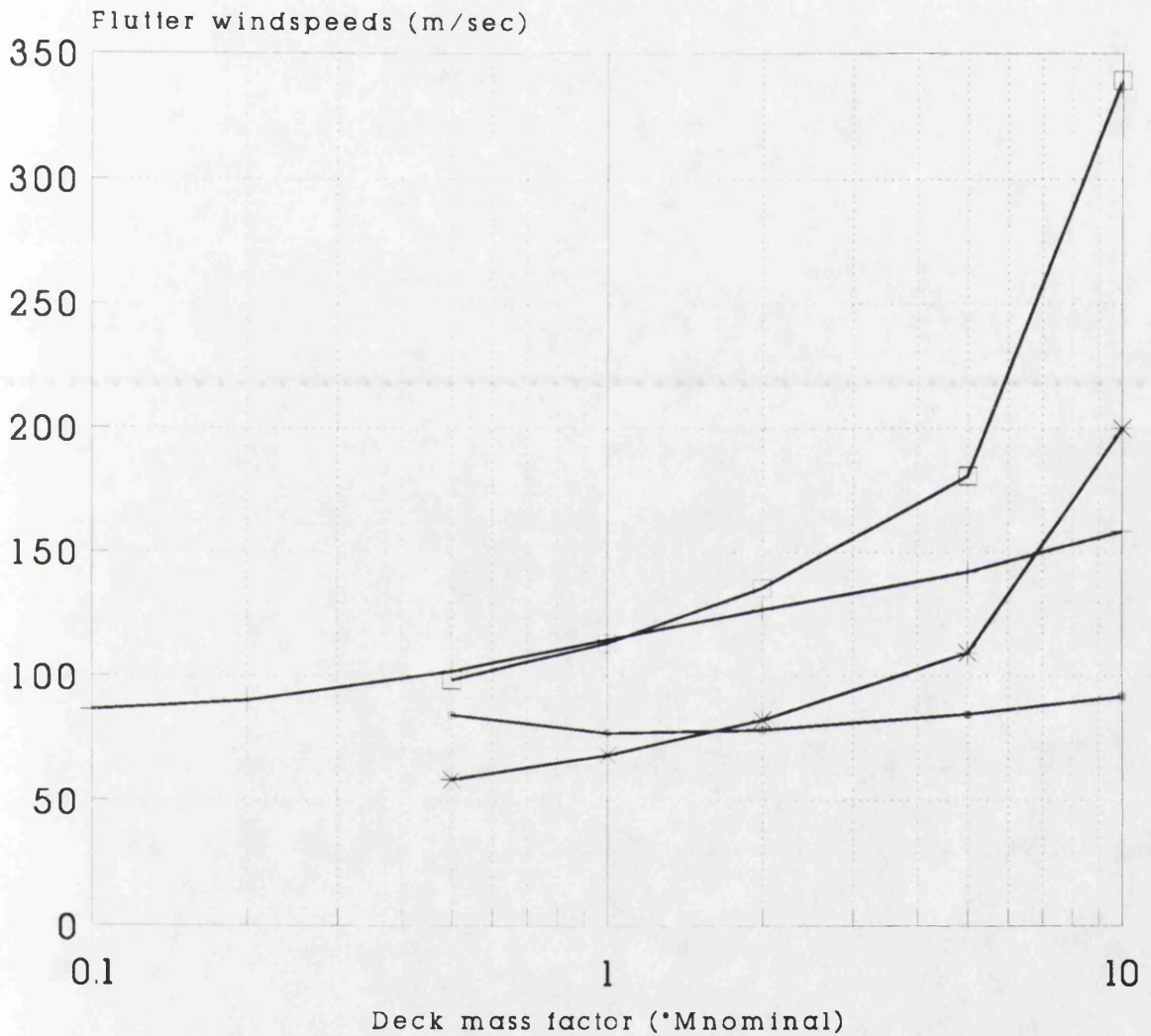
Natural frequencies calculated by ANSUSP



- | | | | | | | | |
|---|-------|---|-------|---|-------|---|-------|
| — | 1-A-F | — | 1-S-F | — | 2-S-F | — | 2-A-F |
| — | 3-A-F | — | 3-S-F | — | 1-S-T | — | 1-A-T |

Graph18 Effect on natural frequencies of varying deck mass per unit length
All other properties as in (Fig.29)

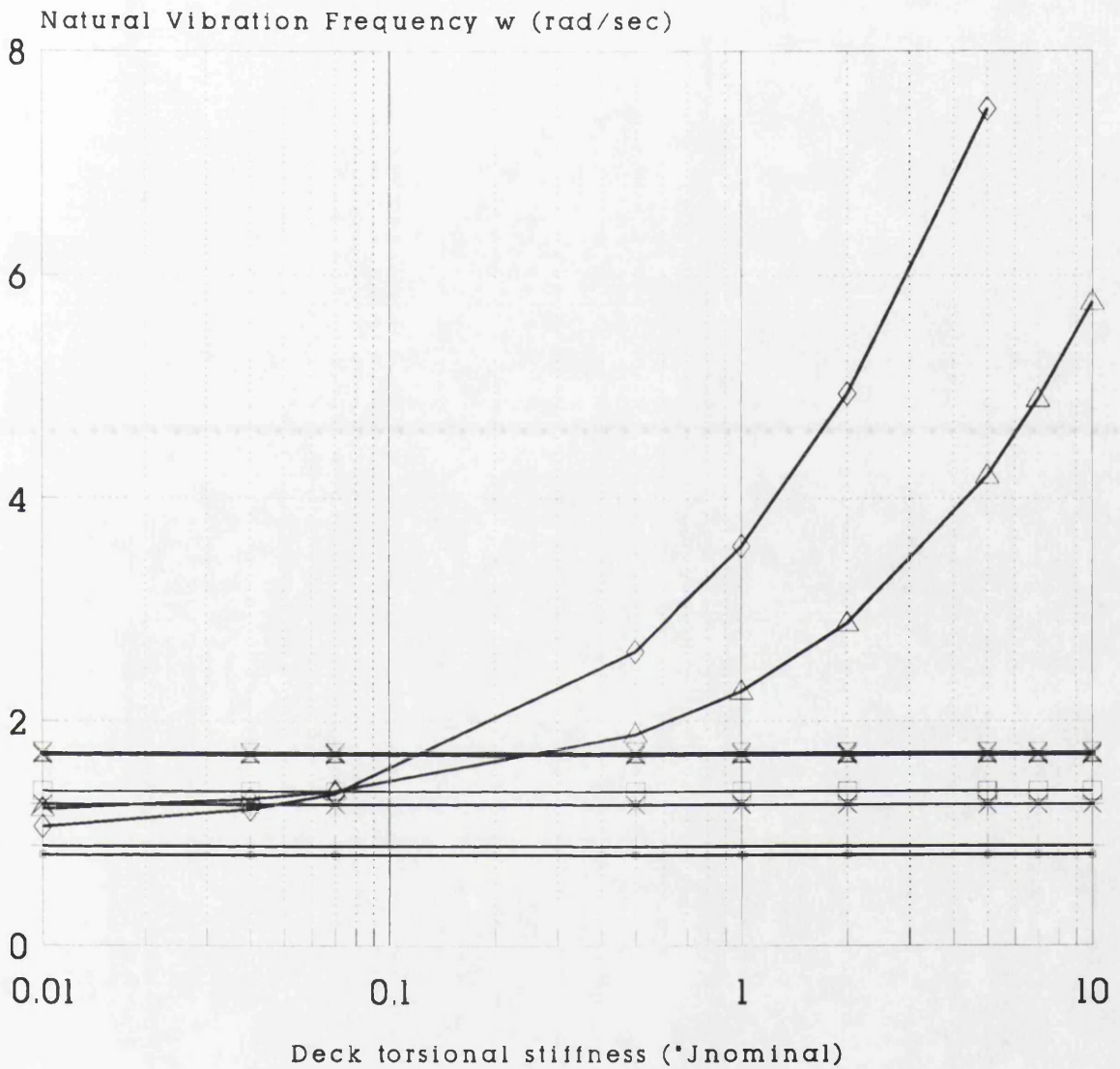
Flutter windspeed calculated by ANSUSP
 Modal flutter analysis including only
 symmetric or only unsymmetric modes



— ANSUSP Modal Symm. — ANSUSP Modal Unsymm.
 * Selberg Symmetric — Selberg Unsymmetric

Graph 19 Effect on flutter windspeed of
 varying deck mass per unit length
 All other properties as in (Fig.29)

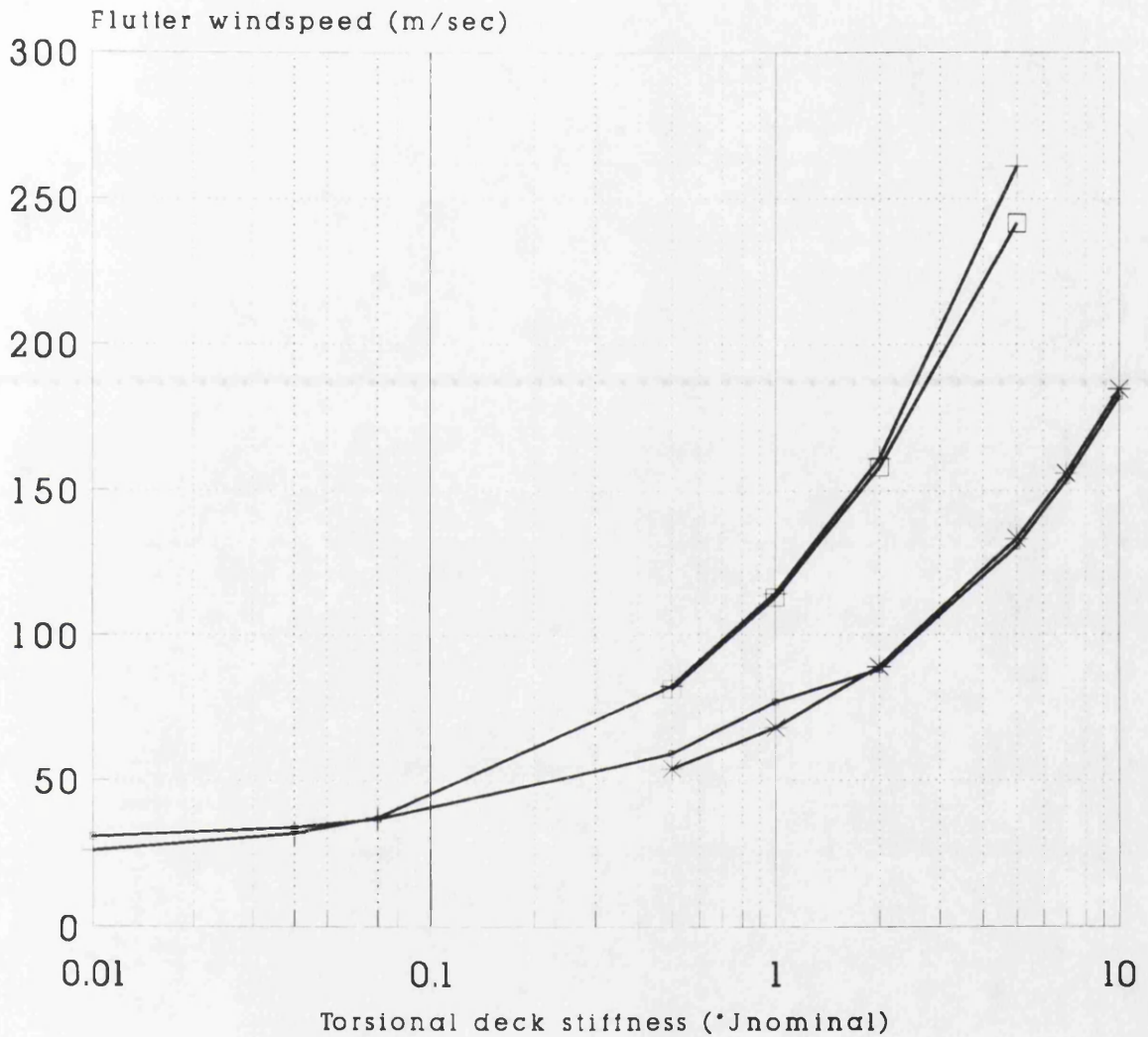
Natural frequencies calculated by ANSUSP



- | | | | |
|-----------|-----------|-----------|-----------|
| —●— 1-A-F | —+— 1-S-F | —x— 2-S-F | —□— 2-A-F |
| —x— 3-A-F | —◇— 1-A-T | —△— 1-S-T | —x— 3-S-F |

Graph20 Effect on natural frequencies of varying deck torsional stiffness
All other properties as in (Fig.29)

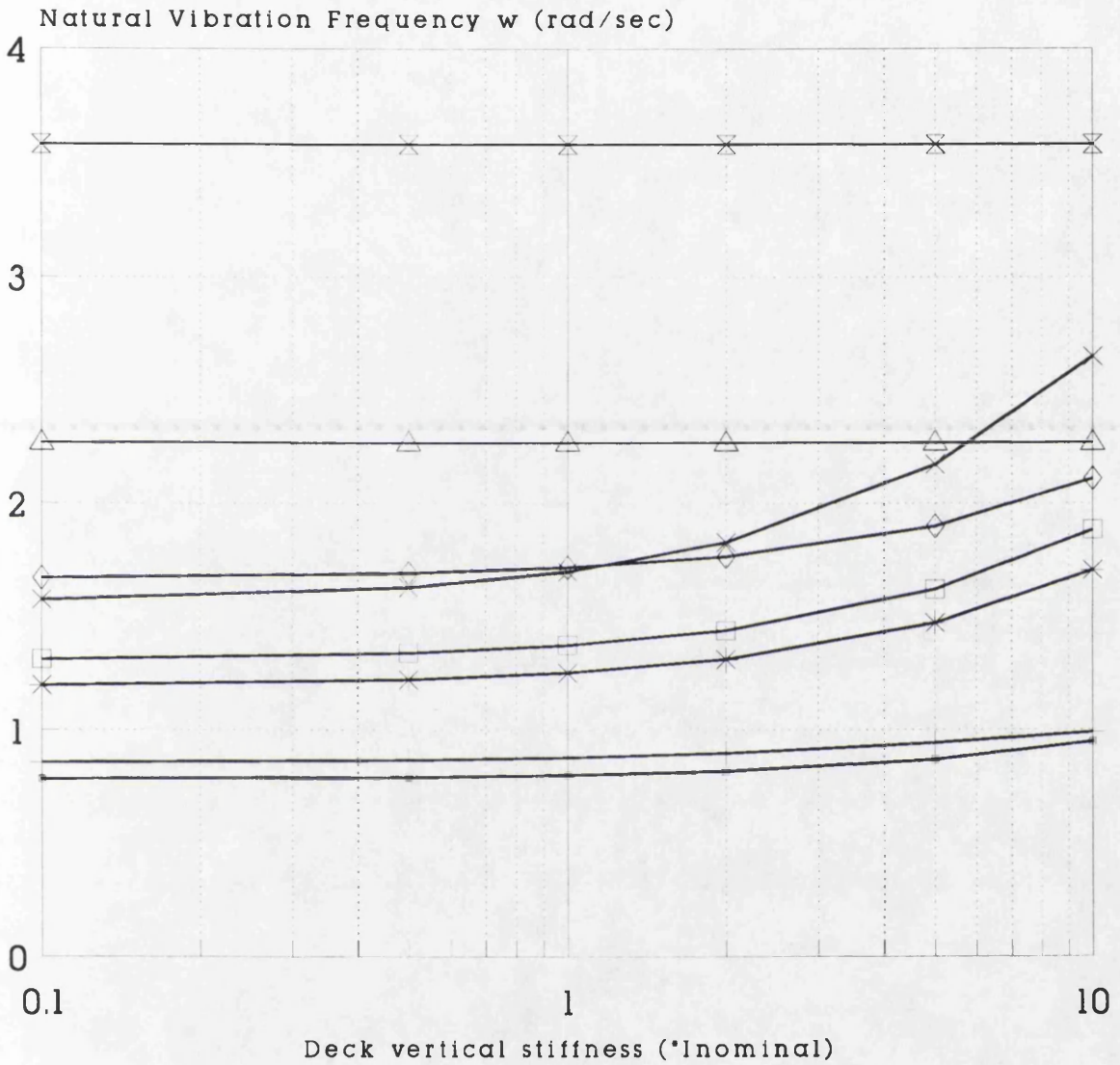
Flutter windspeeds calculated by ANSUSP
 Modal flutter analysis including only
 symmetric or only unsymmetric modes



— ANSUSP Modal Symm. — ANSUSP Modal Unsymm.
 * Selberg Symmetric — Selberg Unsymmetric

Graph21 Effect on flutter windspeed of
 varying deck torsional stiffness
 All other properties as in (Fig.29)

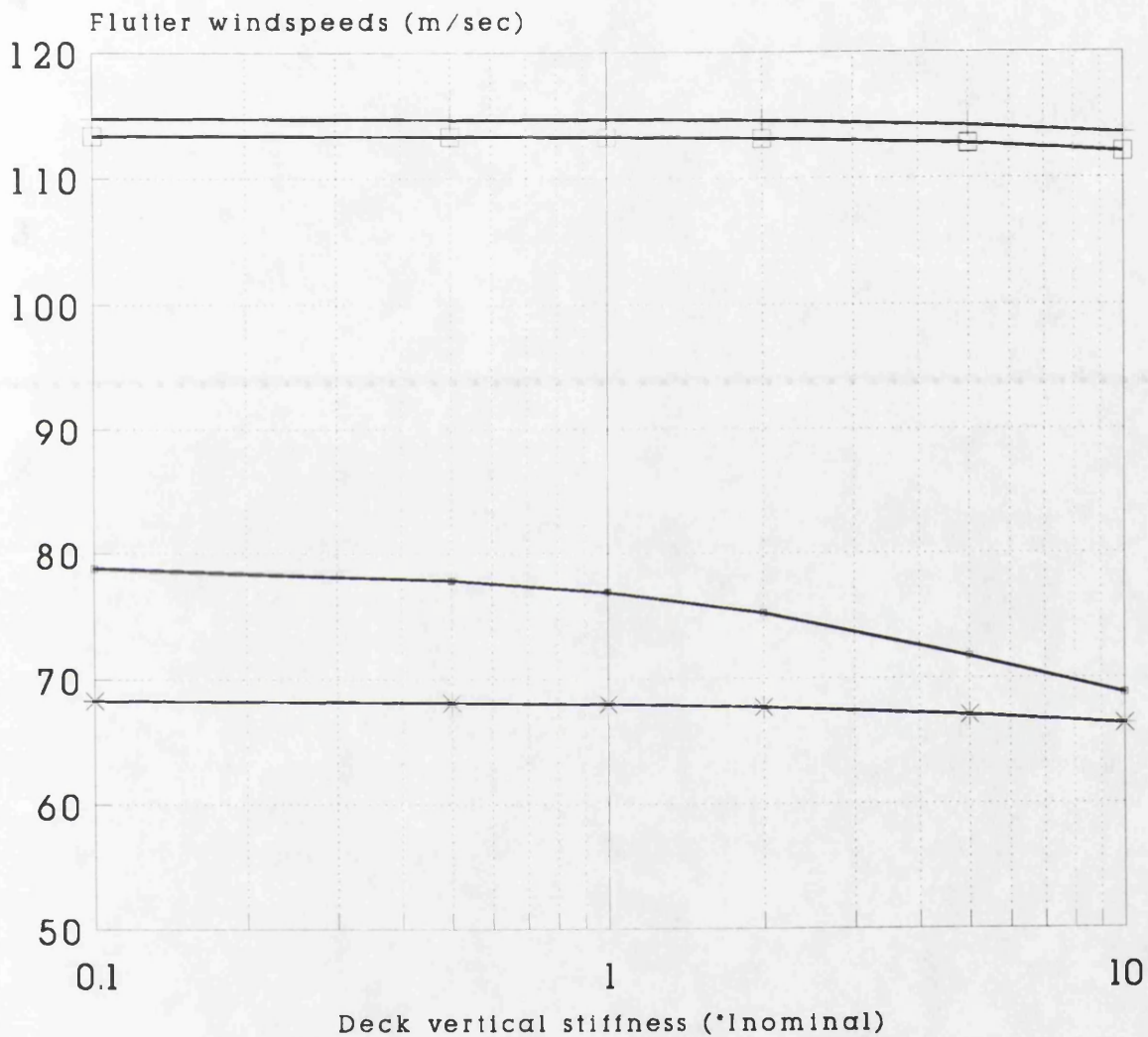
Natural frequencies calculated by ANSUSP



- | | | | |
|-----------|-----------|-----------|-----------|
| — 1-A-F | —+— 1-S-F | —x— 2-S-F | —□— 2-A-F |
| —x— 3-A-F | —◇— 3-S-F | —△— 1-S-T | —x— 1-A-T |

Graph 22 Effect on natural frequencies of varying vertical deck stiffness
All other properties as in (Fig.29)

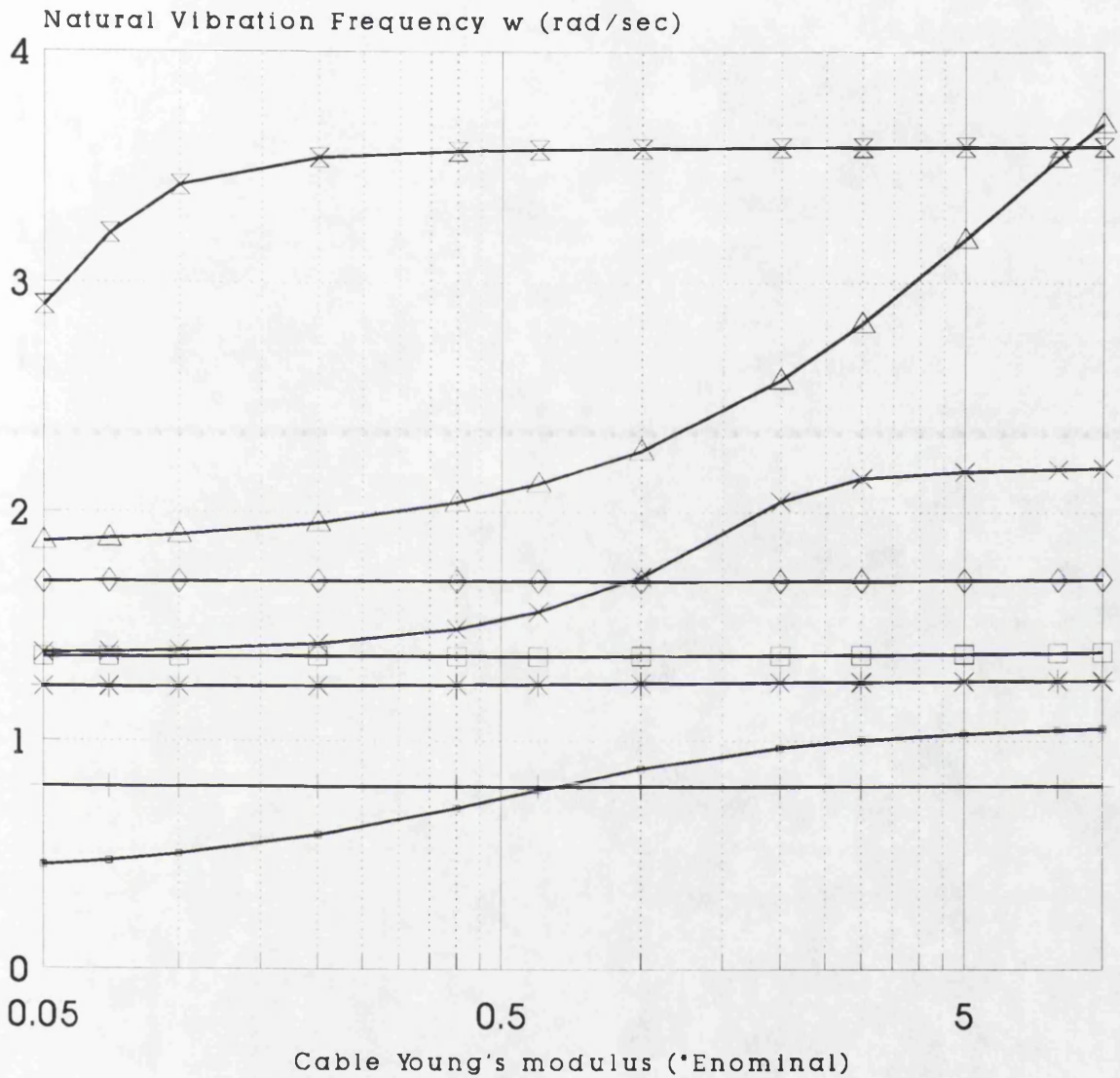
Flutter windspeeds calculated by ANSUSP
 Modal flutter analysis including only
 symmetric or only unsymmetric modes



— ANSUSP Modal Symm. — ANSUSP Modal Unsymm.
 * Selberg Symmetric * Selberg Unsymmetric

Graph23 Effect on flutter windspeed of
 varying deck vertical flexural stiffness
 All other properties as in (Fig.29)

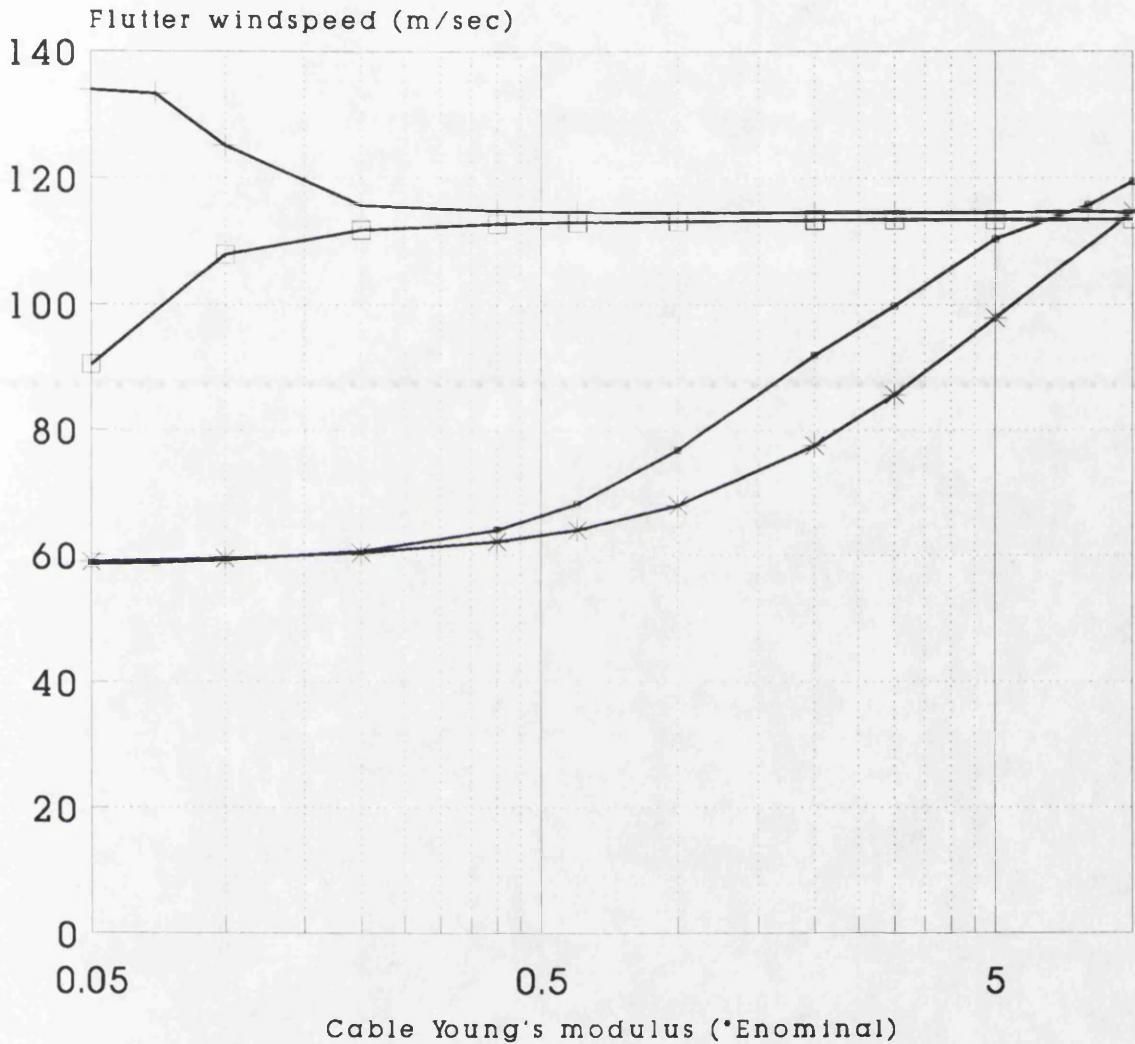
Natural frequencies calculated by ANSUSP



- 1-S-F —+ 1-A-F —x 2-S-F —□ 2-A-F
- x 3-S-F —◇ 3-A-F —△ 1-S-T —x 1-A-T

Graph24 Effect on natural frequencies of varying cable Young's modulus
All other properties as in (Fig.29)

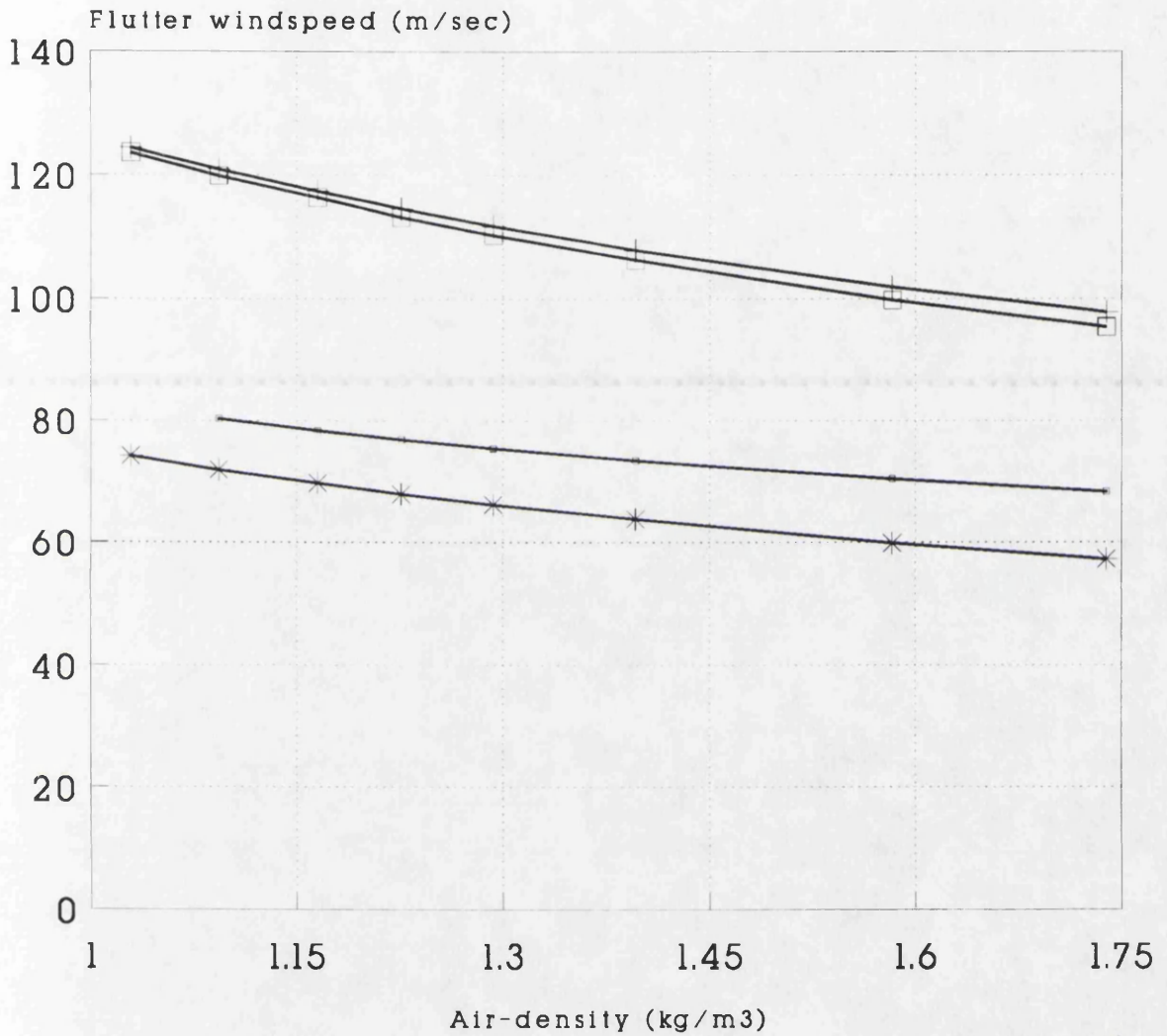
Flutter windspeeds calculated by ANSUSP
 Modal flutter analysis including only
 symmetric or only unsymmetric modes



— ANSUSP Modal Symm. — ANSUSP Modal Antis.
 * Selberg Symmetric — Selberg Unsymmetric

Graph 25 Effect on flutter windspeed of
 varying cable Young's modulus
 All other properties as in (Fig.29)

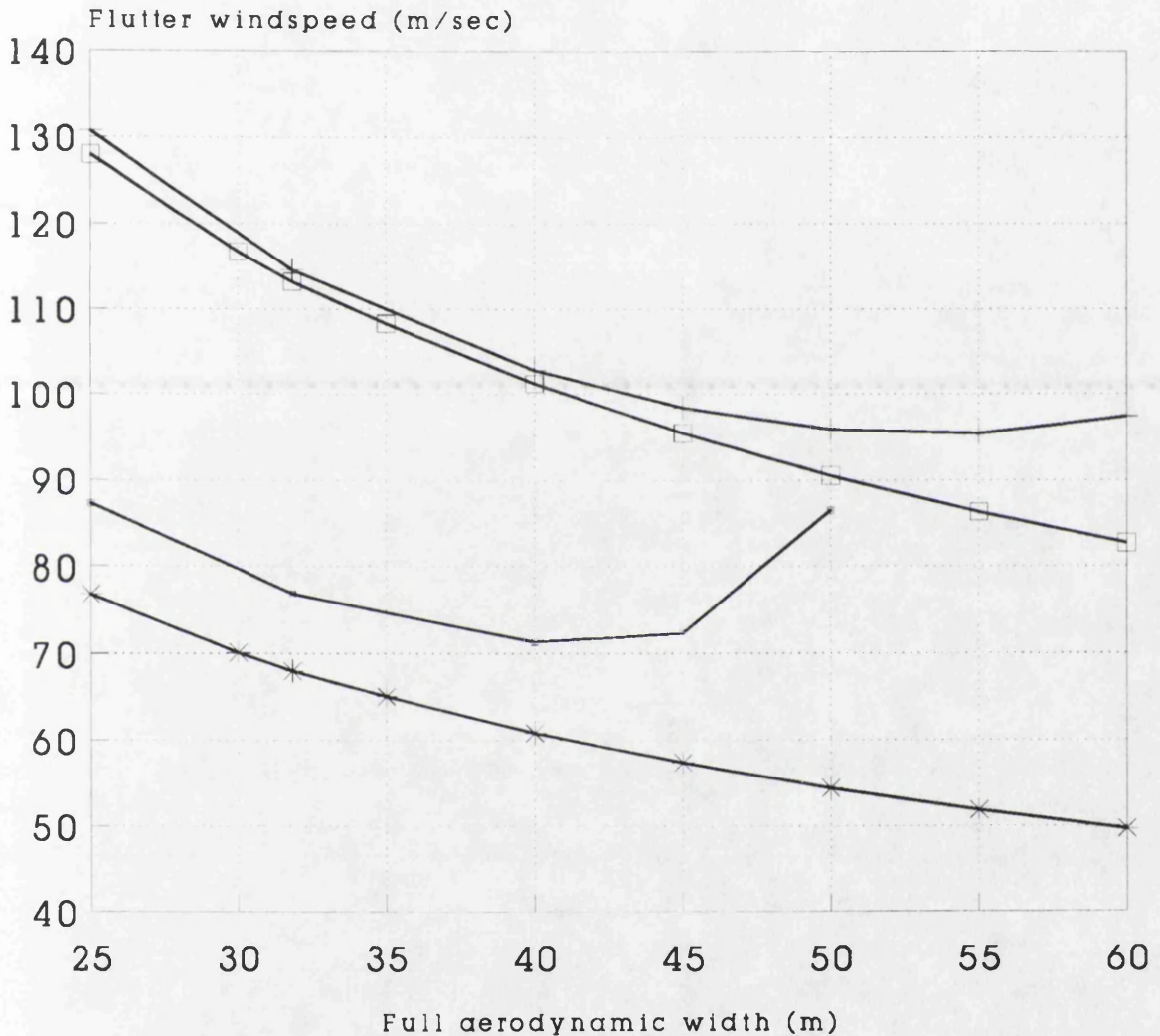
Flutter windspeeds calculated by ANSUSP
 Modal flutter analysis including only
 symmetric or only unsymmetric modes



— ANSUSP Modal Symm. — ANSUSP Modal Unsymm.
 * Selberg Symmetric — Selberg Unsymmetric

Graph26 Effect on flutter windspeed of
 varying air-density
 All other properties as in (Fig.29)

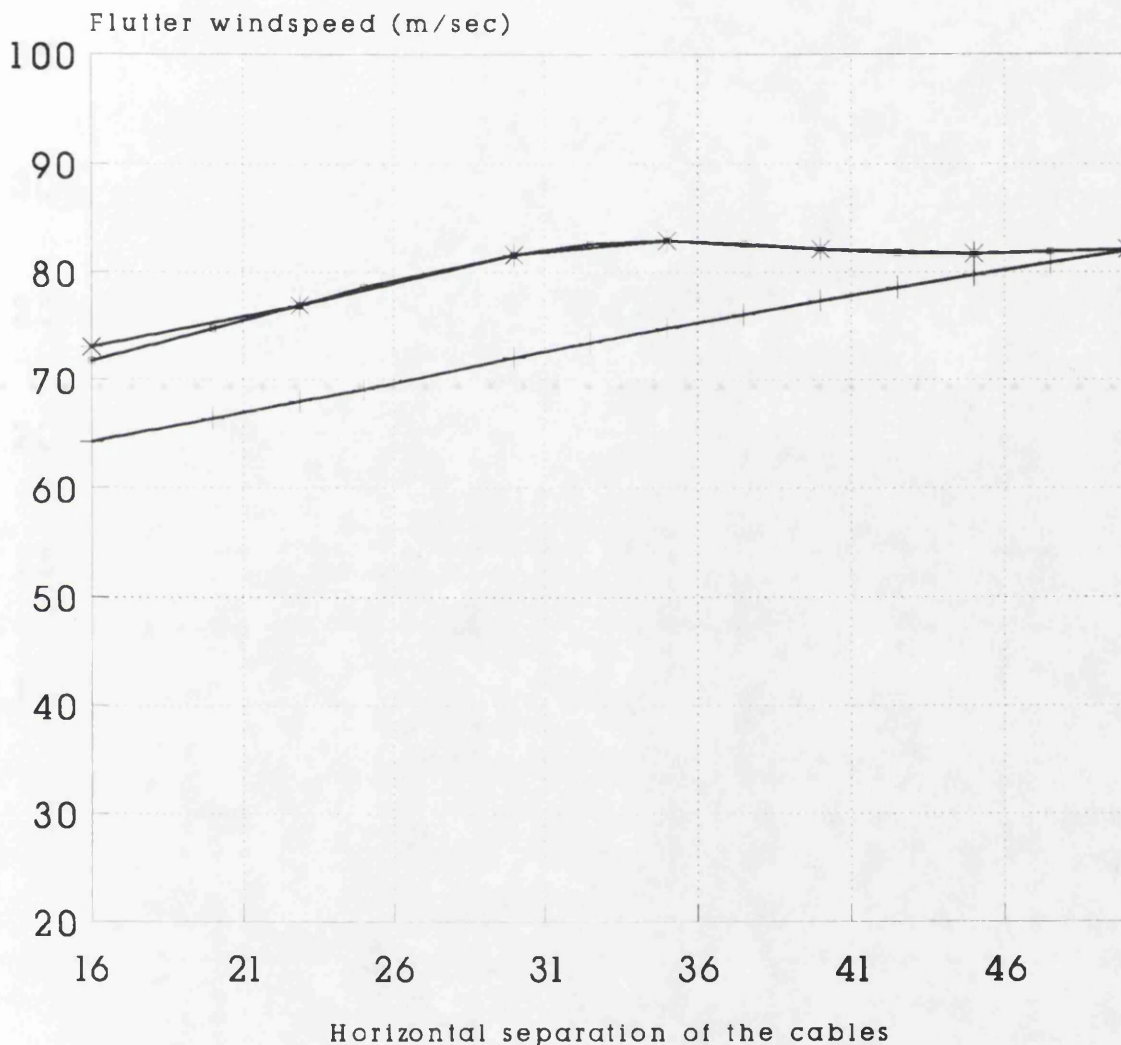
Flutter windspeeds calculated by ANSUSP
 Modal flutter analysis including only
 symmetric or only unsymmetric modes



— ANSUSP Modal Symm. — ANSUSP Modal Unsumm.
 * Selberg Symmetric □ Selberg Unsymmetric

Graph27 Effect on flutter windspeed of
 varying deck full aerodynamic width
 All other properties as in (Fig.29)

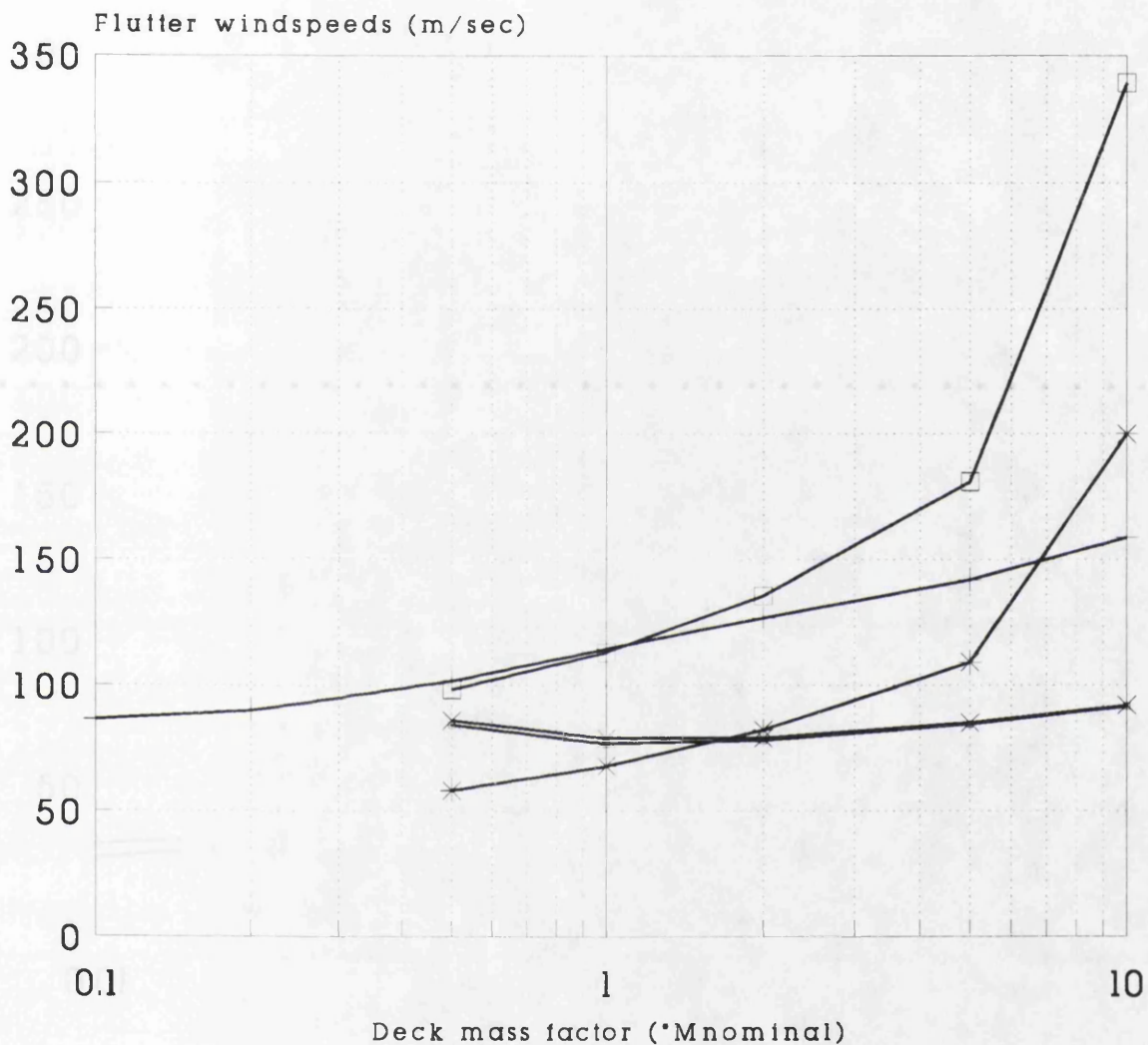
Flutter windspeeds calculated by ANSUSP
Modal flutter analysis including only
symmetric modes



—+— ANSUSP Modal Symm. —+— Selberg
—*— ANSUSP Time history

Graph28 Effect on flutter windspeed of
varying horizontal separation of cables
All other properties as in (Fig. 29)

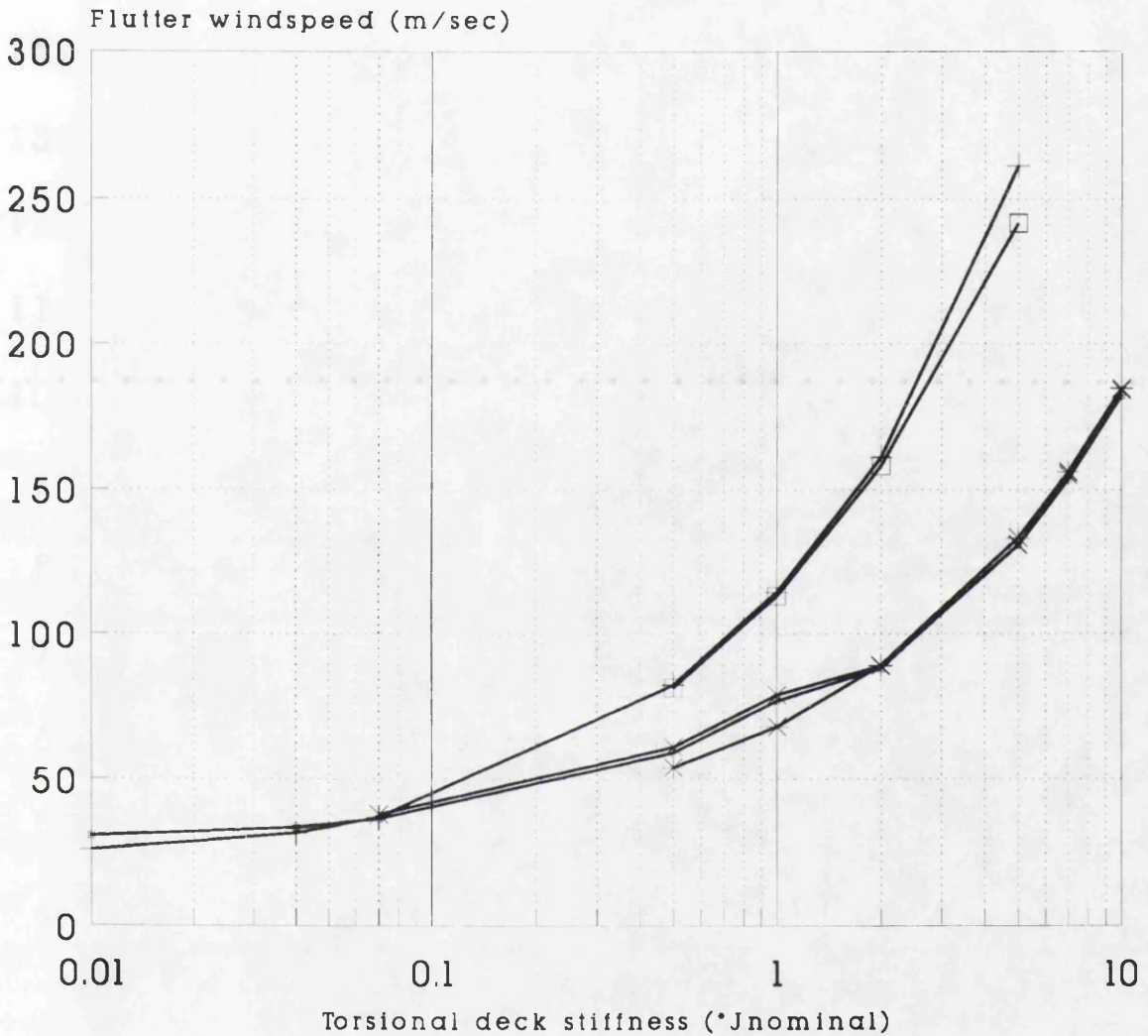
Flutter windspeed calculated by ANSUSP
 Modal flutter analysis including only
 symmetric or only unsymmetric modes



— ANSUSP Mod.S. — ANSUSP Mod.A * Selberg Sym.
 □ Selberg Antis. * ANSUSP Time History

Graph 29 Effect on flutter windspeed of
 varying deck mass per unit length
 All other properties as in (Fig. 29)

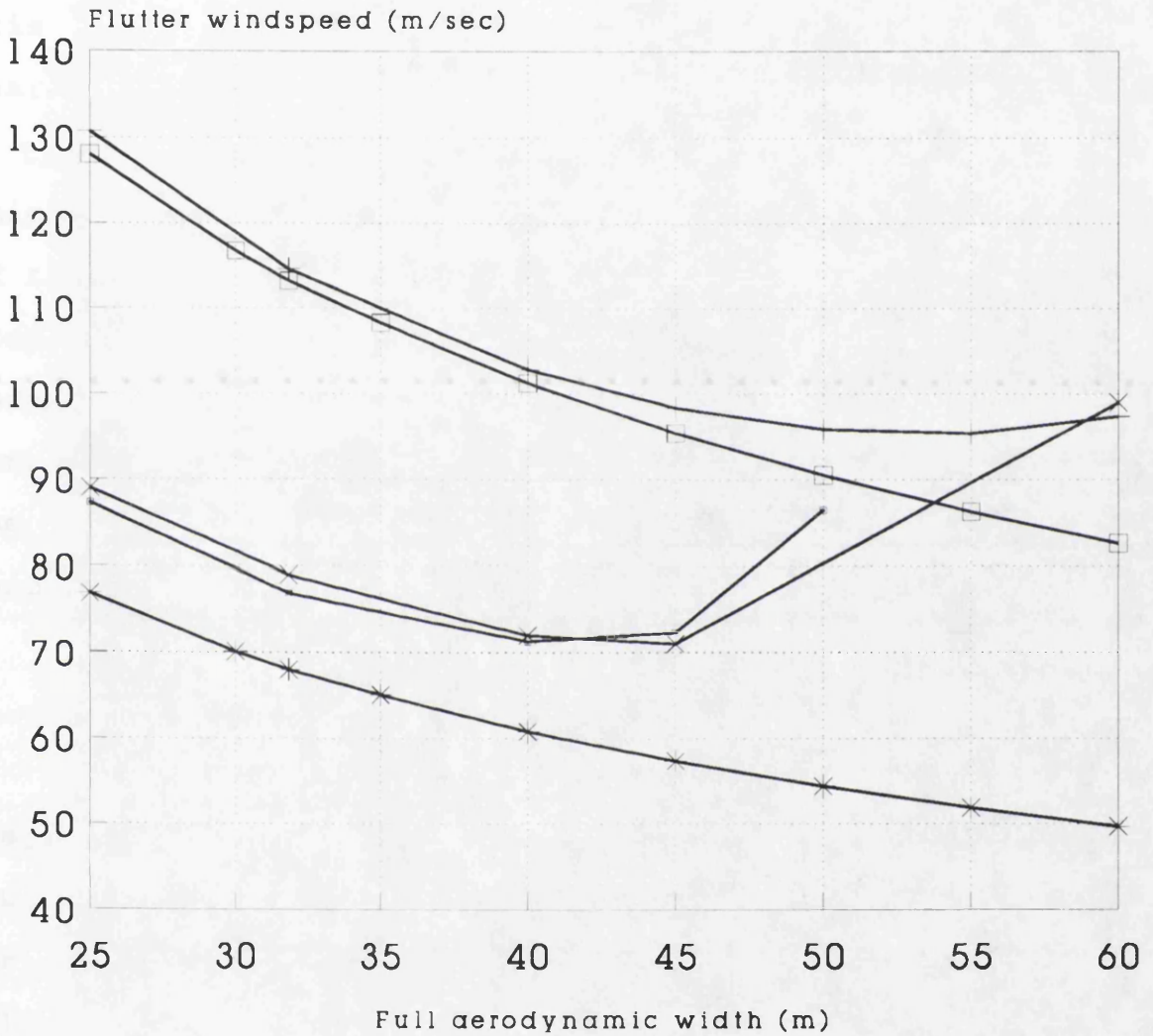
Flutter windspeeds calculated by ANSUSP
 Modal flutter analysis including only
 symmetric or only unsymmetric modes



— ANSUSP Mod.S. — ANSUSP Mod.A. * Selberg S.
 □ Selberg Antis. * ANSUSP Time History

Graph30 Effect on flutter windspeed of
 varying deck torsional stiffness
 All other properties as in (Fig. 29)

Flutter windspeeds calculated by ANSUSP
 Modal flutter analysis including only
 symmetric or only unsymmetric modes



— ANSUSP Mod.S. — ANSUSP Mod.A. * Selberg Sym.
 □ Selberg Antis. * ANSUSP Time History

Graph31 Effect on flutter windspeed of
 varying deck full aerodynamic width
 All other properties as in (Fig. 29)

Chapter 6

Discussion of results

The previous work was carried out with ANSUSP, on the Severn Bridge geometrical and structural properties. This structure was chosen because it incorporates the characteristics of a modern cable suspended bridge and is a typical bridge which satisfies the conditions under which ANSUSP can produce reliable results. The comparison of the results by modal analysis with the results by time step analysis and also by Selberg's semi-empirical formula have led us to the following observations. The percentages quoted below are based on variations from the values corresponding to the nominal properties associated with the Severn Bridge structure as in Fig.29.

6.1 The sag/span ratio of the bridge which is a measure of the bridge gravity stiffness plays a significant role (up to 13%) in determining the flutter speed of the bridge when the sag/span ratio varies within the usual spectrum of design values between 1/14 and 1/10. The effects of changing cable sag/span ratio on symmetric and antisymmetric frequencies are opposite in nature. For symmetric vibration motion the torsional stiffness provided by the cable/hanger system increases with increasing cable sag while the corresponding antisymmetric stiffness decreases thus effecting maximum changes of +10% and -22% in these natural frequencies respectively.

6.2 Horizontal separation of the cables can slightly affect the symmetrical flutter speed by up to 9% approximately. However when combined with towers that are 10,000 times stiffer than the nominal tower properties, increasing horizontal cable separation by a factor of 1.2 can affect the behaviour of the bridge in symmetrical flutter significantly by increasing it by 30%. For the case of a reduced deck torsional stiffness by a factor of 0.04 times, the nominal Severn values the flutter speed variation is 60% of the flutter speed for the nominal cable separation.

6.3 Cable mass affects the overall bridge rotational inertia considerably since it is positioned towards the outer edges of the deck. The other major part of torsional inertia is due to the deck rotational inertia. Consequently the critical flutter speeds of the bridge are affected by both those factors. The characteristics of the bridge improve by up to 10% with cable mass decreasing by a factor of 10 and also improve by up to 7% by decreasing deck rotational inertia by a factor of 10.

6.4 The deck mass affects the gravity cable stiffness modifying the symmetric flutter speed by only 8% for a 10 fold increase in deck mass, but has a much larger effect on the antisymmetric flutter speed by almost doubling it.

6.5 Deck torsional stiffness affects the behaviour of the bridge in flutter according to the proportion of the overall torsional stiffness that it provides since the cables contribute the other major part. The higher the deck torsional stiffness the larger the role it plays in the behaviour of the bridge in flutter increasing the symmetric flutter speed by 130% for a 10 fold increase of deck torsional stiffness.

6.6 Deck vertical stiffness plays a small role in the behaviour of the bridge in flutter. It is interesting to mention that increasing the vertical stiffness of the deck by a factor of 10 reduces the critical windspeed of the bridge in flutter by 5%.

6.7 The Young's Modulus of the cables (E_{cable}) significantly affects the flutter characteristics of the bridge if the cables provide a considerable proportion of the total bridge torsional stiffness in comparison to the deck torsional stiffness. Consequently the larger the contribution of the cables to the overall bridge torsional stiffness the more important is the cable Young's modulus in changing flutter speeds. Particularly when E_{cable} is smaller than 50% the nominal Severn Bridge values the symmetric flutter speeds are unaffected. When E_{cable} increases by 10 fold compared with the nominal Severn value symmetric flutter speed increases by 55%.

6.8 The effect of the air density on the flutter speed of the bridge is to increase the flutter speed

by as much as 15% of the original Severn bridge flutter speed if the air density varies from the lowest possible value (1.029kg/m^3) for very thin air (in temperature of $+70^\circ\text{C}$) to the highest possible value (1.779kg/m^3) for the thickest possible value (corresponding to -70°C). In more realistic terms the variation in flutter speed is more likely to vary by approximately 9% for atmospheric conditions where very high windspeeds are expected to occur.

6.9 Aerodynamic width affects the aerodynamic behaviour of the bridge by up to 20% for widths which correspond to between 2 and 6 lane carriageways. The results though indicate there are no constant trends for the flutter speed when altering aerodynamic width particularly for the symmetric oscillation flutter.

Chapter 7

Conclusions

The work presented in this thesis represents an effort to gain some insight into the aerodynamic characteristic behaviour of flat-plate deck suspension bridge models, which satisfactorily simulate modern faired box deck cross sections.

By changing the numerical model of the original Severn bridge and altering factors which were assumed to be significant for its aerodynamic behaviour, the following conclusions have been reached on the importance of these various factors that affect the flutter stability of this type of bridge.

Some of the parameters examined in the present analysis using ANSUSP produced predictions which were the straight consequence of changes in the bridge stiffness or the bridge inertial properties. Other parameters tested produced results which were not easily predictable or explained. This was the case particularly when changing these parameters affected both inertia and stiffness properties. In these cases a succession of decreasing and increasing flutter wind speed trends was shown when these parameters increase.

The coupling effect being essential for the flutter phenomenon relies on the torsional and vertical frequencies and how close together their values are. It was observed that when a bridge property was changed and the vertical frequencies are affected if their values

approach torsional frequencies, or vice versa, flutter windspeeds usually tend to decrease, the coupling of the two motions being facilitate. On the contrary, when the difference of vertical and torsional frequencies was increased flutter windspeeds were in most cases increasing.

In the following, some general qualitative conclusions will be presented based on observations on the flutter behaviour of cable suspended bridges as some of their properties are modified.

The distribution of mass of a bridge cross section has a large effect on the flutter speed of the bridge. The torsional frequency increases with decreasing deck rotational inertia while the fundamental vertical frequencies, symmetric and antisymmetric remain unaffected and so the coupling effect between vertical and torsional natural frequencies occurs when higher wind speeds are reached.

The torsional stiffness of the deck is one of the most significant factors of the bridge and when it increases, the flutter windspeeds increase accordingly. However, the other large part of the bridge overall torsional stiffness is provided by the cables. Consequently the effects of the deck torsional stiffness are more significant the higher proportion of the overall

torsional stiffness of the bridge is provided by the deck.

The horizontal separation of the main suspension cables affects the part the cables play in the overall torsional stiffness of the bridge and simultaneously the proportion they contribute to the overall rotational inertia. The other contributions to the overall torsional stiffness and vertical inertia is provided by the deck. It has been found that increasing cable separation (increasing torsional stiffness and also rotational inertia provided by the cables) results in increasing flutter speed up to a limit after which the flutter speed is essentially constant. These unexpected effects on flutter speeds are of medium importance. The effects of the cable separation on bridge torsional stiffness is larger if the tower stiffness (both in bending and in torsion) increases very significantly (10,000 fold) and in this case flutter speeds generally increase with increasing cable separation.

The material of the cables can have a large effect on the flutter windspeed of the bridge. When the Young's modulus of the cables increases, the role of the cables in the overall bridge torsional stiffness increases, increasing flutter speeds. Antisymmetric flutter speeds initially decrease up to a point with increasing E_{cable} and for any further increase remain the same.

Antisymmetric flutter becomes the critical case for a Young's modulus 10 times the nominal Severn value.

Increase of vertical deck stiffness in bending has only a minor effect on aerodynamic stability reducing the flutter speed by up to 5% within the range of the parameters tested. The introduction of deep truss stiffening girders in some bridges in the past as referred to in [17] did not necessarily improve the flutter characteristics of these structures except if it also increased the bridge torsional stiffness.

The deck mass is a factor which brings rather unpredictable effects of minor importance. When deck mass increases although the flutter windspeed increase and vertical frequencies reduce the symmetric flutter windspeed remains relatively constant with only an 8% difference from the flutter speed for the Severn bridge nominal properties. The antisymmetric flutter speed is affected somewhat more than the symmetric flutter speed, increasing by 40% for a 10-fold increase in deck mass.

Aerodynamic width is a factor which affects the aerodynamic forces and results in unpredictable effects of medium significance. Within the range of aerodynamic width values tested with ANSUSP a variation on flutter speeds of up to 13% from the flutter speed for nominal Severn properties was observed. Although initially the flutter speed as expected reduced with increasing aerodynamic width, a point was reached where further

increase in aerodynamic width produced increase in flutter speeds. This is true for both symmetric and antisymmetric modes.

The behaviour of the bridge in different air-density conditions was predictable, showing an almost linear proportional relationship of the flutter windspeed with air-density. The higher air density could be the result of low temperatures occurring in reality.

Here it should be emphasized that these conclusions refer to a bridge where symmetric flutter is critical. It is possible when symmetric flutter speed increases because of alterations to the bridge properties and the antisymmetric flutter becomes the prominent case, relative adaptations on the conclusions should be made regarding the structure's critical flutter mode.

The comparison of the results of the two numerical methods (modal and time history) show the modal analysis to produce satisfactorily accurate results with a much lower cost than the time history method. This justifies it as a useful tool for initial understanding of the behaviour of a cable suspended bridge of a flat or a similarly shaped deck. The computing time saved by using a combination of the two numerical methods was shown to be significant when compared with the use of the time history method alone.

One of the major difficulties, during the present study was encountering incontinuity in trend for flutter speed both in the time history method and in modal analysis predictions. In the time history method there were cases where the damping would not become zero no matter how high the windspeed. In modal analysis two kinds of discontinuity were encountered. In some cases the response frequency corresponding to the lower damping, when inserted in the formulas for the aerodynamic forces resulted in a significantly different response frequency. In other cases damping was high no matter how high was the wind speed. This could be due to instabilities in the algorithm. A further investigation, including theoretical proof of the existence or lack of continuity of solutions, would support the validity of the present study.

Chapter 8

Further work proposals

So far the cable suspended bridge has been assessed only for the complete structure. In an incomplete bridge the response of the structure subjected in wind flow may differ significantly from the response of the complete structure. Thus the results of the present analysis carried out for the complete bridge does not apply to the construction stages, and consequently a full flutter analysis of the various construction stages of the bridge will also be required in practise.

As the flutter windspeed during construction may often be lower than for the completed bridge condition it may also be of some importance to investigate the effects of modifying the basic bridge geometric and structural properties for the erection conditions.

The parametric analysis presented in this thesis could also be applied on cable stayed bridges. These structures even though they retain some similarities with the cable suspended bridges as for example their susceptibility to wind effects, are in other aspects quite different structures. The construction of cable stayed bridges all over the world is presently expanding as they are more rigid structures than the cable suspended bridges.

Cable elements have lately appeared modelling the non-linear behaviour of cables, [18]. The introduction of those elements in the modelling of cable suspended

bridges in both numerical methods, modal and time step could improve the accuracy of the results produced by ANSUSP.

Chapter 9

Reference

- 1) Navier, ''Memoires sur les ponts suspendus'', Paris, 1823.
- 2) Geographical Journal, August 1942.
- 3) Melan, J., (translated by D.B. Steinman), ''Theory of Arches and Suspension bridges'', Chicago, 1913.
- 4) Robert H. Scanlan, ''On the state of stability considerations for suspended-span bridges under wind, '' | IAHR/TOTAM Symposium, Karlsruhe 1979.
- 5) Wardlaw, R.L. ''Sectional versus Full Model Wind Tunnel Testing of bridge road decks.'', DME/NAE Quarterly Bulletin No 1978(4), Ottawa, Canada, 25-47, (Jan.1979).
- 6) Walshe, D.E.J., ''Wind excited Oscillations of Structures.'', National Physical Laboratory, H.M.Stationary Office, London, Ch.7, (1972)
- 7) Yoshimura, T. and Nakamura, Y., ''On the Indicial Aerodynamic Moment Responses of Bridge Deck Sections.'', Proceedings, 5th International conference on wind Engineering, Fort Collins, Colorado, (July 1979).
- 8) Ishiro Konishi, Naruhito Shiraishi, Masaru Matsumoto, ''Vortex shedding oscillations of Bridge deck sections.''' | IAHR/TOTAM Symposium, Karlsruhe 1979.
- 9) Melbourne, W.H., ''Model and full scale

response to wind action of the cable stayed box girder West Gate Bridge.'', IAHR/TOTAM Symposium, Karlsruhe 1979.

10) Wardlaw, R.L., ''Approaches to the suppression of wind induced vibrations of structures '', IAHR/TOTAM Symposium, Karlsruhe 1979.

11) Toshiro Miyata, Isao Okauchi, ''Torsional flutter of large-scale model of suspension bridge deck in natural turbulent wind''. IAHR/TOTAM Symposium, Karlsruhe 1979.

12) Simpson, A.G., D.J.Curtis, Y-L.Choi, ''Aeroelastic aspects of the Lantau fixed crossing''. Proceedings of a conference, Institution of Civil Engineering, London, 25-26 March 1981, Bridge Aerodynamics.

13) Iwegbue, Phd. diploma Thesis, 1976, Manchester Umist.

14) Agar, T.J.A., The analysis of aerodynamic flutter of suspension bridges, Computers and Structures, Vol. 30, No 3, pp. 593-600, 1988.

15) Agar, T.J.A., Aerodynamic flutter analysis of suspension bridges by a modal technique. Eng.Struct., Vol. 11, pp. 75-82, April 1988.

16) Leonhardt, F., New trends in the conception and design of suspension bridges, Proceedings of symposium on suspension bridges, Lisbon 1966, pp. 125-148.

17) Gimsing Niels, J., Cable supported bridges concept and design, Chichester, Wiley 1983.

- 18) Panagiotopoulos, P.D., A variational Inequality Approach to the Inelastic Stress-Unilateral Analysis of Cable-Structures, Comp. and Struc. 6(1979) 133-139.
- 19) Wyatt, T.A., Mechanisma of Damping, Symposium on dynamic behaviour of bridges, Crowthorne, Berkshire, 19 May 1977, pp. 10-21.
- 20) Scanlan, R.H. and Tomko, J.J., 'Airfoil and Bridge Deck Flutter Derivatives', J. Eng. Mech. Div., ASCE, Vol. 97, No. EMZ, 1818-1737, Dec. 1971.
- 21) Iwegbue, I.E. and Brotton, D.M., A numerical integration method for computing the flutter speeds of suspension bridges in erection conditions, Proc. ICE, Part 2, pp. 63,785-802, 1977.
- 22) Frandsen, A.G., Wind stability of suspension bridges. Application of the theory of 'thin airfoil', Symposium of suspension bridges, Lisbon 1966, p. 610.
- 23) Curtis, D.J., Hart, J.J., Scruton, C., Walshe, D.E., "An aerodynamic investigation for the suspended structure of the proposed Tsing-Ma bridge," Engineering Structures, vol. 7, January 1985.
- 24) Brown, W.C., Parson, M.F and Knox, H.S.G., 'Bosporus Bridge. Design and construction', Proc. of the ICE, Part 1, vol. 58, Nov. 1975.
- 25) Timoshenko, S., Collected papers, Mc Graw-Hill, New York, 1953.
- 26) Clericetti, C., 'The theory of Modern American Suspension Bridges'. Proc. Inst. Civ. Engrs., London, Vol. 60, 1880.

- 27) Southwell, R.V., and Atkinson, R.J., 'On the Problem of Stiffened Suspension Bridges and its treatment by relaxation Method'', Proc. Inst. Civ. Engrs., London, 1939.
- 28) Bleich, F., 'Dynamic Instability of Truss Stiffened Suspension Bridges Under Wind Action'', Proc. ASCE, Vol. 74, No.8, 1948.
- 29) Bleich, F., Mc Coulough, C.B., Rosecranz, R. and Vincent, G.S., 'The mathematical Theory of Vibration in Suspension Bridges'', U.S.Government Printing Office, Washington D.C., 1950.
- 30) Van der Woude, F., 'Analysis of Suspension Bridges using Energy Principles'', The Structural Engineer, Vol.54, No.4, April 1976.
- 31) Abo-Hamad, M. and Utku, S., Proc. ASCE, J. Eng. Mechanics, vol. 104, p.537, 1978.
- 32) Chaudhury, N.K., 'The Dynamic Behaviour of Non-Linear Structural Frameworks'', PhD Thesis, Univ. of Manchester, 1966.
- 33) Chaudhury, N.K., Brotton, D.M. and Merchant, W., 'A Numerical Method for Dynamic Analysis of Structural Frameworks'', Int.J. Mech. Sciences, Vol.8, 1966.
- 34) Allman, D.J., 'The Natural Frequencies of Elastic Structures'', PhD Thesis, Univ. of Manchester, 1968.
- 35) Bell, A.J., 'Critical Wind Speeds of Elastic Structures'', PhD Thesis, Univ. of Manchester, 1971.

- 36) Bell, A.J., and Brotton, D.M., 'A Numerical Integration Method for the Determination of Flutter Speeds', Int.J. Mech. Sci., Vol.15, 1973, pp.473-483.
- 37) Frazer, R.A. and Duncan, W.J., 'The Flutter of Airplane Wings', R&M Aeronautical Research Committee, No.1155, August 1928.
- 38) Farquharson, F.B., Smith, F.C. and Vincent, G.S., 'Aerodynamic Stability of Suspension Bridges', Parts 1 to 5, Structural Research Lab., Bulletin 116, Univ. of Washington, 1949-1954.
- 39) Steinman, D.B., 'Rigidity and Aerodynamic Stability of Suspension Bridges', Proc. ASCE, Vol. 69, No. 9, 1943.
- 40) Selberg, A., 'Oscillation and Aerodynamic Stability of Suspension Bridges'. Acta Polytechnica Scandinavica, Civ. Eng. and Building Const. Series No. 13, Oslo, Norway, 1961.
- 41) Smith, I.P., 'The Aeroelastic Stability of the Severn Suspension Bridge', NPL/Aero/1105, 1964.
- 42) Sabzevari, A. and Scanlan, R.H., 'Some basic Studies on the Aeroelastic Stability of Suspension Bridges', Research Report, Dept. of Civil Engineering, Princeton University, USA, 1967.
- 43) Sabzevari, A. and Scanlan, R.H., 'Aerodynamic Instability of Suspension Bridges', Proc. ASCE, Vol. 94, No. EM2, April 1968, pp.489-519.

44) Bathe, Klauss Jurgen and Wilson, Edward L. 'Finite Element Method', 1976.

45) Theodorsen, T., 'General Theory of Aerodynamic Instability and the Mechanism of Flutter', NACA Report 496, 1934.

46) Bowen, C.F.P. and Charlton, T.M., 'A Note on the Approximate Analysis of Suspension Bridges', The Structural Engineer, Vol.45, No.7, July 1967.

47) Roberts, Sir Gilbert, 'Severn bridge, Design and contract arrangements', Proc. ICE, Vol.41, Sept.1968.

48) Wardlaw, R.L., and Goettler, L.L., 'A Wind Tunnel Study of Modifications to Improve the Aerodynamic Stability of the Long's Creek Bridge', Report No.LTR-LA-8, NAE, National Research Council, Ottawa, Canada, 1968.

49) Agar, T.J., 'Analysis of suspension bridges-programme ANSUSP userguide, Mott Hay & Anderson Computer Department, 1980.

50) The failure of the Tacoma Narrows Bridge, Bulletin No.78, School of Eng.Tex.Eng.Stat.,1944.

51) Okubo, T., and Narita, N., 'A comparative study of aerodynamic forces acting on cable stayed bridge girders', Proc. 2nd, US-Japan. Seminar on Wind Effects on Structures, Kyoto, University of Tokyo Press, 1976, pp. 271-283.

52) Okubo, T., and Yokoyama, K., 'Some approaches for improving wind stability of cable-stayed bridges', Proc.4th Int. Conf. on Wind

Effects on Buildings and Structures, London, 1985,
Cambridge University Press, 1986, pp.241-249.

53) Loiseau, H., and Szechenyi, E., 'Etude du
comportement aeroélastique du tablier d'un pont à
haubans'', T.P.1975-75, Office National d'Etudes et
de Recherches Aérospatiales, Chatillon, France.

54) Wyatt, T.A., and Scruton, C., 'A brief
survey of aerodynamic stability problems of bridges'',
Bridge aerodynamics, 25-26 March 1981, Thomas Telford
Limited, London 1981.